Development and Evaluation of a Topology Optimization Framework for District Thermal Energy Systems to Lower Life Cycle Cost and Carbon Emissions

by

Amy Elizabeth Allen

B.S., University of Illinois, 2012

M.S., Stanford University, 2014

A thesis submitted to the

Faculty of the Graduate School of the

University of Colorado in partial fulfillment

of the requirements for the degree of

Doctor of Philosophy

Department of Civil, Environmental, and Architectural Engineering

2021

Committee Members:

Gregor Henze, Kyri Baker, Co-Chairs

Moncef Krarti

Gregory Pavlak

Wangda Zuo

Allen, Amy Elizabeth (Ph.D., Architectural Engineering)

Development and Evaluation of a Topology Optimization Framework for District Thermal Energy Systems to Lower Life Cycle Cost and Carbon Emissions

Thesis directed by Prof. Gregor Henze and Asst. Prof. Kyri Baker

It is accepted that the most cost-effective approach to decarbonizing energy systems will involve widespread electrification of combustion processes, including space heating. So-called "fifth-generation" district thermal energy systems, which operate at near-ambient temperatures, have the potential to provide significant reductions in source energy use intensity in appropriate applications, as well as facilitating beneficial electrification of heating, and the integration of renewable and waste heat sources. However, obstacles remain to the adoption of such systems, including a large "search space" of potential network configurations. This research addresses that obstacle through the development of a framework for network topology optimization of district thermal energy systems. The topology optimization framework seeks to address the question, for a given set of buildings with known locations and loads, "What is the optimal subset of buildings, if any, to connect to a district thermal energy system, and by what network should they be connected, to minimize life cycle cost?"

Though the topology optimization framework is extensible to district thermal energy systems in general, the problem is particularly interesting and relevant in the context of fifth-generation (or "advanced") systems. To motivate the focus on fifth-generation district thermal energy systems, this research also evaluates the potential for reduction in source energy-use intensity from the use of low-exergy building level HVAC systems, which would be compatible with a district thermal energy system operating at near-ambient temperatures. The topology optimization problem is addressed in two parts: the selection of the best subset of buildings (if any) to connect to a district thermal energy system, and the selection of the network by which to connect them. The particle swarm optimization (PSO) algorithm is applied to the first part of the problem, and a heuristic

–the use of the minimal spanning tree, a concept leveraged from graph theory, which connects the given buildings and plant with a network having the least possible total edge length–is applied to the second part of the problem. This research validates those two approaches for use in network topology optimization in the context of fifth-generation systems. This research also demonstrates the value of network topology optimization through the application of the developed framework to a case study.

Dedication

I wish to dedicate this work to my parents, Brian and Susan Allen, for their unflagging love and support throughout every phase of my life, and to my late grandparents, Bill and Lois Allen and Bill and Emma Lou Little, who helped instill in me a keen sense of curiosity and love of learning. I wish they were still here.

Acknowledgements

I appreciate and am grateful for the advice and support of my committee members, and in particular, owe a great debt of gratitude to my advisors, Professors Gregor Henze and Kyri Baker, as well as Professor Greg Pavlak, for their unending patience and guidance over the last several years. They were always ready to offer insightful direction and feedback, while also encouraging me to work independently. I have learned so much from their classes, papers, and sterling example as researchers, and I hope this is only the beginning of our collaboration.

I am very grateful to my managers, Bill Livingood and Michael Deru, and colleagues at the National Renewable Energy Laboratory for supporting my work, and for offering insightful guidance and feedback. I am grateful to my immediate supervisor and colleague, Nicholas Long, for his unflagging patience and generosity in offering advice on the Metamodeling Framework, as well as many other technical issues that arose during this work —his support was essential. Dr. Brian Ball generously offered insightful advice and feedback on structuring optimization problems, and implementing solutions progammatically. I am also grateful for valuable technical guidance from Dr. Katherine Fleming, David Goldwasser, Andrew Parker, and many other colleagues.

I am grateful for the support of my fellow graduate students in Architectural Engineering at CU, and especially wish to acknowledge the significant contributions of Yangyang Fu in very generously and patiently providing significant technical guidance in the use of Modelica, and Justus von Rhein, for the very solid foundation in topology optimization built through his excellent master's thesis. I wish to also express my gratitude for technical assistance from Dr. Zahra Fallahi and Dr. Mick Murphy.

Contents

Chapter

Tables

Table

Figures

Figure

Chapter 1

Introduction, motivation, and organization

1.1 Motivation

Cities and the urban districts that compose them have been recognized by the UN Environment Programme and other international bodies as ideal laboratories for strategies to reduce carbon emissions. Sources of emissions linked to cities already account for seventy-five percent of carbon emissions globally [1]. The United Nations Environment Programme designated "safe, resilient, and sustainable cities" as one of its 2030 Development Goals, which are focused on human development and protection of the environment [1]. Specifically, "eco-districts", which include a focus on building energy efficiency, in addition to renewable energy, public transportation, and sustainable land use, in a localized area, have been recognized as a successful strategy in European cities that have achieved significant reductions in carbon emissions [2]. Advanced district thermal energy systems have the potential to achieve deep energy savings by leveraging the density and diversity of loads in urban districts. "Conventional" district thermal energy systems, in which a single centralized source or a few sources supply thermal energy to connected loads, generally rely on radial networks, or a ring configuration, if redundancy of supply is essential [3]. Advanced systems, which use water at near-ambient temperatures, enabling connected loads to serve as "prosumers", motivate the consideration of a wider array of network configurations. This larger solution space of potential system configurations, as well as the high infrastructure cost, hinders the adoption of advanced district thermal energy systems. The work of [4] states that expansion of the use of advanced district thermal energy systems in the context of increased penetration of renewable

electricity generation will require "advanced energy system analysis tools of coherent systems."

The work presented in this dissertation seeks to address these barriers to adoption by developing a topology optimization framework for district thermal energy systems. For a given urban district, the framework can answer the questions, "Which subset of buildings, if any, are most advantageous to connect to a district thermal energy system, and by what network topology should they be connected, in order to minimize life cycle cost?" As part of this work, the framework has been applied to several relevant case studies to characterize the nature of the buildings that are most advantageous to connect to such a network, and the factors that influence the optimal topologies for connecting them.

1.2 Introduction

Several concepts from graph theory are useful in characterizing the "search space" of potential thermal network configurations for a given set of buildings. In the mathematical context, a "graph" is a set of nodes (vertices) and edges (pairs of nodes) connecting them. A "connected graph" is a graph in which there exists at least one path between every pair of nodes [5]. A "spanning tree" is type of connected graph in which there exists exactly one path between each pair of nodes, and the "minimal spanning tree" is the spanning tree that connects a given set of nodes with the least total edge length [5]. In this work, thermal networks are represented as connected graphs. The number of potential network configurations for a district thermal energy system is equal to the product of the number of ways a subset of buildings of a given cardinality can be selected, and the number of connected graphs associated with that subset, summed over the number of buildings in the district.

Figure 1.1 illustrates a notional comparison of common types of networks in the context of district thermal energy systems. The radial networks that are often used in older generations of district thermal energy systems constitute spanning trees. However, the consideration of the connectivity between loads, in addition to connectivity between loads and a central plant, is more relevant in the context of advanced systems, in which individual loads can serve as "prosumers" and offset the requirement for thermal energy provision by centralized sources. "Conventional"

district thermal energy systems are generally designed for uni-directional mass flow. Restricting the "search space" further to only minimal spanning tree networks significantly reduces the number of potential solutions. Growth in the size of the search space for the network topology optimization problem for district thermal energy systems when all connected graphs are considered, and for minimal spanning tree networks only, is shown in Figure 1.2.

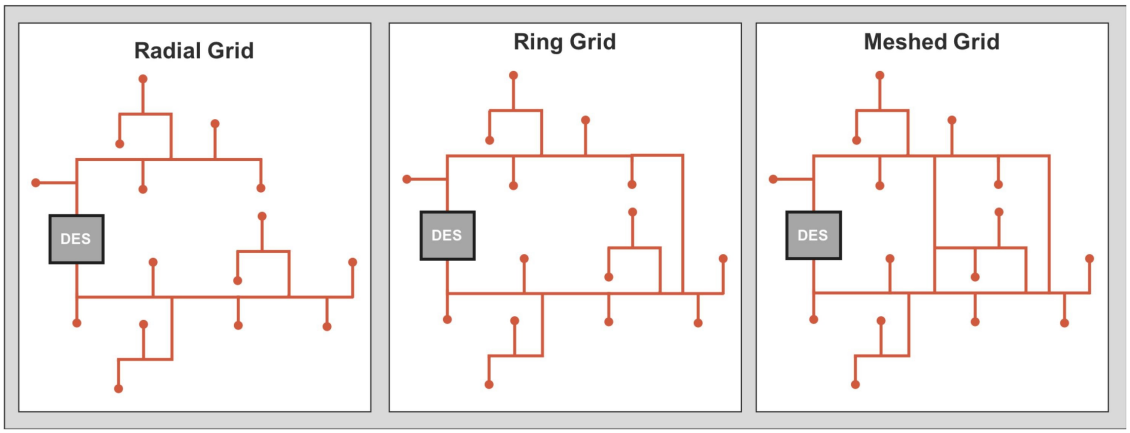

Figure 1.1: Schematic illustration of different types of thermal networks, courtesy of [3].

1.2.1 Advanced district thermal energy systems

In this work, the term "advanced" district thermal energy systems will be used to encompass fifth generation district heating and cooling systems, ambient loops, and other moderate-temperature district networks. The evolution of district thermal energy systems over their 140 years of existence has often been characterized in terms of generations (with most authors recognizing either four or five generations), with the defining feature being a progression from steam to hot water for heating, and to more moderate temperatures of water for both heating and cooling [4]. The diagram in Figure 1.3 illustrates this evolution conceptually. Note that different authors provide different characterizations of particular generations of district thermal energy systems. In this dissertation, consistency with the terms used by the original authors will be maintained.

The topology optimization framework is most relevant in the context of so-called "fifth generation district heating and cooling (5GDHC) systems." Per the work of [7], a 5GDHC system is

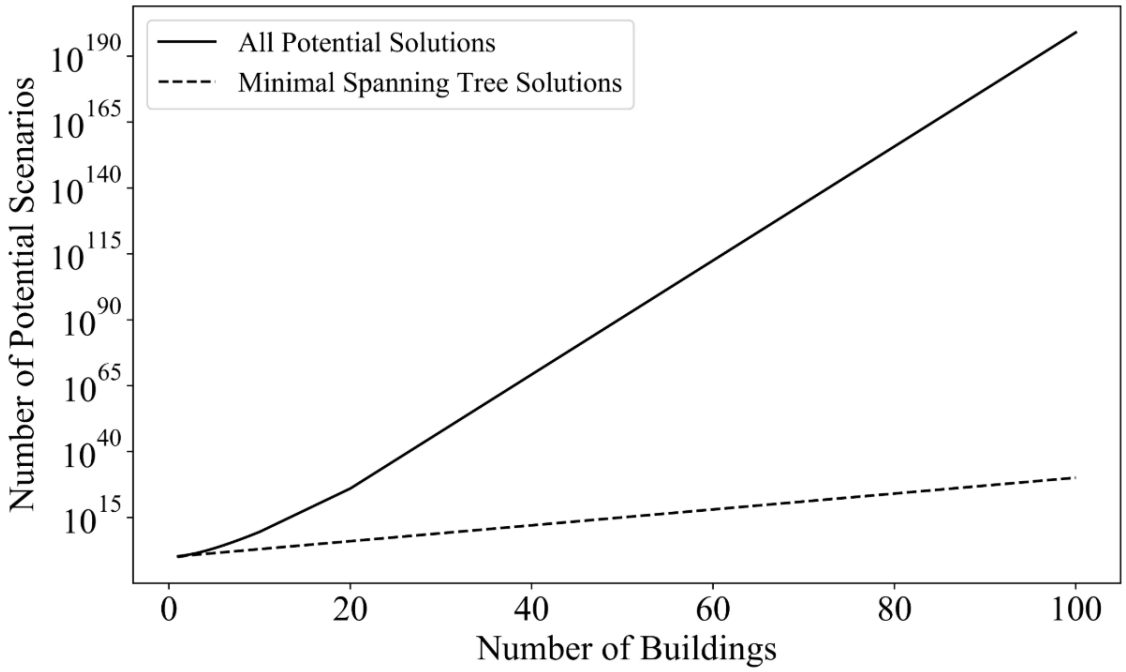

Figure 1.2: Comparison of topology optimization problem search space for all connected graphs vs. minimal spanning trees only, presented also in [6].

distinguished from earlier generations of district thermal energy systems by its use of water (or brine) as a working fluid, and the presence of water-source heat pumps at connected buildings, which use the network as a heat source or sink. The authors of [7] performed a survey of operating 5GDHC systems, and found that most had network temperatures in the range of 15-25°C. The moderate network temperatures require the use of water-source heat pumps to further temper the water to meet the thermal loads of connected buildings.

The work presented in this dissertation has focused on 5GDHC systems, in a two-pipe configuration with bi-directional mass flow and bi-directional thermal flow. In systems of this nature, each connected building is equipped with an energy transfer station (ETS), consisting of a water-source heat pump, heat exchanger, and a distribution pump. The heat pump in the ETS tempers the water further as required. Buildings are connected in parallel to the thermal network. Based on the building's load, the distribution pump draws water from either the system's "cool pipe" or "warm pipe." 5GDHC systems are conducive to the integration of waste heat sources, and of the

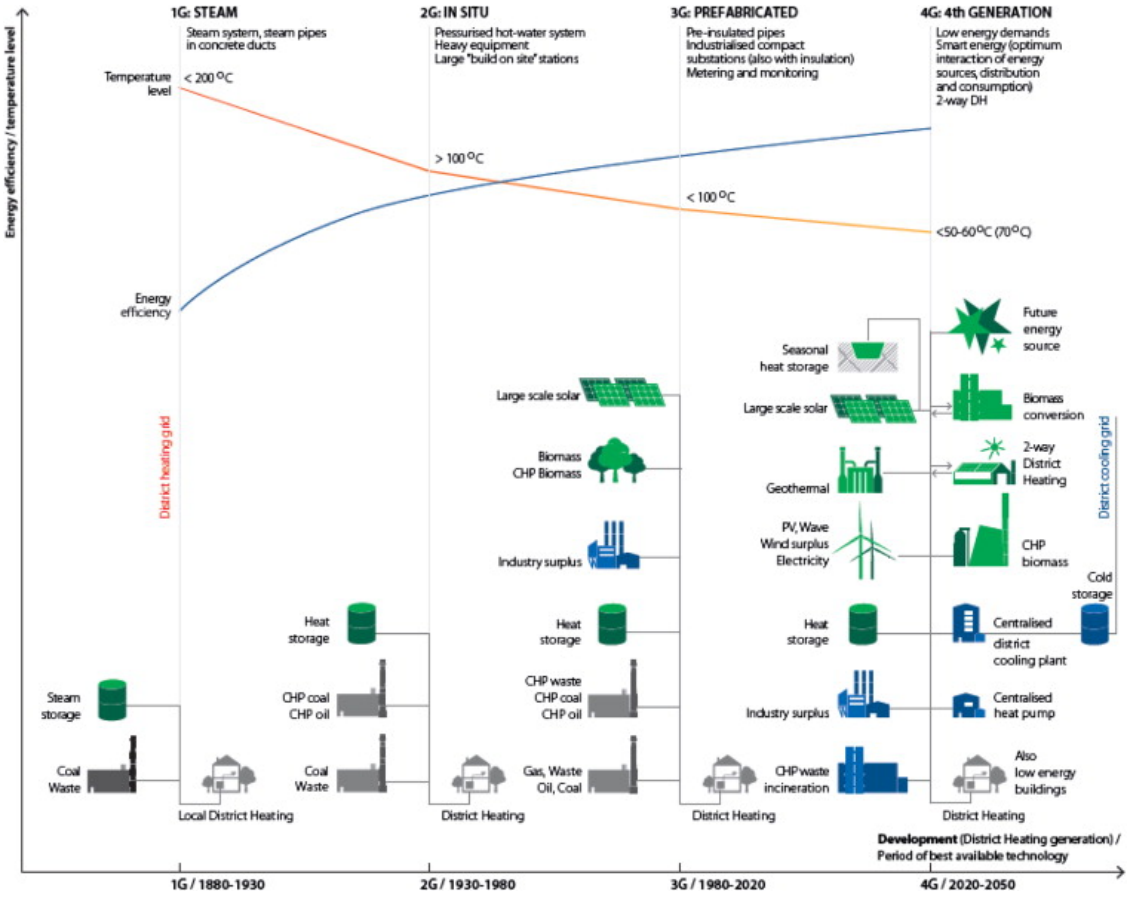

Figure 1.3: Conceptual diagram illustrating the evolution of district energy systems, courtesy of [4].

ability of individual buildings to serve as "prosumers", adding or rejecting heat from the network in a manner that can offset the heating or heat rejection required from centralized supply equipment, if the network topology is designed appropriately. Figure 1.4 shows a schematic illustration of a 5GDHC system with bi-directional thermal and mass flow. In Figure 1.4, $\dot{m}$ represents mass flow and $\dot{q}$ represents heat flow.

Numerous studies have investigated various aspects of advanced district thermal energy systems, including comparisons of these systems to distributed HVAC systems, and optimization of system parameters. The work of [4] identified factors that allow advanced systems to save energy and reduce carbon emissions relative to conventional district thermal energy systems. Moderate water temperatures facilitate the integration of waste heat sources (including through combined heat and power), and renewable heat sources, such as solar thermal and geothermal. Reduced supply temperatures in heating facilitate the use of heat pumps and condensing boilers, and warmer supply temperatures in cooling increase the potential for water-side economizing, reducing the energy intensity of the primary equipment. The use of electric heat pumps in place of natural gas-fired boilers is compatible with decarbonization of source energy. Moderate water temperatures also reduce heat losses and gains in the distribution system [4].

The emerging nature of 5GDHC systems, particularly in configurations with bi-directional mass flow, means that there remains a need for refinement to operational practices. Analysis of existing systems consisting of two-pipe networks by [8] and others has identified pump cavitation, caused by large pressure drops across loads, along with pressure control instabilities. The work of [9] investigated these problems through a simulation study, and concluded that they are a "fundamental property" of thermal energy systems with bi-directional mass flow and variable-speed pumping.

The lack of time scale separation between the responses of compressor speed, pump speed, and valves lead to pressure control instabilities in the system, which can subsequently cause flows to drop below minimum levels at the heat pumps, which can damage the equipment. The work of [9] evaluated an approach of controlling centralized pumps to achieve a zero pressure differential between the warm and cool pipes, and determined that this control approach was also likely to lead

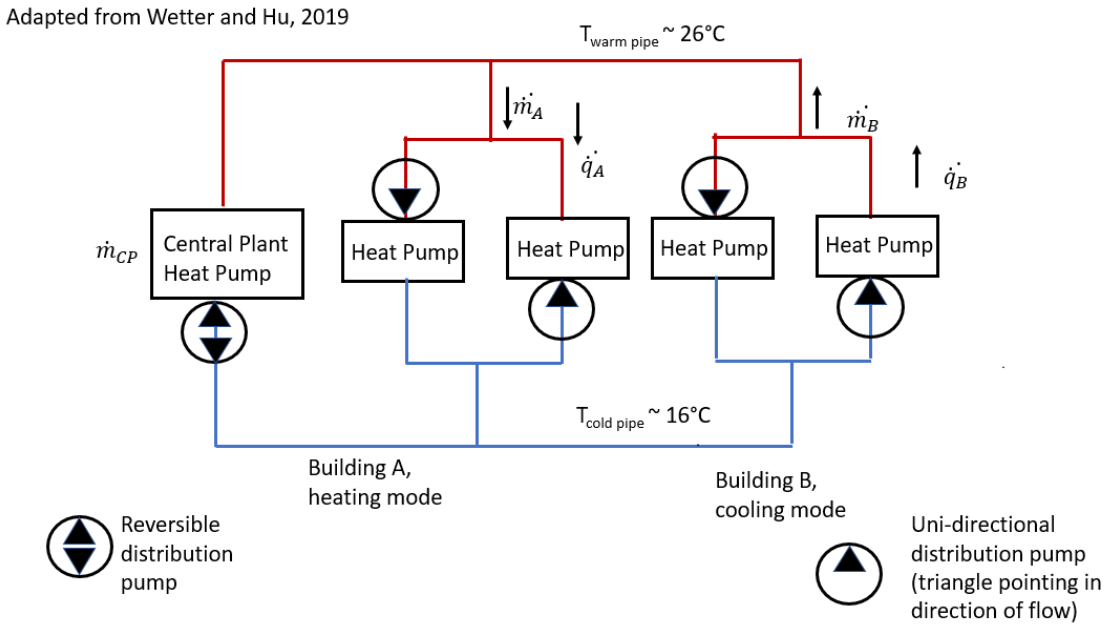

Figure 1.4: Schematic illustration of 5GDHC system with bi-directional thermal and mass flow.

to instabilities in practice. An alternative configuration that addresses the pressure control instabilities uses bypasses lines with dedicated pumps at each load and the central plant [9]. However, this configuration has a higher initial cost, and higher cost and complexity associated with future extensions, due to the need to potentially replace pumps on other bypass lines as additional loads are added. The work of [10] evaluated a potential solution to the pump cavitation problem, by dynamically changing the point in the network at which the expansion vessel is connected. However, shifting the location of the expansion vessel does not address the pressure control instabilities. A modeling analysis by [11] suggests that, at least in a network with a single "prosumer", appropriate pump control can mitigate pressure instabilities resulting from bi-directional flow. Their study leveraged data from an operating district heating system to develop detailed models to evaluate the effects of the integration of a waste heat source on pressure and temperature levels throughout the system. The waste heat source was co-located with a building that was served by the network for space heating. Their work found that use of variable-speed primary pumps, controlled to a pressure differential at the farthest substation, mitigated problems with pressure balance resulting from the injection of waste heat into the system.

As an alternative to two-pipe systems with bi-directional mass flow, [8] and [9] recommend one-pipe uni-directional systems, with each load connected in series. In this configuration, the inlet and outlet of each ETS is kept small, and thus the pressure drop across each load is minimal. Single-pipe uni-directional systems offer reduced complexity in operation, and reduced initial costs and reduced cost and complexity associated with expansion, but also result in greater exergy destruction, which may be significant when large waste heat sources are present. While uni-directional and bi-directional systems differ in their operating principles, it is expected that a similar approach to topology optimization can be applied to advanced district thermal energy systems generally. Both system types facilitate bi-directional thermal flow, and motivate consideration of topology optimization.

Past studies have also sought to characterize the conditions under which district energy systems are preferable to independent, building-level HVAC systems. The work of [12] determined

a metric based on minimum load diversity for characterizing when bi-directional 5GDHC systems under a given set of conditions would use less energy than the aggregation of individual building-level systems. Their study found that bi-directional 5GDHC systems were favorable relative to distributed systems if there were at least 1 unit of cooling energy per 5.7 units of simultaneous heating energy required, or vice versa. The work of [13] also identified "complementary energy use and local production patterns" (when distributed renewable thermal energy sources are considered) as a requirement for advanced district thermal energy systems to be cost-effective, specifically in the context of retrofits of conventional systems. The authors of [13] propose the concept of a "smart dual thermal network" as a retrofit of an existing district heating system to add the provision of cooling, and increase energy efficiency and the potential for use of renewable thermal energy. They define "smart dual thermal networks" as district thermal energy systems tied to a combined heat and power plant that circulate hot water and incorporate bi-directional thermal and mass flow, coupled with building-level absorption chillers and distributed solar thermal collectors. They performed a simulation study comparing the performance of the "smart dual thermal network" and two intermediate variations with a reference case in two climate zones. The intermediate variations consisted of "smart thermal networks" (incorporating bi-directional heat exchange, but not cooling) and "dual thermal networks" (performing heating and cooling but with uni-directional flow only). The authors of [13] found that, relative to a reference case district heating system with uni-directional flow, no solar thermal collectors, and compression-based cooling at the building level, the "smart dual thermal networks" resulted in significant (29%) operational cost savings in the climate of Madrid, Spain. They note that the use of distributed solar thermal collectors can increase the "aggregated demand flexibility" and ease a transition from other types of primary heating equipment to combined heat and power.

1.2.2 Topology optimization

The authors of [14] state that "topology optimization gives answers to the fundamental engineering question: how to place material within a prescribed design domain in order to obtain

the best structural performance?" More generally, topology optimization can be extended to any engineering design problem that involves making choices among multiple potential configurations, wherein all potential configurations satisfy basic functional requirements of the design but can be distinguished by their performance in other domains. Topology optimization has been applied to a variety of different design spaces, including structural elements, and design and distribution of electrical conductors in circuits.

In general terms, the cost function by which the optimum is determined in a topology optimization problem is expressed as a function of the material distribution, and could reflect material costs, compliance (in a structural context, inversely related to stiffness), parasitic resistance in an electrical circuit, or other parameters. The specific constraints of the topology optimization problem are domain-specific and can include limitations on physical size of a component, or requirements for connectivity of components in an electrical circuit. However, there are structures of these constraints that are common to topology optimization problems across different domains.

Solution approaches to topology optimization problems often discretize the volume into a large number of small volumes (known as a mesh), which increases the number of optimization variables. In structural applications, the finite element method is often applied to evaluate the objective function. One challenge in solving topology optimization problems is that the solutions can be mesh-dependent, or sensitive to the particular choice of discretization, which is not desirable. Additionally, discretization makes the problem computationally intensive to solve, and the large number of variables is often intractable with general nonlinear programming algorithms [15]. Early work in the realm of topology optimization applied to electrical conductors was performed by [16]. They applied topology optimization to the design of an electrically small conformal antenna, using the far-field radiated power at a single frequency as the objective function, with a volume constraint. The authors of [16] applied a discretization to the spatial domain of the antenna, and applied a threshold to evaluate intermediate values of the material's density and assign the presence or absence of material.

This binary nature of the optimization variable (representing the presence or absence of mate-

rial at a given point in space) makes the topology optimization problem non-convex, and challenging to solve. This difficulty can be addressed by replacing the binary variable with a continuous one, and adding a regularization term to the objective function to penalize intermediate values of the variable. One method for doing this is known as Solid Isotropic Material with Penalization (SIMP). Approaches like SIMP require a constraint on the overall volume of the component. Adopting a continuous variable allows for the use of gradient-based methods [17]. A challenge of approaches like SIMP is determining a value for the penalty term that has the intended effect. The work of [18] solved a topology optimization problem for design of a Hall effect thruster using the SIMP method for problem formulation and a branch-and-bound algorithm. In their formulation, the optimization variable was the distribution of ferromagnetic material. The authors of [18] used an interval branch-and-bound algorithm.

Topology optimization problems have also been solved with discrete mathematical programming methods on the dual space, such as by [17] for a structural application, in which compliance was minimized. Since compliance cannot be expressed explicitly in terms of the design variables, an approximation was used. The work of [17] imposed upper-bound constraints on the volume and perimeter. (The constraint on perimeter is intended to provide quality control of the solution.) They found dual methods to be well-suited to topology optimization problems because of the reduction in dimensionality provided. In this formulation of the problem, the binary variables are the only source of non-convexity. Due to the non-convex nature of the problem, there is not a guarantee of a zero duality gap; that is, there is not a guarantee that the solution of the dual problem will be the global optimum of the original (primal) problem. The authors of [17] bounded the duality gap for problems with a small number of constraints and a large number of optimization variables (characteristic attributes of topology optimization problems, when discretized) as being about 10^{-5} percent of the objective function. The bound on the duality gap means that the solution achieved by this method is sufficiently close to the global optimum.

1.2.3 Optimization of district energy systems

Topology optimization problems involving networks are distinct from topology optimization problems in the structural context. In network problems, the objective functions generally have more complex dependencies on the network than compliance or other structural properties do on material distribution. Among network problems, advanced district thermal energy systems rely on a more complex physical model than domestic water distribution networks, due to the relevance of thermal losses, and conventional district thermal energy systems, due to the presence of bi-directional thermal flow (even if mass flow is uni-directional). The more complex nature of the advanced district thermal energy system, compared with other types of engineering networks, affects the selection of an optimization approach. Some past work has addressed multiple aspects of thermal network operation by dividing an optimization problem into sub-problems. Optimization problems involving district thermal energy systems often involve non-convex objective functions, which past studies have addressed with genetic algorithms.

Numerous studies have addressed optimization of different aspects of district energy systems. This section will focus on work that addresses thermal energy, alone or in addition to electricity. Studies involving optimization of district energy systems differ in the representation of building loads, the nature of the objective functions, the optimization variables, and the optimization approaches. Past studies have addressed both design and operational optimization problems. The work discussed in this section treats building loads as deterministic. Past studies have addressed aspects of the network topologies, supply temperatures, and pipe diameters as the optimization variables, and life cycle costs, carbon emissions, and operating costs as the objective functions. Among studies using economic costs as the objective function, planning studies tend to use life cycle cost, and operational optimization studies, operating costs. Past studies also differ in the degree of realism reflected in the constraints.

Unit commitment problems for district heating systems have been addressed by [19], [20], and [21]. The work of [19] performed optimization for load allocation among multiple heating

plants in a district heating system to minimize operating cost. They treated network topology as an input and performed optimization over the supply and return temperatures and mass flow rate at each plant. The authors of [19] applied their model to a test case with a radial topology. They applied genetic algorithms to this problem, with a non-convex, and non-smooth, objective function. They used a quasi-steady state physical model, based on known building loads [19]. The work of [20] sought to minimize hourly operating costs for a combined heat and power district heating system, with natural gas and fuel oil boilers. The optimization variables included the order in which equipment was dispatched. They sought to maintain realistic constraints on operating conditions and realistic performance characteristics for steam boilers and gas turbines. The authors of [20] formulated the problem on a multi-period (multi-day) basis, accounting for start-up and shut-down costs for equipment. They formulated the problem using a mixed-integer nonlinear programming (MINLP) approach and compared the results from applying branch-and-bound, and genetic algorithms. Branch-and-bound was applied to a more tightly constrained version of the problem that did not consider continuity of operations for equipment. A focus of their work was on reduced computational time, to allow this optimization approach to be implemented for scheduling daily operations at real plants.

The work of [22] developed a framework for optimization of fourth generation district heating systems, sub-dividing the problem into unit commitment and economic dispatch. The unit commitment problem is discrete, with binary variables corresponding to the operating status of each unit. The authors of [22] formulated the unit commitment problem as a mixed integer quadratically constrained programming problem. They transformed the continuous economic dispatch problem into a non-linear programming problem through a discretization. The authors formulated the economic dispatch problem with minimization of the supply temperature as the objective function, but the approach is generalizable to other objectives. In the work of [22], the unit commitment problem is solved first, and the status of each unit at each timestep is then used as an input for the economic dispatch problem. In the sample cases to which [22] applied this method, individual building loads were aggregated to reduce the complexity of the network.

The work of [23] sought to optimize the supply temperature of an advanced district heating and cooling network to minimize energy consumption. They formulated the problem for a two-pipe system, with a fixed temperature differential between the two pipes. They used a simplex method (Nelder-Mead) to solve the optimization problem. Their study found energy savings on the order of 15% from implementing the optimal supply temperature in an example network, in comparison to allowing the temperatures to float freely between 12 °C and 20 °C. They found that the effect of implementing seasonal resets of the supply temperature was negligible. The authors implemented an agent-based control approach to maintain the loop temperature setpoint. They found that bi-directional near-ambient temperature networks saved energy relative to uni-directional networks in the two locations they analyzed.

The work of [24] and [25] addressed topology optimization for district thermal energy networks. The authors of [24] solved an optimization problem to minimize life cycle cost for the network topology (including location of the central plant) and pipe diameters for a low-temperature (55°C supply/ 25°C return) district heating network. They formulated a mixed-integer non-linear programming problem. The life cycle cost included costs associated with piping and pumping infrastructure, heat losses, pumping energy, maintenance, and a carbon tax. In the topology optimization problem, the optimization variables were the elements of the adjacency matrix representing the connectivity of the thermal network. The network topology was constrained to be a tree, and a connected graph, with twin pipes (supply and return pipes encased in the same conduit). Additionally, it was required that each building be connected to the district thermal energy network. The flow in each pipe was constrained to be uni-directional. The authors of [24] applied genetic algorithms to solve the optimization problem. Building loads were represented with an annual peak load, and a multiplier for each of eight periods dividing the year. The authors of [25] sought to optimize the topology configuration, pipe diameter, and operating parameters of a district heating network for minimal life cycle cost. Included in the life cycle cost were costs associated with infrastructure (primary plant equipment and piping) and energy use (for heat generation and distribution). Piping costs included material costs and trenching, and supply and return pipes

were not constrained to lie in the same trench. Operating parameters included supply and return temperatures for the network, and mass flow rates. Both parallel and series connections of buildings to the district network were considered, as well as the absence of a connection from a given building to the network. The primary application for series connections were buildings with lower temperature supply requirements. They formulated the problem in three sub-problems as a mixed-integer non-linear program, a mixed integer linear program, and a non-linear program. The authors of [25] performed analysis for steady-state conditions only. They considered several sample configurations of building locations and loads, and concluded that the optimal topology was highly context dependent, and not generalizable.

The work of [26] performed network topology optimization for a district heating and cooling system. The authors formulated the objective function as a life cycle cost based on the capital cost of piping and trenching and a limited set of operating costs (related to pumping energy, peak pumping power, and unwanted heat losses and gains through the network). Their study treated building loads and energy consumption by primary equipment as boundary conditions. The authors approached the optimization problem with mixed-integer linear programming. The authors applied their approach to several prototypical districts, and identified limited reductions in life cycle cost (of 0.5% to 1.3%) relative to that of networks designed to minimize capital cost only. However, the internal rate of return associated with the incremental capital investment required by the life cycle cost optimal network relative to the first-cost optimal network was as high as 15%, significantly higher than current borrowing rates for infrastructure. The authors of [26] identified an extension of their problem, in which the connection status of buildings would also be treated as an optimization variable, as an area in which further work was needed.

The work of [27] considered multi-objective optimization (for life cycle costs and carbon emissions) for district-level heating and electrical energy systems. The authors of [27] divided the optimization problem into sub-problems: selection of heating systems for each building (which could be tied to a district system, or independent), design of primary equipment (with energy storage included in the scope) and selection of efficiency measures at the building level, and operation

of primary equipment and energy storage units. They used detailed building load models, formulated with RC networks. The authors considered various topology configurations, but not meshed networks. Their solution process was iterative among the sub-problems and used Pareto fronts to evaluate the solutions. The authors of [27] initially applied heuristics to the first sub-problem, and evolutionary algorithms to the second sub-problem. They did not consider bi-directional flow of heat at the building level in this analysis. Instead of assigning weighting factors to the two objectives, in evaluating chromosomes in the evolutionary algorithms, [27] applied a non-dominated sorting-based algorithm. They applied constraints to the mutations to ensure validity of the resulting solutions. The work of [28] also performed multi-objective optimization, for life cycle cost and carbon emissions, for a district energy system. They sought to optimize the sizing and dispatch of primary equipment for a district energy system, comparing the results of the analysis performed separately for district heating and cooling systems, and for case in which the heating and cooling systems were coupled through the use of an absorption chiller. The authors found that the coupling of district heating and cooling systems resulted in the ability to achieve lower carbon emissions for a given life cycle cost. The authors of [28] formulated the optimization problem as a linear program, and used the epsilon-constrained method to construct a Pareto front. They represented the performance of the primary equipment considered with simplified models, calculating the associated carbon emissions based on a flat ratio of the heating or cooling load delivered by the unit of equipment.

1.2.4 Optimization of networks in other domains

Optimization problems have been also been studied extensively in the context of engineering networks other than district thermal energy systems. The work of [29] performed joint optimization of a water and power system, for minimal operational cost. The optimization variables included nodal voltages and power (active and reactive), mass flow rates, pressures (including pressure drops through valves), and pump speeds. The network considered included water storage tanks. Though valve positions were actuated through the optimization process, the network and loads (required

flow rates) were an input to the analysis. The water and power networks considered were coupled by the water distribution pumps. The authors of [29] formulated an MINLP and applied feasible point pursuit successive convex approximation, which provides stronger convergence claims than genetic algorithms. This approach involves reformulation of non-convex constraints as equivalent non-convex quadratic constraints. The authors implemented this approach in a distributed fashion, with a smaller optimization problem (consisting only of the variables associated with the given network) being solved for each network at each iteration. Information is then exchanged between the two networks regarding only the common variables.

The authors of [30] solved a joint design and optimization problem for a domestic water network within a high-rise residential building. The objective was to minimize the sum of first costs of the pipes and pumps, and the energy costs for the pump operation. The authors solved for the optimal piping layout, optimal diameter of each pipe, optimal pump placement, and optimal pump operating speed. The authors formulated the problem as an MINLP and applied a branch-and-bound approach. The relaxation used involved a linearization of the pump model. The physical model was formulated for steady-state conditions. The sub-problems in the branch-and-bound algorithm involved sub-trees of the network. This was used to create a lower bound on the value of the objective function, since any tree containing the given sub-tree would have a greater value of the objective function. The authors of [30] also considered an additional case with constraints regarding resiliency, characterized in terms of the maximum number of pumps that could fail while still supplying a given fraction of the demand.

1.3 Novelty of contribution

The key factors that distinguish this contribution from past work are its consideration of both the network topology selection and the choice of buildings to connect to the network, its analysis of bi-directional thermal and mass flow, and its consideration of a variety of potential topologies, with refined modeling of building load profiles and the thermal and hydronic operation of the network. The past work that is most relevant to this proposed contribution is that of [24], [27], [25], and

[26]. The combination of characteristics discussed in this section distinguishes this work from that of those authors.

The work of [24] and of [26] imposed a constraint that every building in the considered district be connected to the district energy network. The work of [25] did not constrain all buildings to be connected to the same primary thermal network, and considered the possibility of "isolated" supply equipment. However, [25] performed analysis for design conditions only. The work presented in this dissertation leveraged hourly building load profiles, and analyzed the performance of the hydronic network at one-hour time intervals. Bi-directional thermal flow and bi-directional mass flow influence the choice of optimal topology, and make the physical model more complex, and were not addressed by any of the four most relevant examples of past work. The work of [24], [25], and [27] considered networks supplying district heating only. The work of [26] considered a district energy system supplying heating and cooling, but with no coupling between the two systems. Additionally, the work of [27] and [24] considered only parallel connections of buildings to the thermal network. The work of [25] considered the possibility of series connections of buildings to the network. The work of [27] did not consider meshed networks, and [24] considered only tree networks. The work of [25] considered a wide range of topologies, but under design conditions only. The work of [26] also considered a wide range of network topologies, but treated the energy consumption of primary equipment and the thermal loads of connected buildings as boundary conditions. The work presented in this dissertation considered all potential network topologies, and accounted for the potential effects of variation in network supply temperatures on the HVAC energy use of connected buildings, and primary equipment. The consideration of additional topologies, and nuanced modeling of building loads, adds complexity to the problem, and enhances the value of the ultimate result.

The four most relevant pieces of past work analyzed networks supplying district heating only, or district heating and cooling systems of the third generation. The work presented in this dissertation introduces more complexity by analyzing an advanced district thermal energy system. Ambient loops and low-temperature district heating networks create more interesting opportunities

for optimization, by introducing more potential topologies, and the potential for bi-directional thermal and mass flow. The presented topology optimization framework is novel because it considers both the questions of which subset of buildings to connect (a need highlighted by [26]) and how they should be connected, is flexible to a variety of potential topologies, and considers bi-directional thermal and mass flow. The presented contribution has extended the work of [3] and [31] by leveraging tools developed by those authors (specifically the 5GDHCtat and ROM Framework, to be discussed in Chapter 2) to create a topology optimization framework for district thermal energy systems.

1.4 Objective

This research focused on developing a topology optimization framework to address the question, "For a given set of buildings, with known locations and loads, what is the optimal subset, if any, to connect to a district thermal energy system, and by what network should they be connected, to minimize life cycle cost?" The approaches implemented in the framework–particle swarm optimization and the minimal spanning tree heuristic–were validated in the context of this problem for 5GDHC systems. The framework was applied to a case study to quantify the potential benefits of network topology optimization for district thermal energy systems operating at near-ambient temperatures. While the topology optimization problem is of greatest relevance to 5GDHC systems, the framework is generally extensible to other types of district thermal energy systems.

1.5 Related tools

The topology optimization framework is introduced in the context of related modeling tools, including the URBANopt Advanced Analytics Platform and the OpenStudio Analysis Framework. URBANopt (Urban Renewable Building And Neighborhood optimization) is an analysis platform developed by the National Renewable Energy Laboratory (NREL) for modeling of thermal and electrical energy systems at the building and district level [32]. NREL has developed URBANopt as a software development kit (SDK), on top of which NREL's partners have built user interfaces. UR-

BANopt leverages existing modeling tools (EnergyPlus, Spawn of EnergyPlus, and OpenStudio) to model building-level thermal loads and energy use. The URBANopt District Energy Systems (DES) workflow permits users to programmatically generate models of district thermal energy systems in Modelica to evaluate energy consumption at the district level [33]. The topology optimization framework is being integrated with the URBANopt-DES modules.

The OpenStudio Analysis Framework (OSAF) is a platform for performing programmatic building energy analysis at scale, including optimization and parametric analysis [34]. The OSAF can be accessed through an application programming interface (API). Implementations of algorithms from the OSAF can be leveraged for integration of the topology optimization framework with URBANopt-DES.

1.6 Organization

This dissertation comprises several papers which describe the key elements of the underlying work, and additional chapters that further document the motivation and approach, and intersections between the developed topology optimization framework and relevant modeling tools.

Chapter 2 - Methods discusses in more detail the research questions that underlie this dissertation and the approach used to address each of them.

Chapter 3 - Evaluation of low-exergy HVAC systems and motivation for topology optimization presents a study comparing the energy performance of an fifth-generation district thermal energy system with that of a third-generation system in the context of a prototypical urban district, and the initial validation of the minimal spanning tree heuristic for the network topology optimization problem. The study investigates in depth the factors contributing to the reduced source energy use intensity of a fifth-generation district thermal energy system, relative to an earlier generation system.

Chapter 4 - Evaluation of the minimal spanning tree heuristic for the topology optimization problem presents two studies in which further validation of the minimal spanning tree heuristic is performed, in the context of prototypical urban districts. An exhaustive search is

performed for a prototypical district, in which all possible network configuration scenarios (more than 30,000) are evaluated, and it is confirmed that the minimal spanning tree network consistently minimizes life cycle cost relative to other networks connecting a given subset of buildings.

Chapter 5 - Validation of particle swarm optimization for the network topology optimization problem presents results validating the effectiveness of the particle swarm optimization algorithm as implemented in the topology optimization framework and a comparison of different approaches for incorporating constraints into the problem.

Chapter 6 - Development of the topology optimization framework provides a more detailed discussion of the implementation of the topology optimization framework in Python and the inputs needed to configure the analysis. This chapter also presents how the framework will be integrated with NREL's URBANopt platform and OpenStudio Analysis Framework.

Chapter 7 - Demonstration of the topology optimization framework presents results from the application of the topology optimization framework to a larger prototypical urban district (consisting of seven buildings). The potential benefits of a fifth-generation district thermal energy system in that context are quantified, and the barriers to their adoption are discussed.

Chapter 8 - Conclusion and future work presents conclusions regarding the potential benefits of topology optimization and how it can address barriers to adoption of fifth generation district thermal energy systems, as well as areas for further development of the framework.

Chapter 2

Methods

The research questions that underlie this dissertation were addressed through five main steps: evaluation of the energy performance of low-exergy HVAC systems, evaluation of the minimal spanning tree heuristic, evaluation of particle swarm optimization, development of the topology optimization framework, and demonstration of the framework with a case study. The first step motivates the focus on advanced district thermal energy systems, and the relevance of the network topology optimization problem. The second and third steps were required to select the approaches to be implemented in the topology optimization framework. The fourth step constituted the construction of the framework itself, which is a desired outcome of the work. The fifth step demonstrates the value and relevance of the topology optimization framework. In the following subsections, the motivation for performing each of these steps, and the approach for doing so, is discussed.

2.1 Evaluation of the energy performance of low-exergy HVAC systems

As part of this work, the energy performance of low-exergy HVAC systems, at the building and district levels, was evaluated, and compared with that of "conventional" hydronic HVAC systems, operating at high temperatures in heating and low temperatures in cooling.

2.1.1 Problem description and approach

The work presented in this dissertation is motivated by the need to reduce carbon emissions associated with conditioning buildings. As such, it was necessary to evaluate the energy performance of the HVAC systems that are the focus of the topology optimization framework developed and define the conditions to which they are well-suited. This was done through energy simulation of a prototypical urban district.

To compare the energy performance of "conventional" and "low-exergy" HVAC systems, a prototypical district of residential buildings was constructed using the multi-family residential building model in EnergyPlus format from the US DOE Prototype Buildings [35]. The Prototype Buildings are intended to represent the characteristics of common commercial and multi-family housing buildings in the US. The source energy consumption was compared for two versions of the district: one with radiant hydronic systems at the building level, using warm water supplied at 45 °C and cool water supplied at 16 °C, and one with typical water-to-air systems at the building level, with hydronic coils leveraging hot water at 82 °C and chilled water at 7 °C. In both cases, the building-level hydronic systems were served by a district thermal energy system.

The two versions of the district were identical in all respects but the HVAC systems. The prototypical district was populated with ten versions of the same underlying building model, with certain parameters varied in order to create a realistic thermal load profile for the district energy system, and to reflect the stochastic nature of occupant behavior. The internal load density, occupant density, window-to-wall ratio, infiltration rate, and occupancy and internal load schedules were the varied parameters, and the parameter values for each building were determined through sampling from probability distributions.

To ensure a fair comparison between the two HVAC system types, each of the two system types were controlled at the building level so that they achieved as similar as possible a trajectory of operative temperatures in each space. Operative temperature is calculated as an average of the mean radiant temperatures of the surfaces in a thermal zone and the air temperature, and

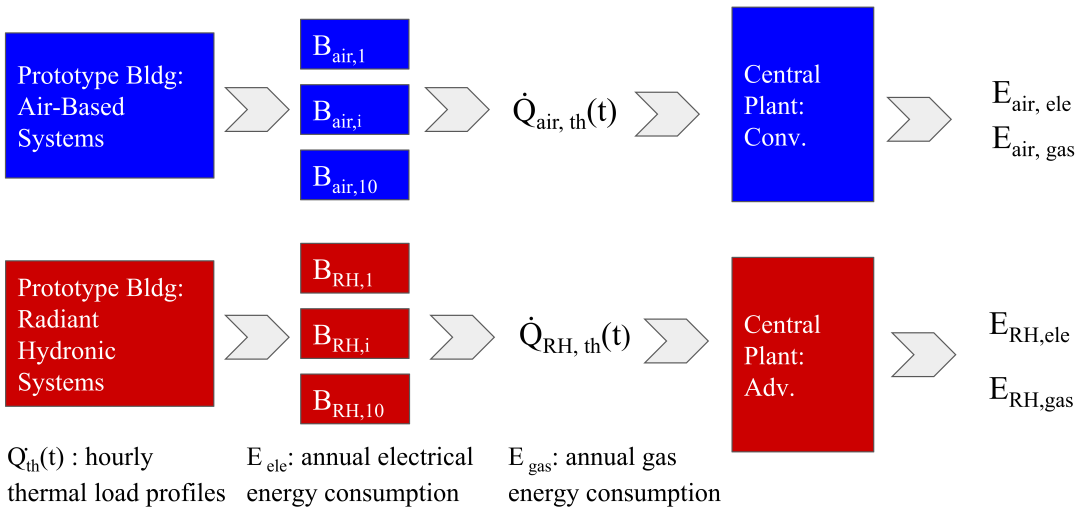

Figure 2.1: Schematic illustration of system comparison.

is an important parameter in human thermal comfort. Thermal comfort is the primary "service" provided by space conditioning systems, and this approach ensured that the energy comparison was being made for HVAC systems providing the same level of service.

A model of the building loads was used to generate the district thermal load profile, which was separately applied to a central plant model. The process by which this was performed is illustrated in Figure 2.1. EnergyPlus does not currently facilitate modeling the interactions between connected loads and a district energy system in a single model, and a limitation of this two-step approach is that it assumes that the district thermal energy system is able to meet the building loads perfectly at each timestep. This approach was refined in the energy modeling that was used to validate elements of the Topology Optimization Framework. The evaluation of the energy performance of low-exergy HVAC systems is discussed in detail in Chapter 3.

2.2 Evaluation of the minimal spanning tree heuristic

The performance of the minimal spanning tree (MST) heuristic was evaluated in order to assess its inclusion in the Topology Optimization Framework.

2.2.1 Problem description and approach

Conceptually, the MST heuristic showed promise as a means of selecting the optimal thermal network by which to connect a given subset of buildings. Its performance was evaluated in the context of a prototypical district, to determine if it should be leveraged by the Topology Optimization Framework.

As shown in Figure 1.2, the "search space" of potential thermal network configurations grows factorially as a function of the number of connected buildings. A district of five buildings creates a search space of 30,770 potential network configurations. This was deemed to be sufficient to evaluate the performance of the MST heuristic through an exhaustive search — evaluating the life cycle cost of all potential network configurations, and determining if, in fact, the MST network provided the least-cost configuration for all thirty-two potential sets of connected buildings.

The heuristic was evaluated in the context of a district thermal energy system operating at near-ambient temperatures, which create the greatest potential for network topology optimization. The prototypical district was constructed such that it was a realistic facsimile of one that would be considered a candidate for district thermal energy systems in terms of its loads. The US DOE Prototype building models were again used to generate the load profiles, and the building types were selected such that, in combination, they provided a favorable value of a thermal load diversity metric that has been proposed by [12] as a threshold for the level at which ambient-temperature district energy systems will operate at a higher exergetic efficiency than building-level HVAC systems. Based on this metric, a district consisting of three multi-family buildings, a retail building, and a hospital were selected.

The HVAC energy use at each building, in both its "connected" and "independent" states (cases in which it was tied to the district thermal energy system or had independent building-level HVAC systems, respectively) was represented with data-driven metamodels that were trained on a data set generated from a parameter sweep over the prototype building models in EnergyPlus format, using the Metamodeling Framework developed by [31]. In the "connected" case, the sup-

ply water temperature from the district system is one of covariates in the reduced order models, ensuring that the building-level HVAC energy use reflects effects from any deviations in network supply temperature. The use of the metamodels structured in this way facilitates accounting for interactions between the building-level energy use and the network conditions, without the computational intensity of a full coupling. The performance of the metamodels in predicting building level HVAC energy use was validated in [31].

The energy consumption of the district thermal energy system was evaluated using an energy model in Modelica, extended from one created by [3]. Modelica is an object-oriented, equation-based language that is commonly used for modeling physical systems [36]. Modelica facilitates modeling of pressure-driven flow and bi-directional mass flow in a hydronic distribution network. The model from which this one was extended was validated in terms of its performance in predicting temperatures at network nodes using data from experiments conducted at EURAC [3]. The evaluation of the minimal spanning tree heuristic is discussed in detail in Chapter 4.

To evaluate the performance of the MST heuristic, the objective function of life cycle cost was evaluated for each potential network configuration of the five-building prototypical district described. For each potential subset of buildings (thirty-two, including the "null case" in which all buildings are served by independent systems), the life cycle cost associated with the corresponding MST network was compared to that of the other possible networks, to determine if it did, in fact, offer the optimal configuration.

2.3 Evaluation of particle swarm optimization

The performance of a particle swarm optimization (PSO) algorithm was evaluated to determine if it should be implemented in the Topology Optimization Framework.

2.3.1 Problem description and approach

PSO is a meta-heuristic optimization algorithm that can be applied to continuous, non-convex functions, and was originally developed by [37]. As such, it is compatible with the use of a "black-

box" function evaluator, since it does not require an explicit definition of the objective function or its derivative. PSO does not provide a guarantee of convergence at a global optimum, but past work has shown that relative to other meta-heuristic approaches, PSO has a lower risk of getting "stuck" at a local minimum [37]. Based on these attributes, the PSO algorithm was a promising candidate for integration in the Topology Optimization Framework. Its performance was evaluated to determine if it should be incorporated in the framework.

The performance of a PSO algorithm in identifying the optimal subset of buildings to connect to a DES, as well as the network by which they should be connected, was compared with the results of the exhaustive search described in Section 2.2. The data set derived from the exhaustive search was extended using post-processing by varying high-level parameters in the life cycle cost function, with six different sets of values, to enhance the robustness of the evaluation. This approach leveraged the work of [38] in developing a post-processing framework for the dataset.

Conceptually, as part of the PSO algorithm, candidate solutions are represented by "particles", which traverse a search space, with each particle retaining knowledge of both its previous "best" location with respect to the objective function, and the best prior location visited by the "swarm" as a whole. The network of other particles with which a given particle can communicate this knowledge is known as a *neighborhood*. When this neighborhood is smaller in size than the swarm as a whole, the approach is known as *lbest.* When each particle can share knowledge with the entire swarm, the approach is known as *gbest.* Past studies have concluded that the relative performance of *lbest* and *gbest* is generally problem-dependent, and thus both approaches were initially evaluated for this problem. It was concluded that *lbest* was preferable in this case. An implementation of PSO for binary-valued variables was selected for the full evaluation [39]. Values of hyperparameters were selected based on recommendations in the literature.

The post-processing framework to be documented in [38] was used to select six sets of parameter values, each one corresponding to a different optimal level of network connectivity in terms of the number of loads served by the DES. The electricity and natural gas rates, unit cost of piping and trenching, and carbon intensity of electricity were the considered parameters. The ranges of

the utility rates and maximum carbon intensity of electricity were selected based on historic values in the mainland U.S., and a lower limit of zero was selected for carbon intensity of electricity, corresponding to a 100% renewable electricity supply. The range of unit costs for piping and trenching were selected based on a literature review. Thus, each of these six sets of scenarios corresponds to a reasonably likely set of conditions that could exist or occur in the US now or in the future. The performance of the PSO algorithm was evaluated under each of these sets of conditions. For each set of conditions, the optimal solution returned by the algorithm after a fixed number of iterations was compared with the "ground truth" value, consistent with the approach taken by [40] and others. The evaluation of particle swarm optimization is discussed in detail in Chapter 5.

2.4 Development of the Topology Optimization Framework

The focus of the work presented in this dissertation is the development of the Topology Optimization Framework. The framework is intended to answer the question, for an urban district with known building locations and loads, "What is the optimal subset of buildings, if any, to connect to a district thermal energy system, and by what network should they be connected, to minimize life cycle cost?"

2.4.1 Problem description and approach

The Topology Optimization Framework is intended to be flexible to a variety of district thermal energy systems, and extensible to different cost functions. The framework was assembled in the form of Python scripts. The evaluation of the cost function is based on the simulation of an energy model representing the district thermal energy system and all buildings in the considered district, in FMU format.

At each iteration, a PSO algorithm, implemented using the PySwarms Python package, is used to generate a "swarm" of candidate solutions, in the form of binary vectors corresponding to the connectivity status of each building and the centralized heat pump [41]. Evaluation of the "swarm" (20 particles) at each iteration is executed in parallel. Each candidate solution is checked

for validity (that the centralized heat pump is connected to the network if any loads are), and valid solutions are then evaluated, through modifying the FMU energy model accordingly, and then simulating it. (Invalid solutions are penalized with a high value of the cost function.) The PyFMI Python package is used to modify and simulate the FMU. The cost function value is calculated based on results from the energy model simulation, and parameters that can be modified by the user. The algorithm continues until it reaches a convergence or termination criterion. A schematic illustration of the workflow of the framework is shown in Figure 2.2. The development of the Topology Optimization Framework is discussed in detail in Chapter 6.

2.5 Demonstration of the Topology Optimization Framework

The performance of the Topology Optimization Framework was demonstrated with a case study, which was also used to quantify the potential benefits of network topology optimization in the context of 5GDHC systems.

2.5.1 Problem description and approach

Quantification of the potential benefits of network topology optimization is important in illustrating the value of the presented Topology Optimization Framework. The framework was applied to a prototypical new-construction district as a case study.

A prototypical new-construction district of seven buildings situated on a university campus was created, using the US DOE Prototype Building models [35]. The building types (three multi-family buildings, three offices, and a restaurant) were selected such that the thermal load density of the district would make it a viable candidate for an ambient-temperature district thermal energy system, based on metrics that have been proposed for previous generations of district thermal energy systems, and operating examples of ambient-temperature systems. Thus, this prototypical district served as a valid "test case" for assessing the value of network topology optimization in this context. An energy model representing the district thermal energy system was extended from the one used for the exhaustive search analysis described in Sub-section 2.2. The framework was

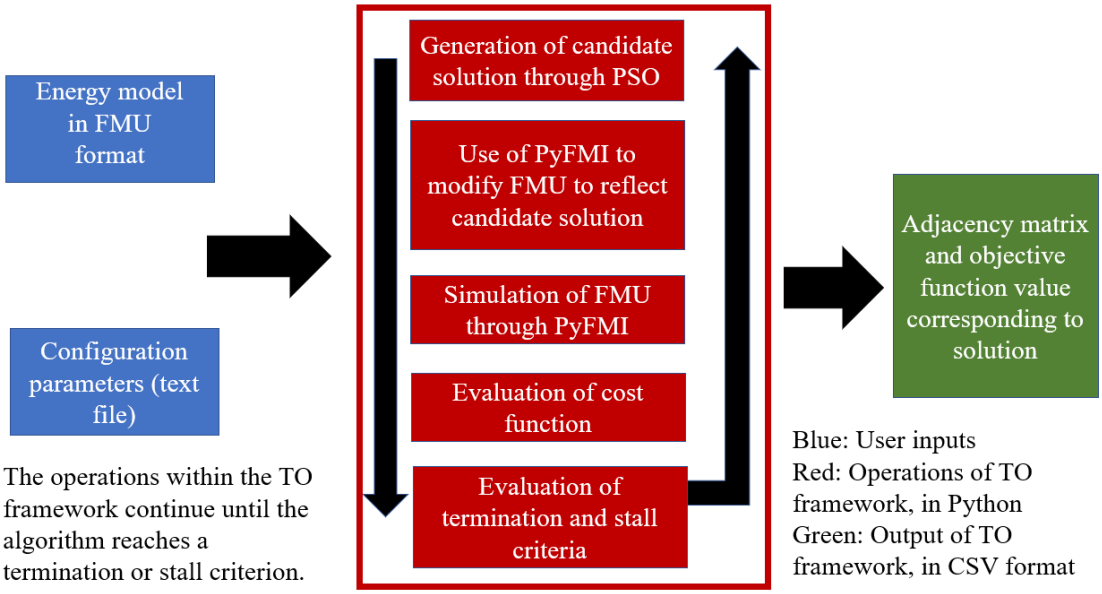

Figure 2.2: Schematic illustration of workflow of the Topology Optimization Framework.

applied to the prototypical district, and the optimal solutions that it determined were compared to four base cases, each of which entailed the connection of all buildings in the district to the DES, with varying network configurations.

The comparison of the optimal solutions to the base case designs, which reflected common heuristics, in terms of life cycle cost, carbon emissions, and source energy use intensity, provided a means of quantifying the benefits of network topology optimization. The results also revealed insights about the economic and policy conditions that would be necessary for ambient-temperature district thermal energy systems to be favorable on a life-cycle cost basis relative to building-level systems. The presented framework is distinct from existing contributions in that it provides a flexible interface to network topology optimization for district thermal energy systems, leveraging validated techniques. The demonstration of the topology optimization framework is discussed in detail in Chapter 7.

Chapter 3

Evaluation of low-exergy building HVAC systems and motivation for topology optimization

This chapter has been published as:

A. Allen, G. Henze, K. Baker, and G. Pavlak, Evaluation of low-exergy heating and cooling systems and topology optimization for deep energy savings at the urban district level.
Energy Conversion and Management, vol. 222, p. 113106, 2020.

3.1 Abstract

District energy systems have the potential to achieve deep energy savings by leveraging the density and diversity of loads in urban districts. However, planning and adoption of district thermal energy systems is hindered by the analytical burden and high infrastructure costs. It is hypothesized that network topology optimization would enable wider adoption of advanced (ambient temperature) district thermal energy systems, resulting in energy savings. In this study, energy modeling is used to compare the energy performance of "conventional" and "advanced" district thermal energy systems at the urban district level, and a partial exhaustive search is used to evaluate a heuristic for the topology optimization problem. For the prototypical district considered, advanced district thermal energy systems mated with low-exergy building heating and cooling systems achieved a source energy use intensity that was 49% lower than that of conventional systems. The minimal spanning tree heuristic was demonstrated to be effective for the network topology optimization problem in the context of a prototypical district, and contributes to mitigating the problem's computational complexity. The work presented in this paper demonstrates the potential of advanced district thermal energy systems to achieve deep energy savings, and advances to addressing barriers to their adoption through topology optimization.

3.2 Introduction

Governing bodies worldwide have recognized the importance of reducing carbon emissions. Beneficial electrification of energy end uses, in conjunction with decarbonization of electricity generation, is widely recognized as a critical strategy to accomplish this goal [42]. Electrification of transportation has made promising strides in this direction, but space heating and cooling pose greater challenges. In 2016, the European Union introduced a Heating and Cooling Strategy which seeks to promote decarbonization of space heating and cooling, and greater utilization of industrial waste heat [43]. In this context, the potential of low-exergy heating, ventilation and air-conditioning (HVAC) systems, which are compatible with electrically-driven primary heating and cooling equip-

ment, and the beneficial use of waste heat, is demonstrated as a strategy to accomplish electrification of space heating and cooling. However, these systems require district thermal energy networks, which are expensive to build and difficult to screen for cost-effectiveness. Expansion of the use of district thermal energy systems in the context of increased penetration of renewable electricity generation will require new analysis tools capable of addressing integrated thermal and electrical systems [44]. Specifically, selecting the best network topology for a district thermal energy system is a key challenge, in both retrofits and new construction. A topology optimization framework is proposed to address this problem.

The work presented in this paper is part of a larger effort to develop a framework for topology optimization of district thermal energy systems, which seeks to answer the questions, for a given urban district, "Which subset of buildings, if any, are most advantageous to connect to a district thermal energy system, and by what network topology should they be connected, in order to minimize life cycle cost?" The work presented in this paper demonstrates the potential of advanced district thermal energy systems to achieve deep energy savings, and steps to addressing barriers to their adoption through network topology optimization. This paper presents results from a comparison of "conventional" and "advanced" district thermal energy systems at the level of a low-energy urban district, and an evaluation of a heuristic for part of the topology optimization problem.

3.2.1 Advanced district thermal energy systems

In this work, the term "advanced" district thermal energy systems will be used to encompass fifth generation district heating and cooling systems, ambient loops, and other moderate-temperature district networks. The evolution of district thermal energy systems over their 140 years of existence has often been characterized in terms of generations (with most authors recognizing either four or five generations), with the defining feature being a progression from steam to hot water for heating, and to more moderate temperatures of water for both heating and cooling [4].

The work of [45] introduced the concept of "deep energy savings" in the context of design strategies that address interactive effects among multiple building systems to achieve significant reductions in energy use. In this work, the concept of deep energy savings is extended to systems implemented at the urban district level. Advanced district thermal energy systems have the potential to achieve deep energy savings by leveraging the density and diversity of loads in urban districts [32]. An analysis found that wide-scale expansion of district heating, in conjunction with building energy efficiency, would allow the European Union to achieve its target for reducing carbon emissions 80% from 1990 levels by 2050, at a 15% lower cost than through energy efficiency strategies at the individual building level alone [46]. The work of [4] identified factors that allow advanced systems to save energy and reduce carbon emissions relative to conventional district thermal energy systems. Moderate water temperatures facilitate the integration of waste heat sources (including through combined heat and power), and renewable heat sources, such as solar thermal and geothermal. Reduced supply temperatures in heating facilitate the use of heat pumps and condensing boilers, and warmer supply temperatures in cooling increase the potential for water-side economizing, reducing the energy intensity of the primary equipment. The use of electric heat pumps in place of natural gas-fired boilers is compatible with decarbonization of source energy and a transition to 100% renewable energy [44]. Moderate water temperatures also reduce undesired heat losses and gains in the distribution system [4]. Advanced district thermal energy systems can also be leveraged for beneficial grid interactivity, such as through the use of "excess" renewable electric generation to charge thermal energy storage [47].

This work will focus on so-called "fifth generation district heating and cooling (5GDHC) systems." The work of [7] defines a 5GDHC system as a thermal energy network circulating water or brine that leverages water source heat pumps to temper the supply fluid at the connected loads. A study of operating 5GDHC systems found that most had network temperatures in the range of 15-25°C [7]. In the analysis of the topology optimization problem in this study, a 5GDHC system with a two-pipe configuration, permitting bidirectional thermal and mass flow, is considered, with buildings connected in parallel to the thermal network. Each connected building is equipped with

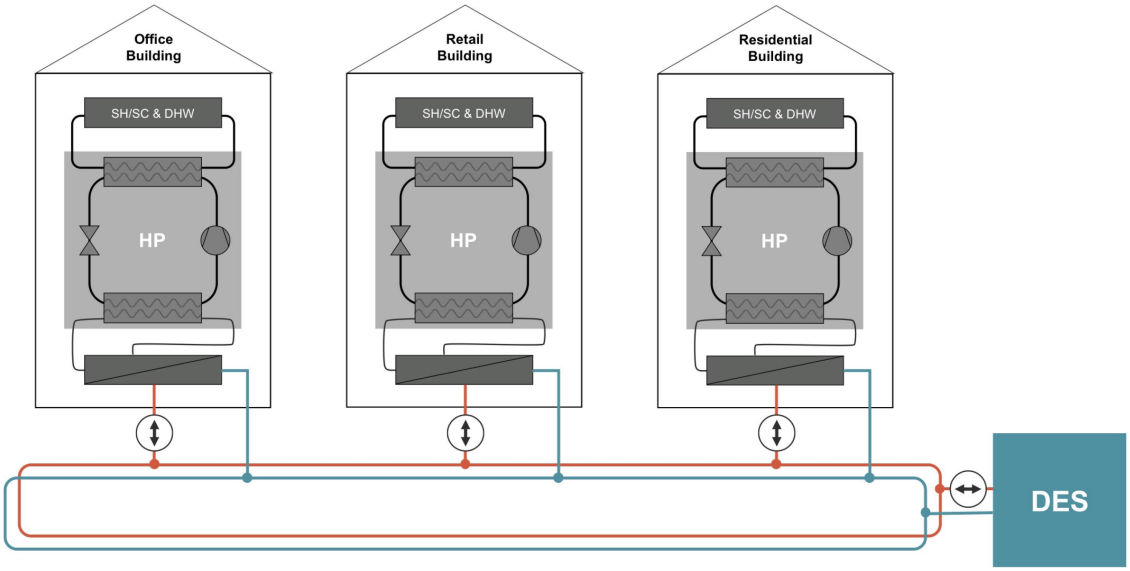

Figure 3.1: Schematic representation of 5GDHC system, courtesy of [3].

an energy transfer station (ETS), consisting of a heat pump, a heat exchanger, and a distribution pump. The heat pump in the ETS will temper the water from the district energy network as required for the building's load. Based on the building's load, the distribution pump or pumps will draw water either from the system's "cool pipe" or "warm pipe." A schematic representation of this system is shown in Figure 3.1.

3.2.2 Low-exergy building systems

The benefits of the use of more moderate water temperatures by advanced district thermal energy systems can be characterized in terms of their lower exergy requirements compared with conventional district thermal energy systems. The concept of exergy combines the first and second laws of thermodynamics, and refers to the maximum work obtained if a system is brought into thermodynamic equilibrium with its environment [48]. Analysis on the basis of exergy facilitates direct comparison of different types of energy flows [12]. To maximize the exergetic efficiency, advanced district thermal energy systems must be paired with low-exergy HVAC systems at the building level, of which radiant hydronic HVAC systems are one example [49]. Low-exergy hydronic HVAC systems are characterized by lower temperature differentials between both supply water temper-

atures and outdoor air temperatures, and supply water temperatures and zone air temperatures, which allow for lower-lift operation of chillers and heat pumps and reduce distribution losses [12]. The flow exergy associated with meeting a heating or cooling load can be calculated as a function of the supply temperatures of the working fluid, the rate of heat transfer to the zone, and the ambient temperature [12]. Note that for purposes of this analysis, since average site-to-source energy conversion factors for electricity and natural gas are readily available for the US, the comparison between the two HVAC system types is performed on the basis of source and site energy, instead of exergy itself.

Radiant heating and cooling systems transfer and reject heat to a conditioned space through both radiation and convection. Specifically, radiant heating and cooling systems have been defined as HVAC systems that transfer more than 50% of their total heat flux by thermal radiation [50]. In this work, radiant hydronic thermo-active building systems (TABS), specifically, hydronic coils embedded in concrete slab floors, will be analyzed. These types of systems are considered "thermo-active" because building components, in this case, mass floors, are charged and discharged with thermal energy, which is then transferred to (or absorbed from) the conditioned space through convection and radiation [49]. Radiative transfer with the active heated and cooled surface can increase the differential between inside and outside surface temperatures for the non-activated zone surfaces [51]. A high-performance building envelope mitigates this effect and minimizes an increase in conductive heat transfer for the non-activated surfaces, making low-exergy HVAC systems particularly well suited to buildings with high-performance envelope designs and limited cooling load densities, such as those considered in this study. Due to their different operating mechanisms, load profiles differing in both timing and magnitude would be observed on radiant hydronic and air-based HVAC systems conditioning the same space and different metrics are used to assess their performance [52]. In assessing energy performance of radiant hydronic systems, it is important to consider heat transfer at both the surface level and the hydronic loop level. Due to the thermal mass inherent in TABS, the peak rate of surface heat removal or addition is expected to be different from the peak rate of heat removal or addition to the hydronic loop [52]. In sizing radiant hydronic

systems, the peak loads imposed on the hydronic loop are generally the relevant parameter [52]. Several studies analyzing radiant hydronic systems at the building level have found the peak cooling loads observed by radiant systems to be higher than those observed by air-based systems [53]. In a simulation study of air-based and radiant hydronic HVAC systems in the form of TABS, in which ventilation and latent loads were not considered, the peak surface cooling rate was found to be 23% to 84% higher, and the peak hydronic cooling rate, 33% to 70% higher, than the peak cooling loads for an air-based system. The wide variation reflects variation in several parameters, including solar heat gain, level of envelope thermal insulation, radiative/convective split associated with internal gains, and orientation of the radiant surface (ceiling or floor) [52]. Another comparison study of air-based and radiant hydronic HVAC systems, in which the radiant systems were coupled with an air system to supply ventilation air, found comparable peak cooling loads between the two system types, with the radiant system having a higher annual cumulative cooling load. The higher annual cooling load for the radiant system was attributed to a higher level of thermal comfort in cooling mode being provided [49].

Radiant hydronic and air-based HVAC systems are generally controlled by different mechanisms, making a direct comparison of the two system types challenging [51]. Due to their thermal inertia, TABS cannot respond quickly to changes in load or setpoint [49]. Air-based HVAC systems are generally controlled to air temperature, and in practice, radiant hydronic HVAC systems can be controlled based on surface temperature, water temperature, or other parameters [51]. Controlling the radiant system to operative temperature and controlling the air-based system to the sequence of operative temperatures that results in the space conditioned by the radiant system, is one approach that has been used in other simulation studies comparing the two system types [52]. Operative temperature is defined as the average of the mean radiant temperature of the zone surfaces and the air temperature and is a key factor in influencing human thermal comfort [49]. Through their use of heated or cooled surfaces, radiant HVAC systems can achieve a comparable level of thermal comfort to air-based systems at lower air temperatures in heating, and higher air temperatures in cooling [53].

3.2.3 District-scale energy analysis

In performing energy simulation of urban districts, to avoid modeling each building individually, archetypal buildings are often selected to represent either specific existing buildings, or typical buildings of the type that are to be represented [54]. However, archetype-based models tend to perform more poorly at a finer time resolution, such as in capturing the district's hourly load profile [54]. Whether existing buildings or hypothetical ones are being modeled, realistic hourly load profiles are key to the meaningful analysis of district thermal energy systems, due to the nonlinear nature of the performance curves of primary equipment such as chillers, boilers, and heat pumps. One factor contributing to the deficiency of many archetype models in predicting energy use at a short time resolution is a reliance on deterministic values of modeling parameters, which fail to capture the wide degree of variation in the actual values of those parameters, even among buildings with similar characteristics [55].

Parameters related to occupant behavior, including schedules for occupancy and lighting and plug loads, have some of the highest levels of uncertainty and are also key drivers of energy use in residential buildings [55]. The work of [56] developed methods for Bayesian calibration of normative energy models in the context of large-scale retrofits, and used the Morris method for parameter screening. The authors identified lighting and plug load densities as highly influential parameters. In [57], a sensitivity analysis was performed for building heating and cooling energy end-uses specifically, considering occupancy and load densities, material properties, and design considerations such as window-to-wall ratio. The authors identified infiltration rate as being one of the most influential parameters. To address these sources of uncertainty, past studies have attached probability distributions to uncertain input parameters, and generated distributions of expected building energy use. This approach is also generally extensible to representing energy use of districts, with individual buildings being assigned parameter values through probability distributions.

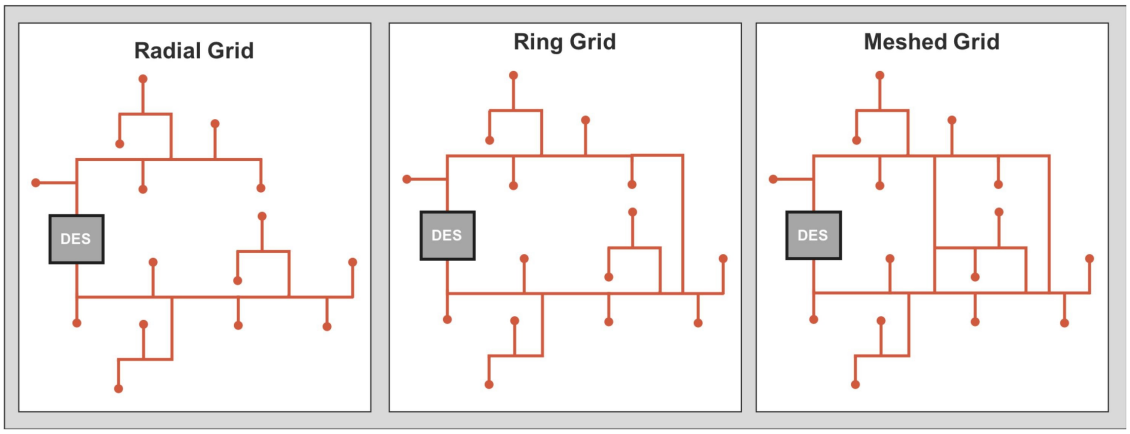

Figure 3.2: Grid topologies for district thermal energy systems, courtesy of [3].

3.2.4 Topology optimization

In this work, district energy system network topologies are represented using the mathematical concept of *undirected graphs*. An undirected graph consists of a set of vertices, or nodes, and a set of edges, which can be expressed as unordered pairs of nodes [5]. A *connected graph* is one in which there exists a path between each and every pair of nodes. The connectivity of a graph can be represented by an *adjacency matrix,* $\boldsymbol{A}$, in which an element $A_{i,j} = 1$ if there exists an edge between nodes i and j and 0 otherwise. In graph theory, a cycle is a path that starts and ends at the same node, and passes through at least three distinct nodes [5]. A connected graph without cycles is considered a spanning tree. A minimal spanning tree is the spanning tree with the least total edge length. Interpreted in the context of district energy system topologies, the minimal spanning tree represents the network that achieves the connectivity of a given set of buildings with the least infrastructure cost. In this study, the minimal spanning tree (MST) heuristic is evaluated to select the network by which a given set of buildings should be connected.

Topology optimization is particularly relevant in the context of 5GDHC systems. Such systems create the potential for buildings and industrial processes to act as "prosumers", supplying or rejecting heat to the thermal network in a way that can offset the load on centralized primary equipment. As a result, more complex network topologies, such as ring and meshed configura-

tions, are often implemented for systems of this type [3]. In the context of conventional district thermal energy systems, where heat and mass flow are typically uni-directional, radial networks are generally used, unless redundancy of supply is essential [3]. Figure 3.2 shows a schematic of radial, ring, and meshed network topologies. Initial work by others suggests that ring and meshed networks can deliver benefits in energy- and exergy-efficiency under certain conditions. The work of [58] compared ring and radial networks for a 5GDHC system through a simulation study, and found that ring networks could incorporate distributed sources of waste heat more effectively. A simulation study by [59] compared two different configurations of 5GDHC systems. The authors found that a two-pipe system with bi-directional flow, similar to the one considered in this study, with a meshed network configuration, resulted in a greater exergetic efficiency than a single-pipe system with uni-directional flow. However, the costs associated with piping and trenching are a significant part of the overall life cycle cost of the district thermal energy system, as concluded by [24] and others. These potential trade-offs between initial capital cost and energy performance motivate the need for a topology optimization framework to guide decisionmaking.

Past studies addressing topology optimization for district thermal energy systems differ in terms of the range of topologies considered and whether connected loads were treated as boundary conditions, as well as in the nature of the thermal networks considered, and the fidelity of building load profiles. Topology optimization problems in this context have often been formulated as mixed-integer non-linear programs (MINLPs), and genetic algorithms have often been leveraged for solving the problem. Life cycle cost, accounting for operating energy as well as the annualized capital cost, has often been chosen as the objective function. In [24], an optimization problem was solved for the network topology (including location of the central plant) and pipe diameters to minimize life cycle cost for a low-temperature district heating network. The network topology was constrained to be a tree and a connected graph and the connection status of each building was taken as a boundary condition. Building loads were represented with an annual peak load, and a multiplier for each of eight periods dividing the year. The authors of [24] concluded that the spatial lay-out of the district considered, building heat loads, and pressure and temperature requirements for

the network were key factors influencing the optimal topology. The authors of [60] performed a simultaneous optimization for sizing of a combined heat and power (CHP) plant and topology of the associated district heating network, with annual net profit as the objective function, accounting for initial capital investments and operating income from the sale of electricity and heat. Thus, the interactions between the network topology and operating energy were not directly reflected in the objective function. The analysis was performed for only one set of load conditions. With the constraint of at least one connected building, the connection status of other considered buildings was an optimization variable. The authors considered radial and ring, but not meshed, topologies. They applied their methods to several study cases and concluded that the simultaneous optimization of the plant design and network topology resulted in increased profitability relative to separate optimizations due to the interactions between the thermal and electrical systems.

Other studies have considered more flexible thermal network configurations. The work of [25] sought to optimize the topology configuration, pipe diameter, and operating parameters of a district heating network for minimal life cycle cost. Operating parameters included supply and return temperatures for the network, and mass flow rates. Both parallel and series connections of buildings to the district network were considered, as well as the absence of a connection from a given building to the network. The primary application for series connections were buildings with lower temperature supply requirements [25]. The authors of [25] formulated the problem in three sub-problems as a mixed integer nonlinear program, a mixed integer linear program, and a nonlinear program and performed the analysis for steady-state conditions only. They considered several sample configurations of building locations and loads, and concluded that the optimal topology was highly context dependent, and not generalizable.

Other studies have considered objective functions other than economic cost, or multiple objectives. The work of [61] applied topology optimization to a district heating network, with an objective of robustness to fluctuations in minimum supply pressure head. In their work, pipe diameter (with a minimum value of zero, corresponding to the non-existence of the thermal connection) was the optimization variable, and meshed networks were considered. The authors applied

a method of moving asymptotes approach to the optimization problem. The connection status of buildings to the network was treated as a boundary condition. The authors of [61] found that the network connectivity was much more influential on robustness than the sizing of pipes. The work of [27] considered multi-objective optimization (for life cycle costs and carbon emissions) for district-level heating and electrical energy systems. In [27], the optimization problem was divided into three sub-problems: selection of heating systems for each building (which could be tied to a district system, or independent), design of primary equipment (with energy storage included in the scope) and selection of efficiency measures at the building level, and operation of primary equipment and energy storage units. The authors of [27] used detailed building load models, formulated with resistor-capacitor (RC) networks. They considered various topology configurations, but not meshed networks. Their solution process was iterative among the three sub-problems. The authors of [27] concluded that, for the hypothetical district considered, distributed CHP and auxiliary heat generation was more cost-effective than a centralized CHP system. The work of [62] performed a multi-objective optimization for design and control of a low-temperature district heating network leveraging renewable thermal and waste heat sources. The consumption of imported primary energy, annualized costs, and carbon emissions were the considered objective functions. The optimization variables included the sizing and location of solar thermal collectors, seasonal thermal energy storage, and waste heat injection, as well as the diameters of network pipes, with a zero diameter corresponding to the absence of a pipe from the network. Individual building loads were aggregated to larger nodes representing neighborhoods, and the connection of these nodes to the network was treated as a boundary condition. The authors applied a master-slave approach to the joint design and control optimization. The authors of [62] concluded that their results for a study case were not readily generalizable to design guidelines, but supported the heuristic that thermal sources should be located close to large loads.

Other studies of topology optimization for district thermal energy systems have investigated the effects of the selection of the objective function. The work of [26] compared the outcomes of optimized design of a district heating and cooling network under two different objective func-

tions: capital costs and life cycle cost, formulating the problem as a mixed-integer linear program. The authors effectively constrained the analysis to radial or ring topologies, and considered energy consumption associated with distribution pumping and heat losses, but treated the energy consumption at loads, and their connection status, as boundary conditions, and performed the analysis for a static load condition. In a study case, the authors identified differences between the topologies of the networks optimized under the two objective functions, due to differences in pumping energy and heat loss associated with the networks, further motivating the need for network topology optimization. The authors of [26] identify consideration of higher-fidelity load profiles, as well as greater flexibility in the network configuration, as areas for future work in the optimization of district thermal networks.

3.2.5 Novelty and contribution

Among past works addressing topology optimization for district thermal energy systems, some studies, such as [61], have addressed objective functions that are not influenced by energy consumption. Others, such as [24], [25], [62], [60], and [27] addressed objective functions influenced by energy consumption, but in the context of district heating networks only. This study introduces greater complexity by analyzing an advanced district thermal energy system, with an objective function influenced by energy consumption and investment and operating costs. Addressing the need identified by [26], ambient loops and low-temperature district heating networks create more interesting opportunities for optimization than high-temperature heating only networks, by introducing more potential topologies, and the potential for bidirectional thermal and mass flow. The larger effort to develop a topology optimization framework, of which this study is a part, presents a departure from past work because it considers both the questions of which subset of buildings to connect as well as how they should be connected, is flexible to a variety of potential topologies, and considers high-fidelity building load profiles. This effort extends the work of [3] and [31] by leveraging tools developed by those authors (specifically the 5GDHC Topology Analysis Tool and the Metamodeling Framework), to evaluate the minimal spanning tree heuristic for a larger use

case, and test the hypothesis that the heuristic is effective in selecting the least-cost network.

An additional novelty of this contribution is the joint consideration of building- and district-level HVAC system energy performance, and the network topology optimization problem. Low-energy districts are an ideal case for the analysis of radiant hydronic HVAC systems, and comparisons with air-based systems. Existing literature, such as [52] and [63], has focused on comparisons of TABS and air-based systems at the building level. Prior work has not addressed district thermal energy systems serving multiple buildings with load profiles accounting for stochasticity of energy use. To test the hypothesis that radiant hydronic HVAC systems will save energy at the district level relative to air-based systems, a detailed comparison of the energy performance of two hypothetical districts is performed.

3.3 Methods

This study comprises two analyses, both of which evaluate the potential of advanced district thermal energy systems: the comparison of the energy performance of two HVAC system types at the urban district level, and the evaluation of a heuristic for topology optimization of district thermal networks.

3.3.1 Heating, ventilation, and air-conditioning (HVAC) system comparison

In this study, the energy performance of two hypothetical low-energy residential districts, one with air-based HVAC systems, and one with radiant hydronic HVAC systems, was compared. Both districts were served by district thermal energy systems. In both cases, to generate the district energy model, a representative building energy model was perturbed to reflect a larger number of buildings. The following steps were performed to carry out this analysis:

(1) Adapt a prototype building model for each HVAC system type under consideration (air-based and radiant hydronic systems).

(2) Perturb each base building model to generate ten building models for each district.

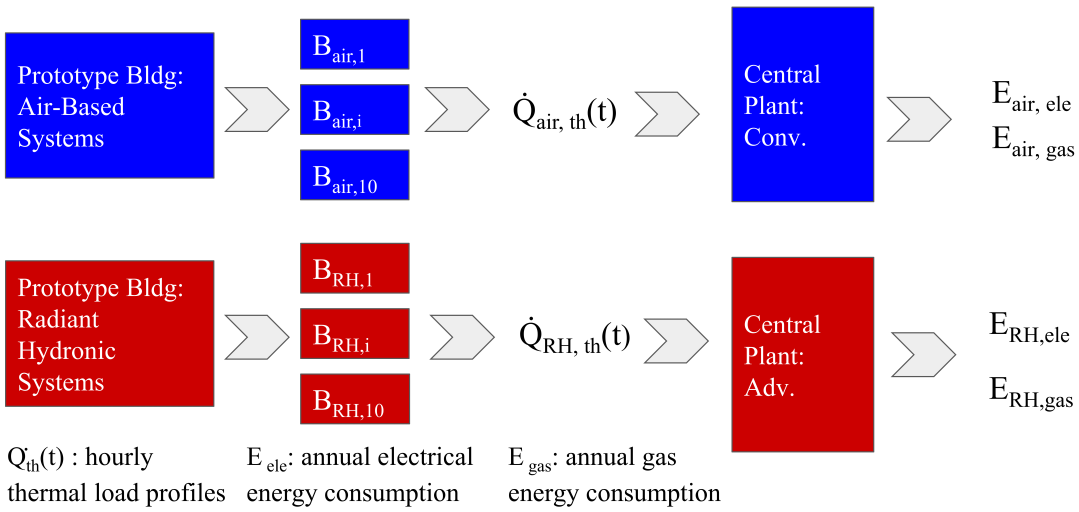

Figure 3.3: Analysis process performed for HVAC system comparison.

(3) Perform energy simulations at the individual building level for the districts, with the building models controlled to achieve an equal level of thermal comfort. Generate heating and cooling load profiles for the district thermal energy systems.

(4) Assemble energy models for the primary heating and cooling plant serving each district, using EnergyPlus components, and simulate with the load profiles generated in step 3.

(5) Evaluate results based on load intensity and annual heating and cooling energy use intensities.

(6) Derive general conclusions from the particular case study.

The process for this analysis is also illustrated in Figure 3.3. In Figure 3.3, energy models representing air-based systems and the conventional central plant are shown in blue, and energy models representing radiant hydronic systems and the advanced central plant are shown in red.

Energy simulation for this analysis was performed using EnergyPlus v8.9 [64]. The analysis was performed using a typical meteorological year (TMY3) weather file for Denver, Colorado, a climate with both heating and cooling loads. Energy consumption results were analyzed in terms of both site energy and source energy, with source energy used as the ultimate basis for comparison.

Site energy refers to the energy delivered to a site (in this case interpreted as a district). Source energy encompasses all the inputs required to generate the delivered energy, including losses in electricity generation, transmission, and distribution, and in natural gas distribution [65].

Base building energy models The intention of this analysis was to isolate the effects of the difference in HVAC systems between the two districts. Thus, the building models for the two districts were identical, except for the HVAC system types. To represent a low-energy district, a base building model with a high-performance envelope and efficient HVAC systems (compliant with 2013 ASHRAE 90.1 [66]) was adapted from a prototype building model. The U.S. Department of Energy publishes prototype building energy models in EnergyPlus format, which are intended to represent the characteristics of typical commercial and multi-family residential buildings in the U.S. [35]. The multi-family prototype model, located in ASHRAE Climate Zone 5B and compliant with 2013 ASHRAE 90.1, was modified to create the base building energy models. The multi-family prototype building model represents a four-story building, of 3,130 m^2 in floor area, composed of residential units and a small office space on the ground floor. The construction is steel frame, and the building has a window-to-wall ratio of 20%. Windows are double-pane with a low-emissivity coating. The prototype building model is configured with split systems with direct expansion cooling and natural gas heating to serve each thermal zone. Internal loads other than lighting in each residential unit include kitchen appliances, a washer and dryer, and miscellaneous plug loads, all of which are powered by electricity. Characteristics of the envelope and loads of the prototype building model, which are retained in the base building model, are summarized in Table 3.1.

The HVAC systems in the prototype building model were modified to generate the base building models for this study. For the district with air-based systems, the split systems were replaced with air handling units with hydronic coils, in order to allow integrating the building level systems with district thermal energy systems. Heating hot water from the district loop was supplied to these systems at 82°C, and chilled water was supplied at 7°C. The air-based systems were controlled to achieve neutral thermal comfort in the space, as reflected in the Fanger model

Table 3.1: Summary of base model envelope and load characteristics.

Parameter	**Value**
Space allocation	
Residential area (%)	87%
Corridor area (%)	10%
Office area (%)	3%
Envelope properties	
Wall U-value($\frac{W}{m^2K}$)	0.31
Roof U-value($\frac{W}{m^2K}$)	0.17
Floor U-value($\frac{W}{m^2K}$)	0.24
Window U-value($\frac{W}{m^2K}$)	0.42
Window SHGC	0.40
Internal loads	
Occupant density ($\frac{person}{1000m^2}$)	25
Lighting power density ($\frac{W}{m^2}$)	14
Internal load density ($\frac{W}{m^2}$)	6.7

(using the control object (Thermostat:ThermalComfort) in EnergyPlus).

For the district with radiant systems, the split systems were replaced with low-temperature, variable-flow, radiant hydronic heating and cooling systems, integrated in the floor slabs. Due to the large area available for heat transfer, heating hot water and chilled water were supplied at moderate temperatures. Heating hot water from the district loop was supplied to the radiant systems at 45°C and chilled water was supplied at 16°C. The flow rate of hot water or chilled water through the radiant hydronic coils was controlled based on operative temperature in the zone, consistent with the approach taken in [49]. A dedicated outdoor air system (DOAS) was added to the model to supply tempered ventilation air, at a constant volume. The DOAS units were each equipped with a direct-expansion (DX) cooling coil and a gas heating coil to temper the outside air. The radiant hydronic HVAC system model incorporated in EnergyPlus is documented in [67]. The work of [68] performed a validation of the EnergyPlus radiant hydronic system model in the context of an instrumented residential building with radiant systems, and found a good correspondence between predicted and experimental results for the energy consumption and thermal comfort parameters considered.

The DOAS units were equipped with a heat recovery ventilator (HRV), in the form of a run-around loop. A run-around loop avoids the risk of cross-contamination between supply and exhaust air from different residential units. Heat recovery ventilation is required by 2013 ASHRAE 90.1 for HVAC systems in ASHRAE Climate Zone 5B supplying 100% outdoor air, but not for systems supplying less than 50% outdoor air at full design flow rate, as is the case for the hydronic air handlers serving the buildings with air-based systems [66]. Thus, heat recovery ventilation was not modeled in the hydronic air handling units.

Perturbations of building energy models To generate realistic heating and cooling load profiles for the district thermal energy system, characteristics of the base building model were perturbed in order to generate nine other sets of characteristics, which were then implemented in nine other versions of the base building energy model. The same sets of perturbations were

Table 3.2: Parameter space for building model perturbations.

Parameter	Dist. Type	Min.	Max.	Ref
Internal load density ($\frac{W}{m^2}$)	Triangular	6.7	16	[69]
Occupant density ($\frac{person}{1000m^2}$)	Triangular	17	50	[55] and [69]
Window-to-wall ratio (%)	Uniform	15	40	[69] and [70]
Infiltration rate($\frac{\frac{m^3}{s}}{m^2 \text{wall area}}$)	Triangular	0.2	2.0	[71]
Occupancy schedule shift (hours)	Triangular	-3.0	3.0	N.A.
Internal load schedule shift (hours)	Triangular	-3.0	3.0	N.A.

used for both the district with air-based systems and the district with radiant systems. The following parameters were perturbed using probability distributions: window-to-wall ratio, internal load density, occupant density, and infiltration rate. These parameters were selected based on the uncertainty associated with them in a hypothetical building, and their influence on heating and cooling loads, determined through a literature review. Ranges for the parameter values were selected based on the literature, (as previously discussed, [55], [56], [57]), and existing guidelines for energy modeling of residential buildings. Schedules for occupancy and internal loads were also adjusted using probability distributions to select a duration by which to "expand" or "contract" the schedule, and to shift the schedule values. These schedules were adjusted in order to reflect the stochastic nature of occupant loads and occupant-driven energy use, both of which contribute to the temporal distribution of building heating and cooling loads [55]. Table 3.2 shows the ranges over which these parameters were perturbed, the distributions used, and references used to determine the ranges. The approach for shifting occupant and plug load schedules was developed by the authors.

System comparison and thermal comfort A meaningful comparison of energy performance must ensure that different HVAC system types are delivering the same degree of thermal comfort in a conditioned space. Thus, the two system types were controlled to achieve the same

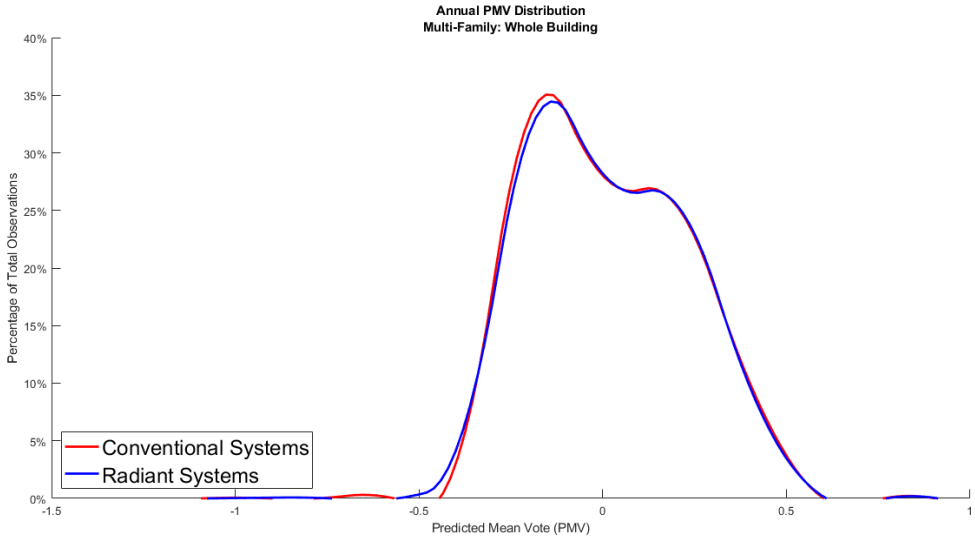

Figure 3.4: Comparison of annual distributions of predicted mean vote between corresponding zones in multi-family buildings served by radiant hydronic and air-based systems.

degree of thermal comfort, as closely as possible, reflected by the Fanger model, which is widely accepted for evaluating thermal comfort [72]. The predicted mean vote (PMV) for occupants in a space is a metric typically used to interpret the results from Fanger's model, with values ranging from -2 (very cold) to 2 (very warm), and a value of 0 corresponding to thermal neutrality. The modeling approach leveraged an option in EnergyPlus to control air-based systems to a thermal comfort setpoint. The radiant systems were controlled to the sequence of operative temperatures that previously resulted in the buildings with air-based systems. This approach resulted in a near-perfect alignment of PMV between corresponding buildings at each timestep and maintained PMV generally within the acceptable band of [-0.5, 0.5] overall. The annual cumulative distributions of PMV for a representative zone for the two system types are shown in Figure 3.4. The analysis of thermal comfort serves to ensure that the same degree of service is being provided by the two HVAC system types considered, and thus that a direct comparison of their loads and energy performance is valid.

3.3.2 District thermal energy system models

The central plants serving the two districts were modeled with the same types of primary equipment, and the same network of distribution pumps and pipes. The primary equipment consisted of water-cooled centrifugal chillers, cooling towers, and hot water boilers. Both districts were configured with a primary and distributed secondary pumping arrangement, with variable-speed pumps.

Characteristics of the chillers and boilers in each plant are shown in Tables 3.3 and 3.4. Note that the COP value listed is for the chiller alone, and not the chilled water plant as a whole.

Table 3.3: Summary of chiller characteristics.

Unit	Cooling Capacity	Chiller Rated COP ($\frac{W}{W}$)	Quantity
Shoulder season chiller	130	5.9	1
Peak load chiller	470	8.2	3

Table 3.4: Summary of boiler characteristics.

Unit	Heating Capacity(kW)	Nominal Efficiency(%)	Quantity
Condensing boiler	200 to 2,900	89%	4
Non-condensing boiler	200 to 2,900	80%	4

Both central plant models were configured with water-side economizers, which use heat exchangers between the condenser water and chilled water loops, to allow heat to be rejected directly from the chilled water return to the condenser water, when the condenser water is sufficiently cool. Chiller characteristics, including performance curves and reference efficiency and capacity values, were obtained from datasets available in EnergyPlus, which represent chillers that are or have been produced by manufacturers [64]. The rated COP values are compliant with the standards

for full-load and integrated part-load efficiency in 2013 ASHRAE 90.1 for equipment manufactured through 2015 [66].

The central plant serving the low-exergy systems is configured with condensing heating hot water boilers. The central plant serving the air-based systems is configured with non-condensing heating hot water boilers. The nominal efficiency values of the boilers are compliant with 2013 ASHRAE 90.1 [66]. The higher return temperatures in the heating hot water loop serving the conventional systems (observed to be 60°C under typical conditions) are too warm to achieve condensing in a condensing boiler [73]. After generating a load profile based on the ten buildings modeled in each district, the thermal and electrical load profiles of each district were multiplied by a factor of four, to better align the cooling load with the capacities of water-cooled chillers available on the market. Thus, each district model effectively represented forty buildings.

3.3.3 Evaluation of minimal spanning tree heuristic

It is hypothesized that topology optimization will enhance the cost-effectiveness of advanced district thermal energy systems, such as the low-exergy systems analyzed in this study. The minimal spanning tree heuristic for the topology optimization problem was evaluated for a prototypical urban district, through a search of all spanning tree networks. The cost function implemented in the topology optimization problem corresponds to the life cycle cost, evaluated over a twenty-year time horizon, with a discount rate of 3%, of piping infrastructure for the 5GDHC system, as well as the energy required to meet the HVAC loads of all buildings in the district, whether or not they are served by the 5GDHC system. (Note that the restriction of infrastructure cost to that associated with the network itself is consistent with a common practice in past topology optimization studies of district thermal energy systems, per the work of [24], and consistent with the cost function formulated by [3]. It was assumed that the difference in capital costs for HVAC equipment between independent and DES-tied systems would be minimal in the scope of the life cycle cost evaluated over thirty years. The capital costs associated with a 5GDHC system (a centralized heat pump and water-source heat pumps at individual buildings) are expected to be more similar to those

associated with independent, building-level systems, than those associated with a "conventional" DES.)

The cost function accounts for projected escalations in electricity and natural gas rates, and for a potential future price on carbon dioxide (CO_2) emissions, based on a scenario outlined by the U.S. National Institute for Standards and Technology [74], as well as projected future declines in the carbon intensity of electricity. The formulation of the objective function leverages uniform present value (UPV) factors for the selected discount rate and time horizon, which represent a ratio of the life cycle cost to the annual cost. UPV factors are obtained from [74] for the operating cost streams (electricity, gas, and carbon) and also reflect the projected escalations in the costs of these quantities over the project lifetime. The analysis is performed based on an application of the energy consumption over a simulated year to all years of the time horizon. This formulation of the cost function is consistent with that implemented by [3]. The cost function for the topology optimization problem is formulated as shown in Eqn. 3.1.

$$\begin{aligned} &\min_{\mathbf{A}} C_{pipes} + C_{elec} UPV_{elec}(E_{de} + \sum_{i=1}^{n} E_{be,i}) + C_{gas} UPV_{gas} \sum_{j=1}^{n} E_{bg,j} \\ &+ \sum_{t=1}^{20} m_{CO2}(t) C_{CO2}(t) UPV_{CO2} \end{aligned} \tag{3.1}$$

subject to:

(1): If there exists a pipe directly thermally connecting building i and building j, $A_{i,j} = 1$. Otherwise, $A_{i,j} = 0$.

(2): If building i is served by the district thermal energy system, there exists a path from the central plant to node i.

where $\mathbf{A}$ is the adjacency matrix describing the thermal network, C_{pipes} is the cost of pipes and trenching, C_{elec} is the electricity cost per unit of consumption, C_{gas} is the natural gas cost per unit of consumption, $E_{be,i}$ is the annual electric consumption for HVAC at building i, E_{de} is the annual

electric consumption for district energy systems, including primary equipment and distribution pumps, $E_{bg,j}$ is the annual natural gas consumption for HVAC at building j, UPV_{elec} is the uniform present value factor for electricity, UPV_{gas} is the uniform present value factor for natural gas, $m_{CO2}(t)$ is the annual carbon emissions in a given year, $C_{CO2}(t)$ is the cost associated with carbon emissions in a given year, and UPV_{CO2} is the uniform present value factor associated with carbon pricing. Note that the time-dependence of carbon emissions and their associated cost is due to the projected future declines in carbon intensity of electric generation, and the projection of an escalating carbon tax.

Note that with n buildings, in addition to a central plant, the graph representing the network has $n+1$ nodes. Due to the complex interactions among building loads in the district energy system context, as well as the equations governing energy consumption by pumps, and heat losses through the pipes, the energy consumption terms in this function are nonlinear. The functions used to evaluate building thermal loads, which are discussed in a following sub-section, are non-convex. Thus, the problem formulated in Eqn. 3.1 is non-convex, due to the binary nature of the elements of the adjacency matrix, and the non-convex functions for energy consumption.

The number of potential solutions to the topology optimization problem formulated in Eqn. 3.1 is a function of the number of possible subsets of buildings in the considered district, and the number of ways in which a given subset can be thermally connected. Specifically, the number of potential solutions is equal to the product of the number of ways to select a subset of buildings of a given cardinality and the number of ways in which that subset can be connected, summed over the number of buildings in the district. There is one additional solution corresponding to the case in which no buildings are connected to the network. Figure 3.5 explores all fifty-four possible solutions to the topology optimization problem for a district consisting of three buildings (shown with blue nodes) and a district energy plant (shown with a red node).

As illustrated in Figure 3.5, the size of the search space quickly expands with an increasing number of buildings. This makes an exhaustive search impractical. A means of addressing this is dividing the analysis of the problem into two steps, first addressing the question of "which subset

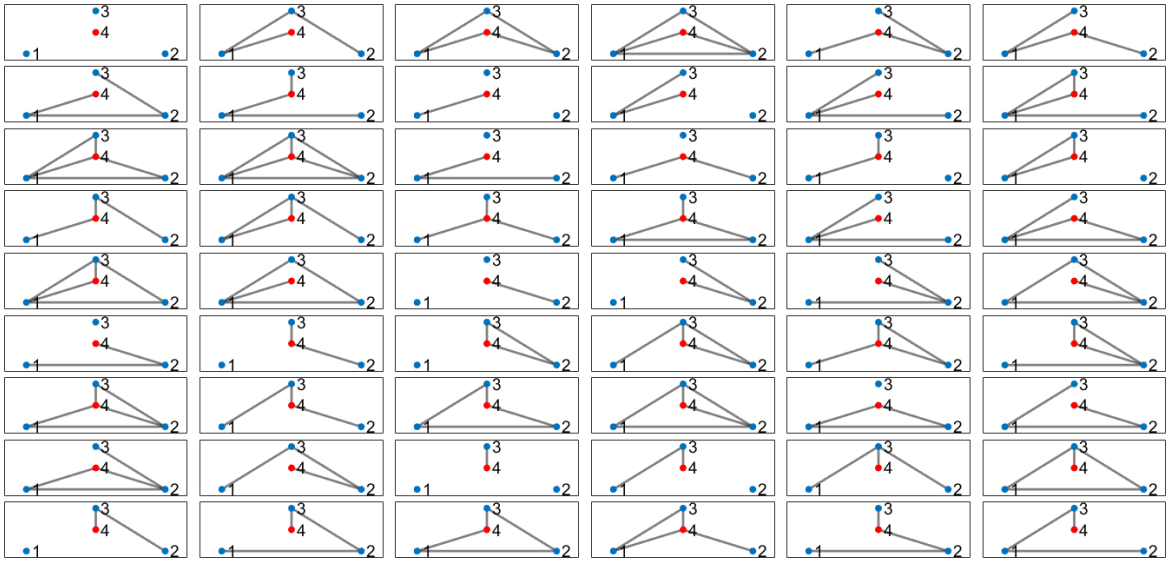

Figure 3.5: Topology optimization search space for district consisting of three buildings and DES plant.

of buildings should optimally be connected to the district energy system," followed by, "given the optimal subset of buildings, what is the best means by which to connect them?" It was hypothesized that a minimal spanning tree may be a suitable heuristic for connecting a given subset of buildings, addressing the second sub-problem. A minimal spanning tree minimizes the piping and trenching costs relative to other potential networks. The costs associated with piping and trenching are a significant part of the overall life cycle cost of the district thermal energy system, as concluded by [24] and others. The use of the minimal spanning tree heuristic would significantly reduce the size of the search space for the topology optimization problem as a whole. As there exists a unique minimal spanning tree for each subset of buildings, the use of this heuristic reduces the search space to the number of distinct combinations of buildings, which is equal to 2^n for a set of n buildings, including the null set. Figure 3.6 compares the number of possible minimal spanning trees to the size of the solution set as a whole as a function of the number of buildings considered. (Note that the y-axis in Figure 3.6 is non-linear.) The number of minimal spanning trees also becomes intractable for districts of increasing size. Additional means of reducing the size of the potential solution space for larger prototypical districts are an area of future work in development of the topology optimization framework.

In this study, all possible spanning tree networks that could serve a district consisting of four buildings and a central plant were analyzed, constituting 212 different cases. A Modelica energy model of the 5GDHC system was used to evaluate the energy consumption terms in the cost function. Modelica is an object-oriented, equation-based language for modeling physical systems [36]. The underlying energy model was assembled and documented in [3] as the 5GDHC Topology Analysis Tool. The model was validated by the authors of [3] using data from a laboratory test bed operated under the FlexyNets Project. FlexyNets is a Horizon 2020 European Project which seeks to develop and deploy fifth-generation district heating and cooling networks [75]. As part of the validation, model parameter values were adapted to reflect those of the FlexyNets test bed, and the model was initialized to a consistent set of conditions. Fluid temperatures calculated by the model at specific points in the thermal network were compared to those measured in the FlexyNets

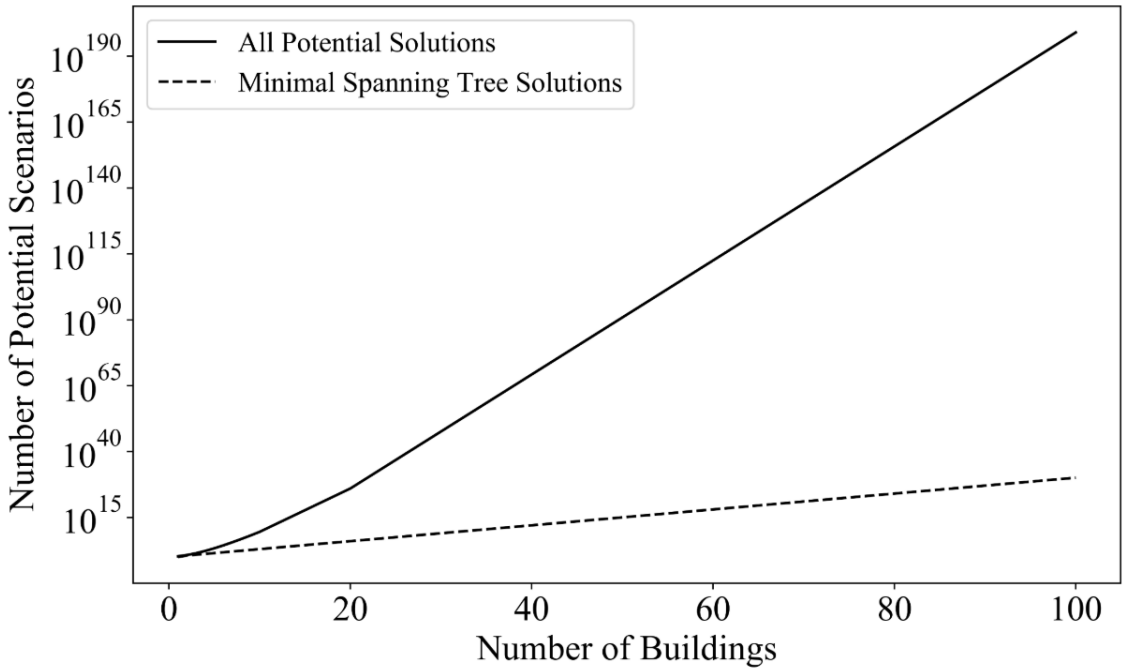

Figure 3.6: Comparison of the sizes of the full search space and search space of minimal spanning trees.

test bed, and a satisfactory correspondence was found [76]. The load side of the energy model was expanded in this work to represent a prototypical urban district consisting of three identical office buildings, and one larger retail building. Based on the work of [12] and [3], it is expected that increased thermal load diversity will enhance the viability of advanced district thermal energy systems. Consistent with the approach taken by [3], in the 5GDHC energy model, building thermal load profiles were represented with data-driven metamodels, generated with the Metamodeling Framework developed in [31]. The Metamodeling Framework has been demonstrated to represent building thermal load profiles accurately, and improves the efficiency of the 5GDHC model simulation, compared with the use of full-order, physics-based models to represent building loads. In the framework developed by [31], metamodels of building thermal load profiles are trained based on a dataset developed using the U.S. DOE prototype building energy models. The Metamodeling Framework offers several model types, and random forest models were used in this study. Two thermal load profiles are developed for each building: one for the case in which the building is tied to the 5GDHC system, and one for the case in which the building is served by independent systems. Separate training data sets are used to generate metamodels for the connected and independent cases. Characteristics of the prototypical buildings used to generate load profiles using the Metamodeling Framework are shown in Table 3.5. For the independent case, the DOE prototype building models, in their current form, are used, with a parameter sweep, to generate training data. For the connected case, the models are modified to use water-source heat pumps for space conditioning. Analysis was performed for the location of Golden, Colorado.

Table 3.5: Building characteristics, evaluation of MST heuristic.

Building Type	**Floor Area(m^2)**	**Baseline HVAC System Type**
Retail	2,294	Packaged units with DX cooling and gas heating
Office	512	Air source heat pumps with supplemental gas heating coils

In this analysis, natural gas and electricity rates obtained from the U.S. Energy Information

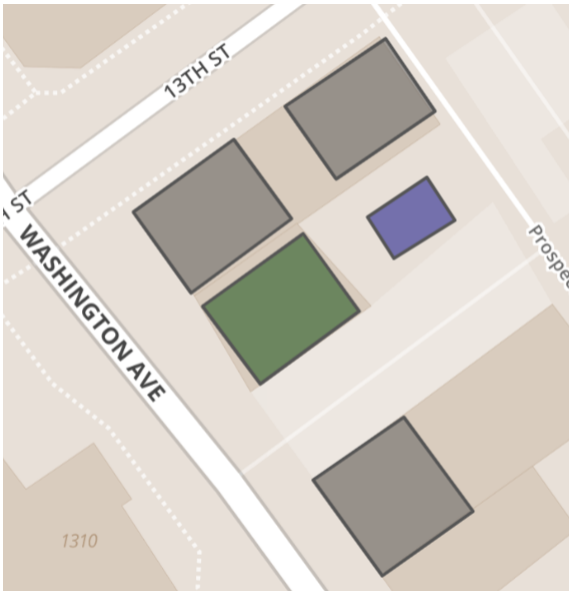

Figure 3.7: Visualization of building locations in hypothetical district (courtesy of GeoJSON.io).

Administration for Colorado in 2017 [77], and unit costs for pipes and trenching ($500/meter), as documented in [76] were used. The twenty-year time horizon used in the analysis is consistent with that used in [76] for evaluation of a 5GDHC system. For purposes of calculating pipe lengths, and for visual reference, the four hypothetical buildings and a district energy system (DES) central plant were located on a block near the intersection of 13th Street and Washington Avenue in Golden, Colorado. A visualization of the GeoJSON data used to plot the building and DES locations is shown in Figure 3.7. In the analysis, this data was used only for calculating pipe lengths. In Figure 3.7, the office buildings are shown in brown, the central plant in blue, and the retail building in green. The relative sizes of the representational buildings shown are not to scale.

3.4 Results

Results from the HVAC system comparison and the evaluation of the minimal spanning tree heuristic for the topology optimization problem are discussed in the following sub-sections.

3.4.1 Heating, ventilation, and air-conditioning system comparison

As part of the HVAC system comparison, thermal comfort, HVAC system performance, and HVAC energy performance were analyzed. Results regarding HVAC system performance at the hydronic loop level and energy performance are presented in this work. Results regarding thermal comfort and zone-level HVAC system performance are presented in [78]. HVAC system performance at the hydronic loop level is quantified using metrics discussed by [52]. For both heating and cooling, cumulative distributions of heat added or extracted, respectively, at the hydronic loop level are shown normalized by building floor area, and disaggregated by the system component. Cumulative distributions of delivered cooling at the hydronic loop level for the base building are shown in Figure 3.8 for air-based systems, and Figure 3.9 for radiant systems. These values represent the cooling delivered by the cooling coil in the air handling unit for the air-based systems, and the sum of the cooling delivered by the DX coils in the DOAS units and the zone radiant hydronic cooling systems for the radiant systems. Note that these values do not represent electrical power input in the case of the DX coils. The disaggregation of the delivered cooling associated with offsetting fan heat is shown for the air-based systems. Due to the lower installed fan power, the cooling load on the DX coil to offset fan heat is negligible for the radiant systems. The radiant systems experience a higher peak cooling load at the hydronic loop level (by 44%) than the air-based systems, which can be attributed to the more immediate conversion of long-wave and short-wave radiation into cooling loads. The ratio between the peak loads on the hydronic loop for the radiant and air-based systems is within the range found by [52]. The latent load constitutes a negligible portion of the total cooling load in both buildings, and thus a disaggregation of sensible and latent loads is not shown on these plots. [1]

As shown in Figure 3.8 and Figure 3.9, a non-negligible cooling load is present at the hydronic loop level in the building with air-based systems for significantly more time of the year than in the

[1]The 0.4% design wet bulb temperature for this location (Denver, Colorado, in ASHRAE Climate Zone 5B) is 18.5°C, with a mean coincident dry bulb of 27.4°C. That combination of wet and dry bulb temperatures corresponds to a relative humidity of 42.8%. The 0.4% design dry bulb temperature for this location is 32.9°C, with a mean coincident wetbulb of 15.9°C. That combination of wet and dry bulb temperatures corresponds to a relative humidity of 13.9% [79].

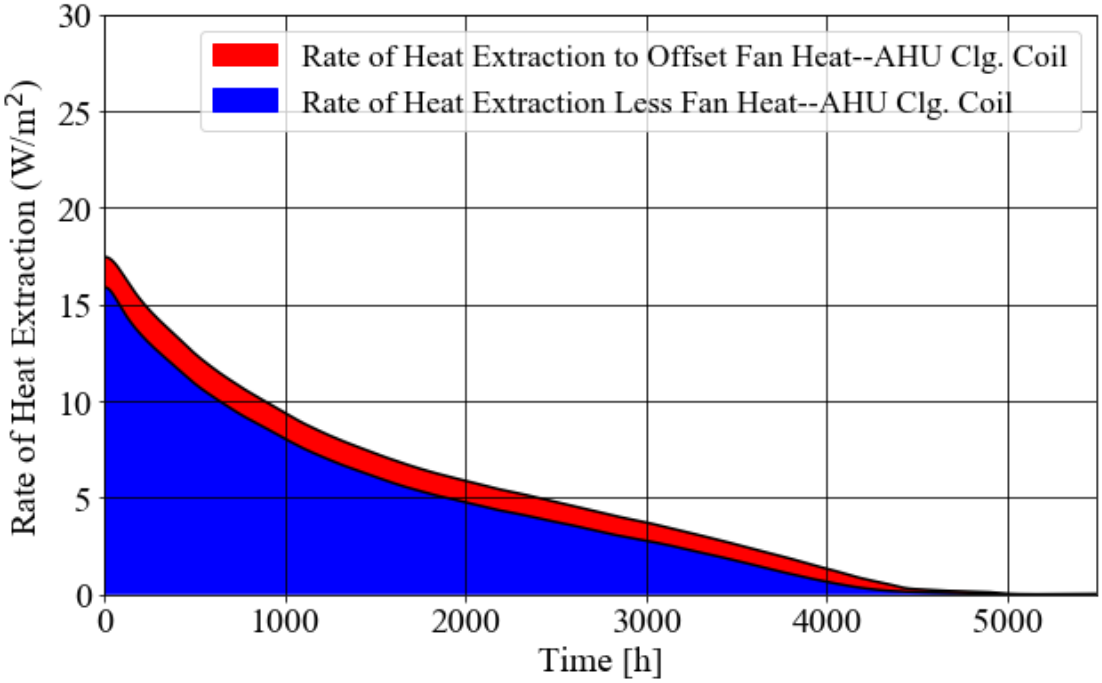

Figure 3.8: Cumulative distribution of cooling load at hydronic loop level, air-based systems.

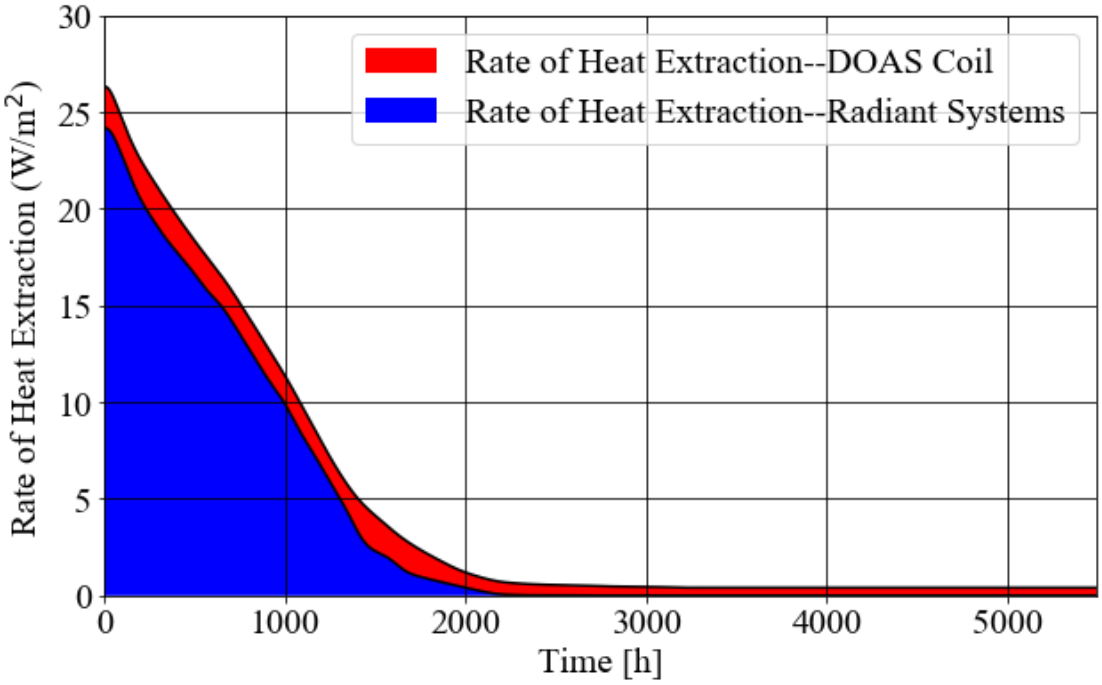

Figure 3.9: Cumulative distribution of delivered cooling at hydronic loop level, radiant systems.

building with radiant systems. This difference is partially explained by the cooling load imposed by offsetting fan heat. Additionally, in the buildings with radiant systems, untempered ventilation supply air offsets a portion of the cooling load. The DOAS supply air is not tempered when outdoor air temperatures are between 12.8°C and 23.9°C. The ventilation supply air provides cooling, or creates a heating load, throughout the year, as the DOAS supply temperature is consistently below the zone air temperatures. During mild outside conditions, the DOAS effectively provides cooling through air-side economizing, though the outdoor air volume remains fixed. The cumulative annual thermal cooling loads of the two districts are similar. Due to the warm air temperatures in the buildings with radiant hydronic systems when the building is in cooling mode, the benefits of the heat recovery ventilator in cooling mode are minimal.

Plots of delivered heating intensities, at the hydronic loop level, are shown in Figure 3.10 for the air-based systems and Figure 3.11 for the radiant systems. These values represent the heating delivered by the heating coil in the air handling unit for the air-based systems, and the sum of the heating delivered by the heat recovery ventilator and the zone radiant hydronic heating systems for the radiant systems. Due to the presence of the HRV, the heating load on the gas coil in the DOAS units is minimal and is not shown on this plot. Note that the heating supplied by the heat recovery ventilator is not associated with additional energy use, but it is shown here for completeness in representing the thermal loads observed with both system types. The contribution of fan heat transferred to the supply air when the building is in heating mode ("useful" fan heat) is also shown for the air-based systems. Useful fan heat is negligible for the radiant systems, due to the lower airflows, and the presence of the HRV. The annual heating loads, also accounting for the effects of useful fan heat and heating delivered by the HRV, are similar between the two system types. The similarity in cumulative annual loads is expected in heating mode, due to the identical nature of the two buildings, expect for the HVAC systems. This result enhances confidence that the two systems are delivering the same service annually, and thus can be fairly compared on the basis of energy performance.

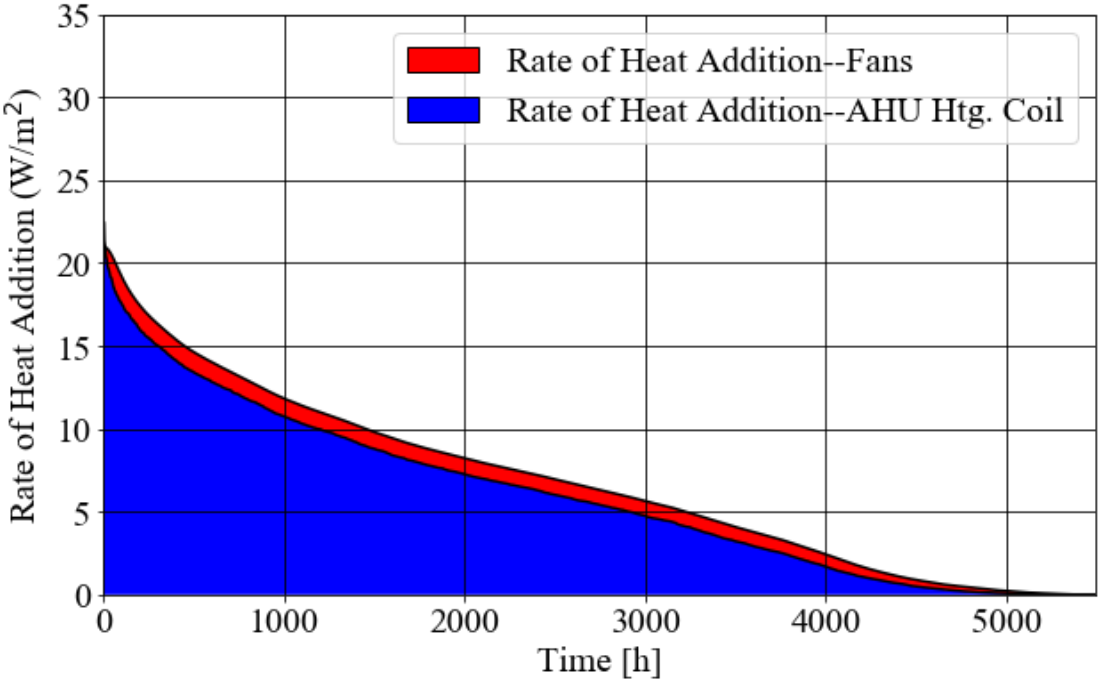

Figure 3.10: Cumulative distribution of delivered heating at hydronic loop level, air-based systems.

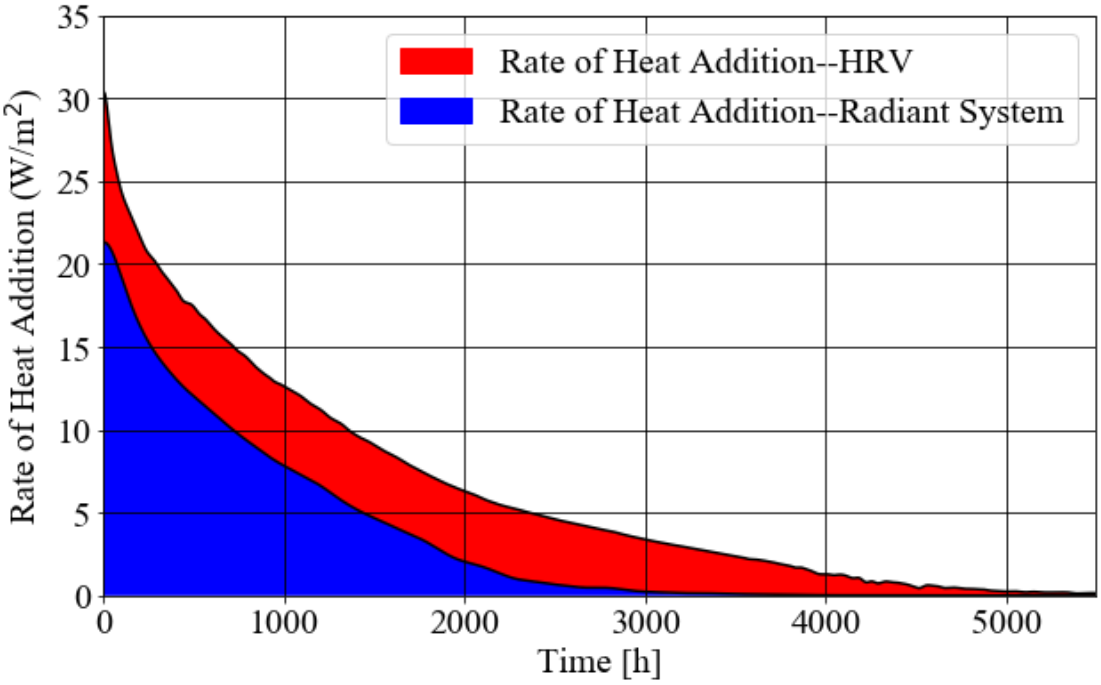

Figure 3.11: Cumulative distribution of delivered heating at hydronic loop level, radiant systems.

3.4.2 Energy performance comparison

The detailed analysis of loads at the hydronic loop level for the two system types provides insight into the expected energy performance comparison. Specifically, the similarity in cumulative annual heating and cooling loads between the two system types suggests that sources of distinction in their energy performance will relate to the presence of the HRV, the operating conditions of central plant equipment, and distribution equipment such as pumps and fans. The dry climate in the location analyzed in this study (Denver, Colorado in ASHRAE Climate Zone 5B) creates ample potential for water-side economizing. Due to the higher chilled water supply temperatures, water-side economizing can meet 53% of the chilled water load in the low-exergy district, compared with only 10% in the conventional district. The effects of water-side economizing are reflected in the ultimate energy use intensity of the chilled water plants. Energy use intensity of the two chilled water plants was compared with a metric including energy use associated with the chillers, cooling towers, and chilled water and condenser water pumps, and all cooling load delivered (including through water-side economizing). Performance metrics for the two chilled water plants, with and without the integration of water-side economizing, are shown in Table 3.6. As shown in Table 3.6, the higher chilled water supply temperatures in the low-exergy plant improve the chillers' efficiency, and the use of water-side economizing significantly improves energy performance for the low-exergy plant. Water-side economizing was implemented in both plants and is reflected in the analysis of their energy performance. The performance of the plants without water-side economizing ("base") is shown for reference.

As shown by the cumulative distributions of annual heating load in Figure 3.10 and Figure 3.11, due to the presence of heat recovery ventilation, the load on the district heating loop and gas heating coils serving the low-exergy systems is significantly lower than that on the conventional district heating loop. The annual requirement for active heating (excluding the heat recovered through the HRV) by the low-exergy district is 53% of that of the conventional district.

Figure 3.12 shows a comparison of the disaggregated site HVAC energy use intensity at the

district level for the two districts, calculated as the ratio of the total HVAC energy consumption in each modeled district to the total building floor area. Note that the floor area value is the same for the two modeled districts. The total site HVAC energy use intensity for the district with low-exergy systems is 51% lower than that of the district with conventional systems. Figure 3.13 shows a comparison of the source HVAC energy use intensity at the district level for the two districts, with the end uses again disaggregated. The total source HVAC energy use intensity for the district with low-exergy systems is 49% lower than that of the district with conventional systems. The difference in the proportions of the two districts in terms of site and source energy use intensity is a result of the fact that the energy use savings of the low-exergy district is largely driven by the gas energy savings associated with the HRV, which has a lower source-to-site ratio than electricity does.

Table 3.6: Summary of chilled water plant performance metrics.

District	Full Load Chiller Power ($\frac{kW}{ton}$)	CHW Plant Power (Base) ($\frac{kW}{ton}$)	CHW Plant Power(WSE) ($\frac{kW}{ton}$)
Low-Exergy	0.33 and 0.43	0.62	0.44
Conventional	0.33 and 0.43	0.83	0.78

3.4.3 Evaluation of minimal spanning tree heuristic

The objective function as shown in Eqn. 3.1 was evaluated for all possible spanning tree networks for the prototypical district consisting of three office buildings, one retail building, and a DES central plant. Figure 3.14 shows the life cycle cost as a function of total piping length for all 211 spanning trees that involve a connection to the DES, with color-coding corresponding to the number of buildings served by the DES. Note that the "null case", in which all buildings have independent systems, is not shown here for compactness, but has the least life cycle cost of all potential solutions considered, a value of $188,000. As shown in Figure 3.14, when grouped by ascending life cycle cost, the potential solutions involving a connection of one, two, or three

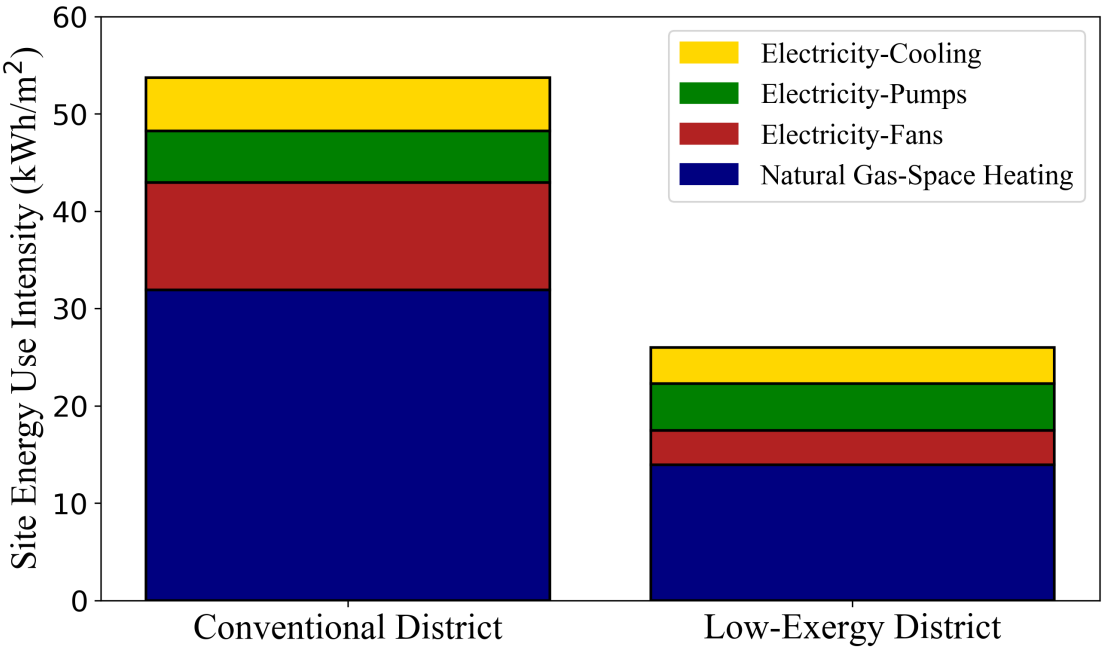

Figure 3.12: Comparison of site HVAC energy use intensity at the district level.

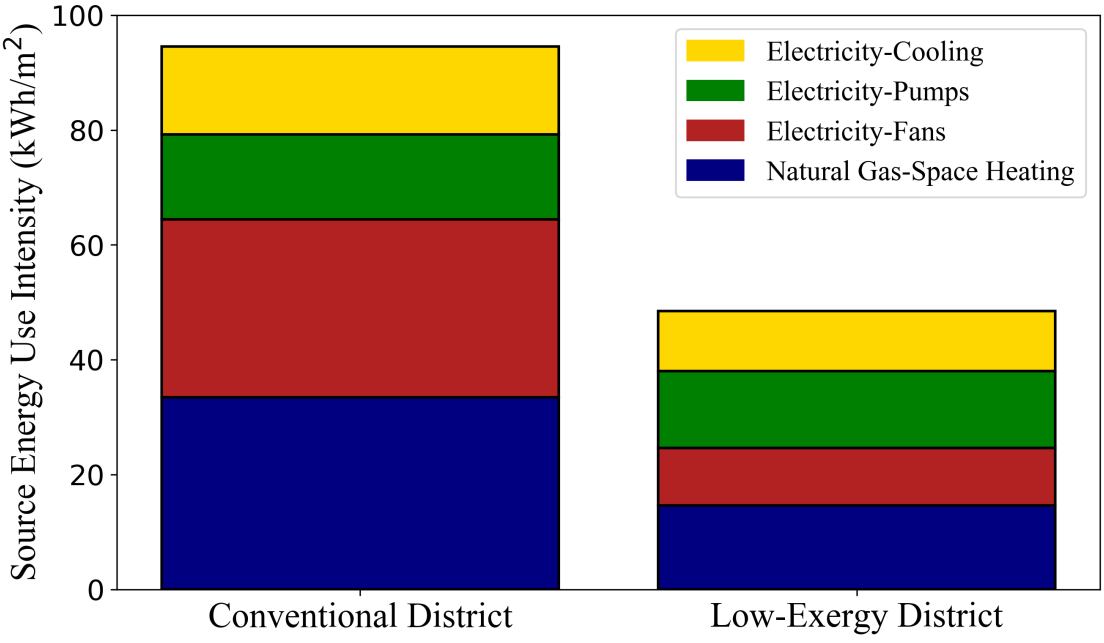

Figure 3.13: Comparison of source HVAC energy use intensity at the district level.

buildings are divided into two bands, based on whether or not the retail building is included in the network. The large step increase in life cycle cost between the two bands corresponds to the addition of the retail building to the network. The primary factor contributing to the bifurcation is the large heating load of the retail building in comparison with the office buildings, which are smaller in floor area and have significantly lower ventilation requirements. (The peak heating thermal load of the retail building is 115,000 W, compared with 15,000 W for the office building, and the annual heating energy consumption of independent systems is also correspondingly higher.) Given the prevailing electricity and natural gas rates for the location considered, it is much more costly to serve this large heating load with electricity as opposed to gas. The significant influence of the particular combination of connected loads on the system's life cycle cost performance is consistent with the results of [12]. As shown in Figure 3.14, within each of the two bands of the solution space, the life cycle cost increases as a function of total pipe length. Of the potential spanning tree topology solutions for the prototypical district considered, infrastructure costs ranged from 2% to 28% of the overall life cycle cost, with the balance attributable to energy costs. Note that this fraction is expected to be higher for non-spanning tree networks, due to the greater length of piping used to connect a given subset of buildings.

From an analysis of the results of the spanning tree search, it is confirmed that, among spanning trees for this prototypical district, the minimal spanning tree network always results in the least life cycle cost for any given combination of buildings (in this case, subsets of two or three buildings, or the full four-building district). This result is expected, as the non-minimal spanning trees result in higher pipe investment costs, without any expected benefits in thermal performance. This result is consistent with the results of [3], who validated the minimal spanning tree heuristic for a district of three identical buildings with an exhaustive search.

3.5 Discussion

The low internal load intensity of the hypothetical residential buildings studied in this analysis enabled the use of radiant hydronic systems, coupled with heat recovery ventilation, to meet almost

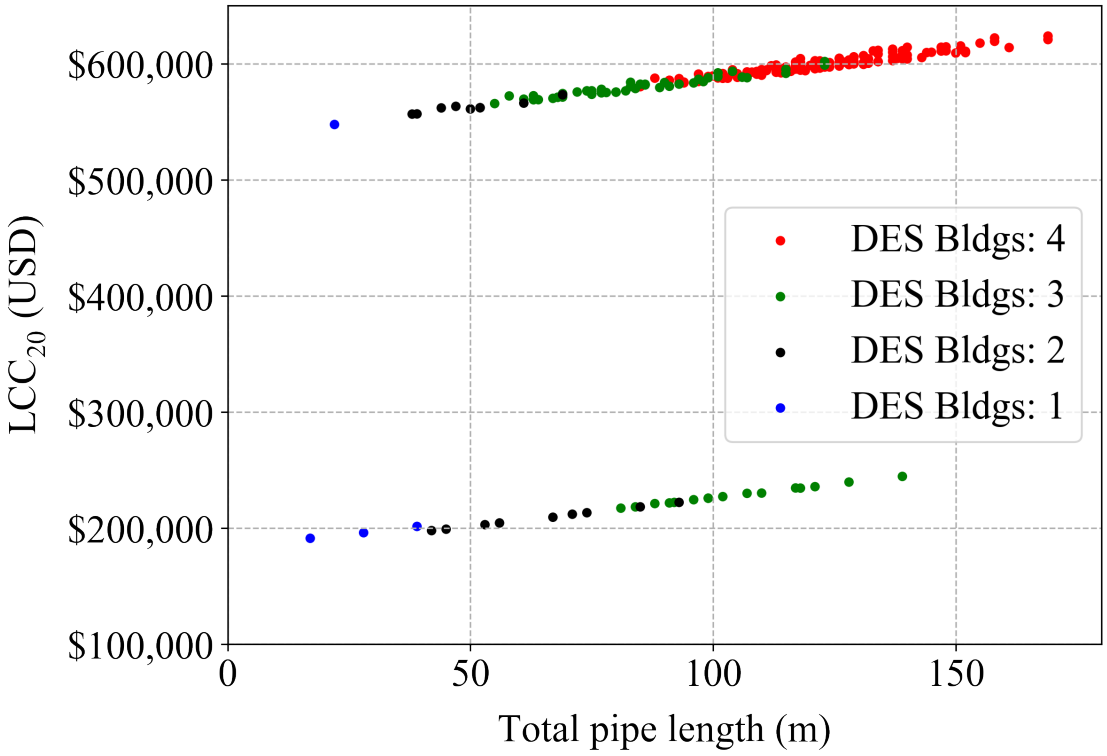

Figure 3.14: Life cycle cost and pipe length for spanning tree topology scenarios.

the entirety of the heating and cooling loads, with minimal contribution from the air system. A building type with higher load intensities or located in a climate with higher latent loads from outdoor air would likely require more supplemental cooling from air-side systems, which would undermine the benefits of the low-exergy primary systems. The detailed analysis of system loads and the validation of the load intensity comparison results with those of [52] provide confidence in the results of the energy use comparison. The HVAC energy savings associated with the low-exergy district are driven by the use of heat recovery ventilation, and the lower energy intensity of the primary plant equipment serving the low-exergy systems. The lower energy intensity of the primary plant equipment is attributable to the higher nominal efficiency of the condensing boiler and its operating efficiency at a high loop temperature differential, more efficient operation of the chillers at the warmer chilled water supply temperatures, and increased potential for water-side economizing. The detailed analysis of loads at the individual building level in combination with analysis of a prototypical district represents a point of departure from previous studies. This analysis highlights the benefits of 5GDHC systems, for which topology optimization can facilitate cost-effective adoption.

Solving the topology optimization problem will require the use of non-convex optimization approaches, which are computationally intensive and can produce multiple solutions. In the future, as part of the development of the topology optimization framework, the minimal spanning tree heuristic will be evaluated with a full exhaustive search for a larger prototypical district with greater thermal load diversity. The prototypical four-building urban district for which the spanning tree search was performed demonstrated the potential of the minimal spanning tree heuristic, but did not offer sufficient thermal load diversity to reveal life cycle cost savings from a 5GDHC system, relative to independent building-level systems. In the full exhaustive search analysis, a sensitivity analysis to utility rates and to the investment costs associated with the district energy system will be performed. Based on the work of [3] and [12], it is expected that a prototypical district with a greater degree of thermal load diversity will be more likely to demonstrate life cycle cost benefits from 5GDHC systems, and from meshed networks specifically, and thus such a case

will provide an evaluation of the minimal spanning tree heuristic under the most relevant, and challenging, conditions. If the heuristic is demonstrated to be valid in a more complex case, it will be implemented as part of the framework. A black-box optimization algorithm that can use the Modelica simulation as a function evaluator, such as particle-swarm optimization [80], will be implemented to address the first part of the topology optimization problem, regarding the selection of a subset of buildings to connect to the district thermal energy system. The implementation of the minimal spanning tree heuristic in the framework will enable topology optimization of 5GDHC networks without constraints on the connection status of individual buildings, providing a much more flexible approach than the current state-of-the-art, and opportunities to investigate complex interactions among building loads in a 5GDHC system.

3.6 Conclusion

The results of the HVAC system comparison demonstrate the potential of advanced district thermal energy systems to achieve deep energy savings. For the prototypical urban residential district considered, radiant hydronic HVAC systems mated with low-exergy district thermal energy systems achieved a source energy use intensity that was 49% lower than that of air-based HVAC systems and conventional district thermal energy systems. However, the high infrastructure costs and large solution space for potential network configurations hinder the adoption of advanced district thermal energy systems. The topology optimization framework proposed by the authors seeks to address those obstacles.

This study leveraged tools developed by [3] and [31] to evaluate a topology optimization heuristic for a four-building district, which demonstrated that the minimal spanning tree network was the most cost-effective means, among spanning trees, to connect a given subset of buildings through a 5GDHC system. This provides validation of the efficacy of the minimal spanning tree heuristic. The use of the minimal spanning tree heuristic significantly reduces the size of the solution space, and thus the computational complexity, of the topology optimization problem. In the future, this heuristic may be adopted by the proposed topology optimization framework.

This study illustrated the promise for topology optimization to facilitate the adoption of advanced district thermal energy systems, which offer significant potential energy savings.

Chapter 4

Evaluation of the minimal spanning tree heuristic for the topology optimization problem

This chapter compiles sections based on the following publications:

A. Allen, G. Henze, K. Baker, G. Pavlak, N. Long, and Y. Fu, "A topology optimization framework to facilitate adoption of advanced district thermal energy systems," in IOP Conference Series: Earth and Environmental Science, Volume 588, 1.01 – 1.05.

A. Allen, G. Henze, K. Baker, G. Pavlak, and M. Murphy. "Evaluation of topology optimization to achieve energy savings at the urban district level," presented at 2021 ASHRAE Winter Conference, February 2021.

4.1 A topology optimization framework to facilitate adoption of advanced district thermal energy systems

4.1.1 Abstract

Advanced district thermal energy systems, which circulate water at temperatures near ambient conditions, and facilitate the utilization of waste heat and renewable thermal sources, can lower the carbon-intensity of urban districts, advancing the U.N. Sustainable Development Goals. Optimization of the network topology — the selection of the best subset of buildings and the best network to connect them, to minimize life cycle cost — can increase adoption of these system in appropriate applications. The potential "solution space" of the topology optimization problem grows factorially with the number of buildings in the district, motivating the consideration of a design heuristic. In this study, a heuristic for the network selection was evaluated with an exhaustive search, for a prototypical four-building district. For the prototypical district considered, the heuristic was effective in selecting an optimal network topology. Additionally, it was found that, in this case, the selection of the subset of buildings was more influential on the life cycle cost than the selection of the network topology. This work is part of a larger effort to develop a topology optimization framework for district thermal energy systems, which is anticipated to address barriers to adoption of ambient-temperature systems.

4.1.2 Introduction

The global trend towards urbanization and the urgency of addressing climate change require addressing the energy- and carbon-intensity of the built environment in cities [81]. Advanced district thermal energy systems, which circulate water at near-ambient temperatures, can leverage the density and diversity of load in urban districts and facilitate the use of renewable thermal resources and waste heat, reducing reliance on fossil fuels, and advancing the U.N. Sustainable Development Goals for Sustainable Cities and Communities, Affordable and Clean Energy, and Climate Action [81].

However, the high infrastructure cost and extensive planning effort required by district thermal energy systems hinder their adoption, motivating the consideration of new approaches [4]. This study is part of a larger effort seeking to address these challenges through development of a topology optimization framework for district thermal energy systems. The topology optimization framework seeks to minimize the life cycle cost associated with meeting the space conditioning requirements of a new or existing district, through answering the questions, "Which subset of buildings, if any, should be connected to a district thermal energy system, and by what thermal network should that subset be connected?" The size of the search space associated with this topology optimization problem grows factorially with the number of buildings considered. For example, for a district of 10 buildings, considering all potential subsets of the group of buildings, and all the potential networks by which they could be connected represents a number of potential configurations on the order of 10^{16}. This motivates the consideration of a heuristic to address the selection of the network by which a given set of buildings should be connected.

In this work, a graph theoretical interpretation is applied to the topology optimization problem. District thermal energy system network topologies are represented as "undirected graphs." An undirected graph comprises a set of vertices, or nodes, and a set of edges (unordered pairs of nodes) [5]. A graph can be represented by an *adjacency matrix,* $\boldsymbol{A}$, in which an element $A_{i,j} = 1$ if there exists an edge between nodes i and j and 0 otherwise. Additional relevant graph theoretical concepts are those of graph connectivity, cycles, and spanning trees. A graph in which there exists a path between each and every pair of nodes is considered a *connected graph.* A path that starts and ends at the same node, and passes through at least three distinct nodes is a *cycle* [5]. A *spanning tree* is a connected graph without cycles, and the spanning tree with the least total edge length is considered the minimal spanning tree. In this context, a network corresponding to the minimal spanning tree will connect a given set of buildings with the least infrastructure cost. However the minimal spanning tree network may not necessarily minimize energy-related costs, since additional thermal connections could potentially improve the efficiency of the network. In this study, the selection of the minimal spanning tree (MST) as the network to connect a given subset of buildings

is evaluated as a heuristic for the topology optimization problem, and will be referred to as the "MST heuristic."

This study and the larger effort focus on applications to fifth generation district heating and cooling (5GDHC) systems. 5GDHC systems circulate water at temperatures near ambient conditions (typically in the range of 15 –25 °C) and leverage water-source heat pumps at the connected buildings to further temper the water [7] either for heating or cooling. This study considers a 5GDHC system in a two-pipe configuration, with bi-directional mass flow permitted. A centralized heat pump maintains the network temperature within a desired range. Buildings are connected in parallel to the thermal network. An energy transfer station (ETS) serves as the interface between each connected building and the district thermal network. The ETS consists of a heat pump, heat exchanger, and a circulation pump. Based on the nature of the building's thermal load, water will be drawn from the network's "cool pipe" or "warm pipe" by the circulation pump. The moderate system temperatures allow individual buildings to add or reject heat to the network in a manner that offsets the load on centralized supply equipment, and would facilitate integration of waste heat and renewable thermal sources such as solar thermal and geothermal [4]. The use of electrically-driven heat pumps as the primary equipment, facilitated by the moderate system temperatures, is compatible with decarbonization of source energy, advancing targets in the U.N. Sustainable Development Goals for substantially increasing the share of renewable energy in the global energy mix [81]. Reducing the carbon intensity of space conditioning at the district scale, which can be accomplished through leveraging 5GDHC systems, represents a scalable approach for lowering carbon emissions, advancing targets in the U.N. Sustainable Development Goals for reducing the per capita adverse environmental impact of cities [2].

With opportunities for buildings to exchange heat synergistically through the thermal network, 5GDHC systems motivate consideration of more complex network topologies, including ring and meshed configurations. Conventional district thermal energy systems are generally configured with radial networks. Examples of these network types are shown in Figure 4.1. Past studies addressing topology optimization for district thermal energy systems have primarily focused on

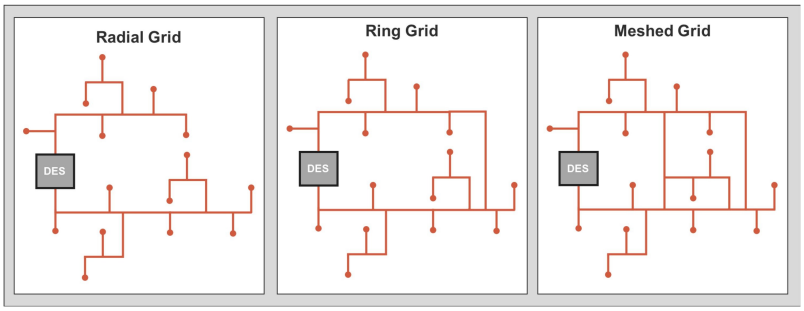

Figure 4.1: Grid topologies for district thermal energy systems, courtesy of [3].

heating-only systems, and a limited set of network configurations. The work of [24] solved an optimization problem for the network topology of a district heating system, including the location of the central plant, and pipe diameters, to minimize life cycle cost. The authors constrained the potential network topologies to exclude ring or meshed configurations, and the connection of each building to the district network was imposed as a boundary condition. Simplified building load profiles based on "time slices" were used. The authors approached the problem with genetic algorithms, and concluded that the relative locations of the buildings, the thermal load, and pressure and temperature requirements for the network significantly influenced the optimal topology.

The work of [25] optimized the network topology, pipe diameter, and supply and return temperatures of a district heating network for minimal life cycle cost. They cast the problem into three-sub problems, which they approached with linear and non-linear programming. The authors considered several scenarios of building locations and loads, and concluded that the optimal topology configuration was not readily generalizable.

A study by [26] performed topology optimization for a district heating and cooling network and compared the outcomes based on two different objective functions: capital cost and life cycle cost. The authors constrained the problem such that only radial and ring topologies were considered, and that the connection status of each building was a boundary condition. With analysis of a study case, the authors concluded that differences in pumping energy and heat loss through the networks led to different solutions associated with the two objective functions, highlighting

the importance of topology optimization. The authors of [26] called for future work in the area of topology optimization for district thermal energy systems to address more flexibility in the network configurations, and higher-fidelity load profiles.

This study, and the larger effort to which it contributes, addresses this need and offers a departure from past work, by considering the full space of potential network configurations, the option for buildings to be served by independent systems, and by leveraging high-fidelity building load profiles. 5GDHC systems, with bi-directional thermal and mass flow, offer greater potential rewards from topology optimization than conventional district thermal energy systems, and pose a more challenging problem, with the larger solution space of network configurations.

Design of a district thermal energy system typically begins with a feasibility assessment in which potential system types and technologies are identified, and parcels in a geographically-defined district are screened for suitability to connect to a district energy system, based on their current or expected base thermal loads, proximity to a potential central plant, and regulatory and economic factors. District thermal energy systems in the U.S. are often developed through a design-bid-build contractual structure, or built, owned, and operated by a third party [82]. Traditionally, design of district thermal energy systems has treated building loads as deterministic. However, the emergence of net-zero energy and other low-energy districts has motivated consideration of more integrated design approaches [83]. The development of the topology optimization framework addresses a need identified by [4] for "advanced energy system analysis tools of coherent systems" to enable the use of advanced district thermal energy systems in the context of increased penetration of renewable electricity generation.

4.1.3 Methods

In this study, an exhaustive search was performed to evaluate the MST heuristic for a prototypical urban district consisting of three multi-family buildings and a hospital. All possible networks that could serve a district consisting of four buildings and a central plant were analyzed, constituting 908 different cases. This topology optimization problem seeks to minimize a cost function representing

the life cycle cost of piping infrastructure for the district thermal energy system, and the energy required to meet the HVAC loads of all buildings in the district, whether or not they are served by the 5GDHC system. The cost function considered also accounts for a potential future price on carbon in the United States, based on a scenario outlined in [84]. The cost function is based on that implemented by [3] and is formulated as follows:

$$\begin{aligned}\min_{\mathbf{A}} & C_{pipes} + C_{elec} UPV_{elec}(E_{de} + \sum_{i=1}^{n} E_{be,i}) + C_{gas} UPV_{gas} \sum_{j=1}^{n} E_{bg,j} \\ & + UPV_{CO2} \sum_{t=1}^{20} m_{CO2}(t) C_{CO2}(t)\end{aligned} \tag{4.1}$$

subject to:

(1) If there exists a pipe directly thermally connecting building i and building j, $A_{i,j} = 1$. Otherwise, $A_{i,j} = 0$.

(2) If building i is served by the district thermal energy system, there exists a path from the central plant to node i.

$\mathbf{A} \in R^{(n+1) \text{ x } (n+1)}$: adjacency matrix describing the thermal network	UPV_{elec}: Uniform present value factor for electricity, accounting for projected escalation in rates
C_{pipes} : Cost of pipes and trenching	UPV_{gas}: Uniform present value factor for natural gas, accounting for projected escalation in rates
C_{elec}: Electricity cost rate	$m_{CO2}(t)$: Annual CO2 emissions, accounting for projections of reduced carbon intensity of electricity
C_{gas}: Natural gas cost rate	$C_{CO2}(t)$: Cost associated with CO2 emissions in a given year, per projections under a scenario by NIST
$E_{be,i}$: Annual electric consumption for HVAC at building i	UPV_{CO2}: Uniform present value factor associated with carbon pricing
E_{de}: Annual electric consumption for district energy systems, including primary equipment and distribution pumps	
$E_{bg,j}$: Annual natural gas consumption for HVAC at building j	

The twenty-year time horizon used for calculating the life cycle cost is consistent with that used in [3] for evaluation of a 5GDHC system. Note that a graph representing a network for a district with n buildings will have $n+1$ nodes, as one node of the graph corresponds to the central plant.

An energy model of the 5GDHC system, implemented in Modelica, was used to evaluate the energy consumption terms in the cost function. The underlying energy model was developed and

documented in [3]. Modelica is a "non-proprietary, object-oriented, equation-based language to conveniently model complex physical systems," such as systems containing mechanical, electronic, hydraulic, and thermal components [36]. The load side of the energy model was adapted to represent the prototypical urban district under consideration in this study. Building types to be included in the district were selected based on an evaluation of thermal load diversity, using a metric defined by [12]. This metric captures the extent to which simultaneous heating and cooling loads are present in the district, which enhance the potential for buildings to recover and reject heat synergistically, improving the exergetic efficiency of 5GDHC systems at the district level. The combination of buildings selected for this study, three multi-family buildings and one hospital, yield a value of the thermal load diversity metric of 0.63, exceeding the threshold of 0.60 identified by [12], for 5GDHC systems to exceed distributed building-level HVAC systems in exergetic efficiency. This study expands on previous work performed by the authors, which analyzed the spanning-tree scenarios only, for a prototypical district with less thermal load diversity present, documented in [85].

In the energy model of the 5GDHC system, building thermal load profiles were represented with data-driven metamodels, developed with the Metamodeling Framework documented in [31]. This is consistent with the approach taken by [3]. The use of metamodels to represent building loads, in comparison with full-order physics-based models, improves the simulation efficiency of the 5GDHC model, and the Metamodeling Framework has been demonstrated to represent building thermal load profiles accurately [31]. Under the Framework, a data set based on the U.S. DOE prototype building energy models for the applicable building types is used to train the metamodels [31]. The Framework offers several model types, and random forest models were selected in this study, based on their accuracy, and the computational efficiency of building the models [31]. Each building has two associated thermal load profiles: one for the case in which the building is connected to the 5GDHC system, and one for the case in which the building is served by independent systems.

Separate training data sets are used to generate metamodels for the "connected" and "independent" cases, i.e., when a building is connected to a district energy system or when it is served by its own dedicated building energy systems. The applicable DOE prototype building models are

Table 4.1: Characteristics of prototypical buildings considered in study.

Building Type	Floor Area(m^2)	Baseline HVAC System Type	Baseline EUI ($\frac{MJ}{m^2}$)
Multi-family	3,134	Packaged units with DX cooling and gas heating	436
Hospital	22,436	Variable-air volume with hot water reheat	924

used, with a parameter sweep, to generate the training data set for the "independent" case. For the "connected" case, the HVAC systems of the prototype building models are modified to use water-source heat pumps. Table 4.1 shows the characteristics of the prototypical multi-family and hospital buildings represented in this study.

The analysis was performed using weather data for Golden, Colorado. Natural gas and electricity rates obtained from the U.S. Energy Information Administration for Colorado in 2017 [77], and unit costs for pipes and trenching ($500/meter) from [3] were used in this study. The four hypothetical buildings and a district thermal energy system central plant were "placed" on a block in Golden, Colorado, for purposes of calculating pipe lengths.

4.1.4 Results and discussion

In order to evaluate the MST heuristic, the life cycle cost associated with each MST network was compared to the costs associated with the other possible networks connecting the same subset of buildings. For each of the fifteen possible subsets, the MST network resulted in either the minimal life cycle cost, or a life cycle cost that was within a negligible margin (1%) of the minimum. This is summarized in Figure 4.2, which shows the ratio of the life cycle cost of a given scenario to the life cycle cost of the MST for the same subset of buildings, as a function of the total pipe length, with scenarios color-coded based on the nature of the buildings connected to the network. Scenarios that represent an MST are depicted with stars, and for these scenarios the value of the ratio is naturally 1.0. (Note that for clarity, only scenarios with a total pipe length under 100 m are shown, which

encompasses all MSTs.)

In this case study, the life cycle cost (LCC) of a particular scenario was more influenced by the selection of the subset of buildings than the network by which they were connected. Figure 4.3 shows life cycle cost as a function of the total pipe length associated with each scenario, with the scenarios grouped by the nature of the buildings connected to the network. As shown in Figure 4.3, for the scenarios consisting of two or three connected buildings, the inclusion of the prototypical hospital building in the network resulted in a significantly higher LCC, due to the high heating load associated with this building, and the high cost of meeting that load with electricity as opposed to natural gas. (Note that in Figure 4.3, a representative sample of the datapoints with four buildings connected is shown, due to the large number of scenarios.)

Figure 4.4 shows a disaggregation of the LCC by component (energy, carbon, and infrastructure) for a randomly selected subset of the topology scenarios. Consistent with the subset represented in Figure 4.4, among all scenarios, the fraction of the life cycle cost attributable to energy costs ranges from 82% to 88%, the fraction attributable to carbon costs from 10% to 17%, and the fraction attributable to infrastructure does not exceed 2%. This dominance of costs related to energy and carbon (which is also proportional to the energy consumption) is attributable to the magnitude of the thermal loads of the prototypical buildings considered. The infrastructure costs are a function of the spatial locations of the buildings. Note that the nature of this disaggregation is not expected to extend to districts with buildings with lower energy use intensity, or lower spatial density, in which cases, the infrastructure costs would be expected to be more significant proportionately.

The small fraction of the LCC that is attributable to infrastructure costs in the scenarios resulting from this case study explains the lack of sensitivity of the LCC to the network by which the subset of buildings is connected. The selection of the network influences LCC through the infrastructure cost component, as well as through thermal interactions that influence the energy consumption of the network. Given the dominance of energy-related costs in the LCC, and the higher costs of electricity relative to gas per unit of delivered energy, a sensitivity analysis was

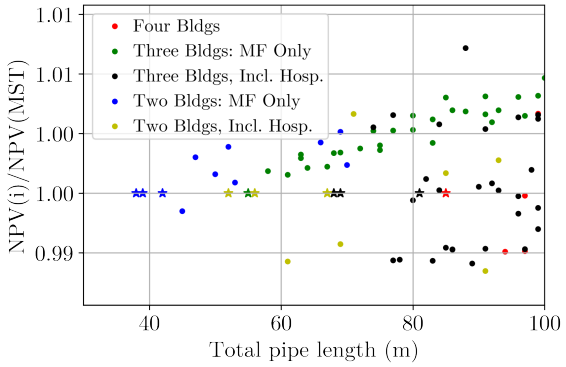

Figure 4.2: Ratio of life cycle cost to life cycle cost of MST as a function of pipe length for topology scenarios.

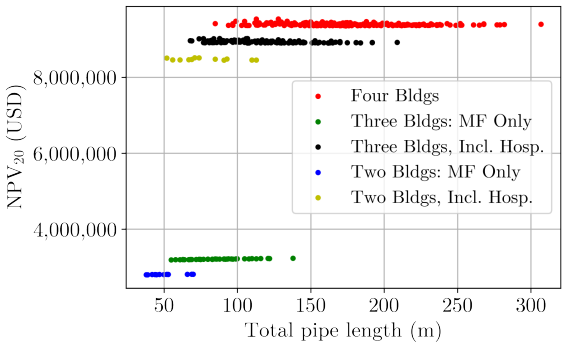

Figure 4.3: LCC as a function of pipe length for topology scenarios.

performed for the electricity cost value. The multiplier applied to the electricity cost was a proxy for a multiplier on the ratio between the electric and gas rates per unit of delivered energy. The results of this analysis are shown in Figure 4.5, for two different values of a ratio (R_{ele}) by which the base case electric rate was multiplied, R_{ele}=0.75, and R_{ele}=0.5.

As shown in Figure 4.5, the maximum and median values of the life cycle cost are reduced with the reduction in electric rates, and as a result, the range of values is also reduced. This shows that a reduction in the ratio of electricity to natural gas rates per unit of delivered energy would reduce the bifurcation of solutions shown in Figure 4.3, corresponding to the presence or absence of the prototypical hospital building in the network. (In the cases considered in the electric rate sensitivity analysis, the minimum values remain approximately the same, as they correspond to cases in which the largest heating load, associated with the hospital, is not connected to the district thermal energy system, and is thus served with natural gas.) This suggests that a reduction in electricity rates relative to natural gas rates could contribute to a greater influence of the network selection, as opposed to the subset of buildings served, on life cycle cost. A shift in building HVAC energy use in the "independent" systems case from natural gas to electricity, as would occur if building heating systems were electrified, would also be expected to increase the influence of the network selection for this reason.

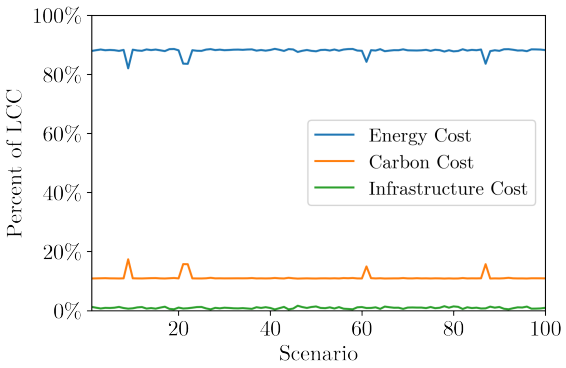

Figure 4.4: Disaggregation of life cycle cost by component for selected topology scenarios.

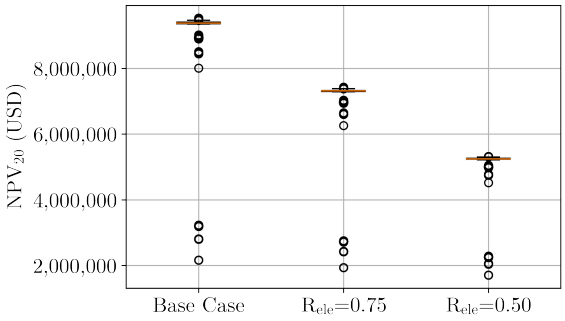

Figure 4.5: Box and whisker plot showing the range of life cycle costs for all scenarios, for the base case and for two cases with a multiplier (R_{ele}) applied to the electricity rates.

4.1.5 Conclusion

This study demonstrated that, for the prototypical urban district considered, with a relatively high degree of thermal load diversity, the MST heuristic is effective in selecting the "best" network by which to connect a given subset of buildings. In this study, due to the relatively high magnitude of the thermal loads present at each building, the selection of a network was relatively unimportant in influencing LCC relative to the selection of the subset of buildings.The results of this study support the inclusion of the MST heuristic in the proposed topology optimization framework. In the future, the MST heuristic will be evaluated for a larger prototypical district, with the integration of a waste heat source, and the robustness of the MST heuristic will be evaluated through Monte Carlo analysis of high-level parameters in the cost function. Future work could also potentially characterize the relative importance of the two elements of the topology optimization problem with a load diversity metric. Further development of the topology optimization framework will include implementation of an optimization algorithm for selection of the subset of buildings to connect to the network. Particle swarm optimization and other meta-heuristic algorithms will be considered, as they are compatible with the use of the Modelica simulation as a function evaluator. It is anticipated that the topology optimization framework, when complete, will result in a useful tool for planners, consultants, and engineers that can expand adoption of advanced district thermal energy systems

in appropriate applications, supporting progress towards the U.N. Sustainable Development Goals.

4.2 Evaluation of topology optimization to achieve energy savings at the urban district level

4.2.1 Abstract

Advanced district thermal energy systems have the potential to achieve significant energy savings and facilitate the integration of renewable thermal resources and waste heat, contributing to reductions in carbon emissions. Such systems, also known as fifth generation district heating and cooling (5GDHC) systems, circulate water at temperatures close to ambient, and leverage electrically driven water-source heat pumps located at connected buildings to further temper the water. However, barriers exist to the adoption of 5GDHC systems, including the factorial growth in potential network configurations as a function of the number of considered buildings. Topology optimization, which seeks to answer the questions, "Which is the best subset of buildings, if any, to connect to a district thermal energy system, and by what network should they be connected, to minimize life cycle cost?" can accelerate the adoption of 5GDHC systems. This study is part of an effort to develop a topology optimization framework for district thermal energy systems. In this study, a heuristic for one important aspect of the topology optimization problem—the use of the minimal spanning tree network to connect a given set of buildings at the least life cycle cost—is validated.

4.2.2 Introduction

Emerging technologies and design practices have enabled significant improvements in building energy performance [86]. Examining energy use intensity (EUI) beyond the level of an individual building, and at the level of an urban district, can unlock even greater reductions in energy use and associated carbon emissions [32]. Past studies have demonstrated that there is significant techno-economic potential for greater adoption of district energy systems (DES) in urban areas in the United States, and that advanced district thermal energy systems can meet targets for reductions in carbon emissions more cost-effectively than building-level systems alone ([87]; [46]).

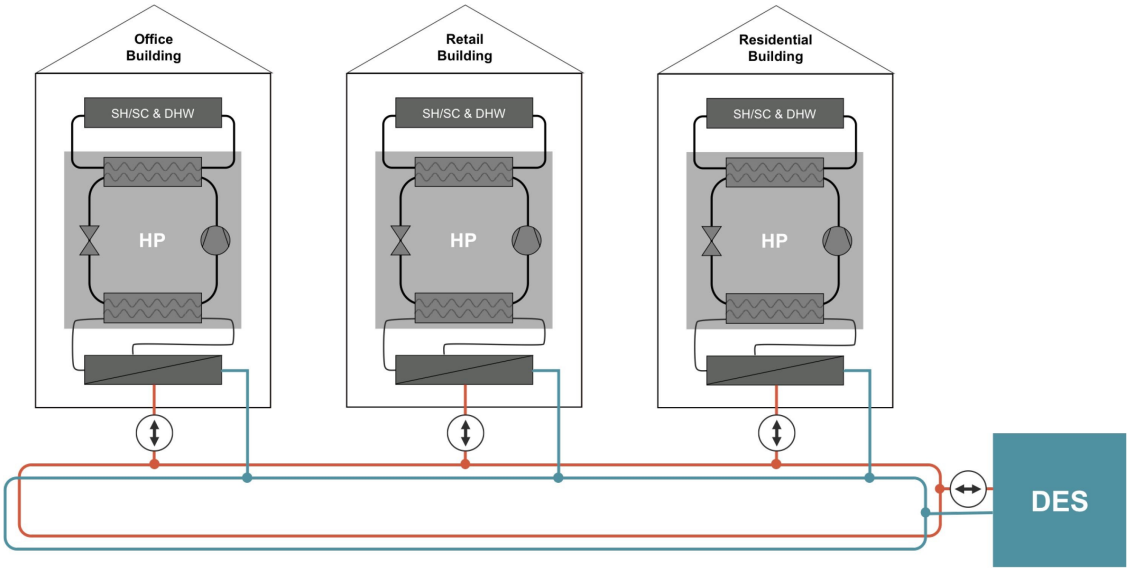

Figure 4.6: Schematic representation of 5GDHC system, courtesy of [3].

Past work has characterized the evolution of district thermal energy systems into either four or five generations, with the later generations circulating water as opposed to steam and leveraging more moderate temperatures [4]. As delineated in the work of [7], fifth generation district heating and cooling (5GDHC) systems are characterized by their use of water at temperatures close to ambient as a working fluid and leveraging water-source heat pumps located at connected buildings to further temper the water as needed to heat and cool the buildings. A schematic representation of such a system is shown in Figure 4.6. This configuration facilitates synergistic exchange of heat among connected buildings and processes, through bi-directional thermal flow, offsetting the requirements for active heating and cooling of the district loop, as well as facilitating the integration of waste heat and renewable thermal sources. However, barriers exist to the adoption of 5GDHC systems, including the factorial growth in potential network configurations as a function of the number of considered buildings. Topology optimization seeks to answer the questions: "Which is the best subset of buildings to connect to a district thermal energy system, and by what network should they be connected to minimize life cycle cost?" Topology optimization has the potential to accelerate the adoption of 5GDHC systems.

Network topology optimization is particularly relevant in the context of 5GDHC systems

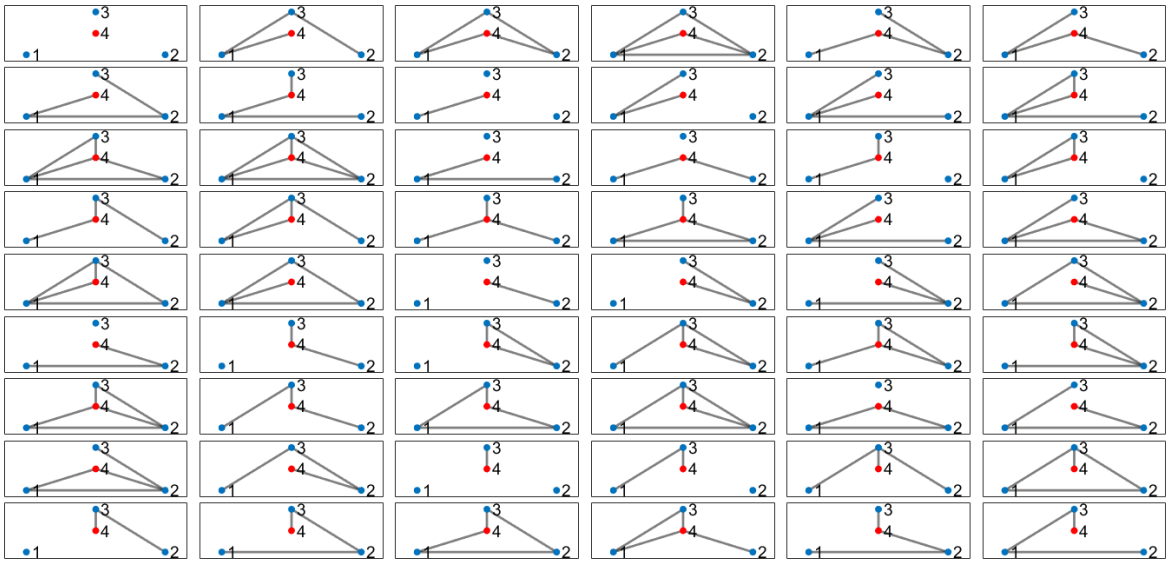

Figure 4.7: Topology optimization search space for district consisting of three buildings and DES plant, also presented in [6].

relative to earlier generations of district heating and cooling systems. "Conventional" district thermal energy systems circulating steam or hot water and chilled water are typically configured with radial networks, or with ring networks if redundancy of supply is essential [3]. The potential for synergistic thermal exchange among buildings tied to a 5GDHC system motivates consideration of ring or meshed networks ([58]; [59]). In the context of the network topology optimization problem, the number of potential thermal networks that could connect a subset of buildings in a given urban district grows factorially with the number of buildings considered and is a function of the number of subsets of buildings that can be selected from the district and the number of potential networks by which a given subset can be connected. Note that in this study, it is not assumed that every building in a given urban district will be served by a district thermal energy system. As an illustration of this concept, all potential networks that could connect buildings in a district consisting of three buildings and a central plant are shown in Figure 4.7.

This study is part of a larger effort to develop a topology optimization framework for district thermal energy systems. The goal of the framework is to assist urban planners and engineers in the design of advanced district thermal energy systems by determining the optimal subset of buildings

(if any) in an urban district to connect to such a system, and the optimal network by which to connect them. In this work, optimality is defined with respect to life cycle cost, encompassing costs associated with infrastructure, operating energy, and carbon. The very large "search space" associated with this optimization problem results in a computationally intractable problem: the search space is on the surprisingly high order of 10^{15} scenarios for a district consisting of 10 buildings, motivating consideration of heuristics to address this part of the problem.

Concepts from graph theory can be leveraged to describe thermal networks. In the mathematical context, an "undirected graph" consists of a set of nodes and a set of edges, which can be represented as unordered pairs of nodes [5] . Such a graph can be represented by an "adjacency matrix," a binary matrix with a number of rows and columns equal to the number of nodes of the graph, in which a given element of the matrix is equal to one if there exists an edge between the corresponding nodes, and zero if there does not [5] . An undirected graph provides a convenient structure for representing thermal networks with "nodes" corresponding to buildings or a central plant and "edges" corresponding to thermal connections. The "minimal spanning tree" (MST) is the graph connecting a given set of nodes with the least total edge length, while providing a path between any two nodes in the set [5]. In the context of DES, the MST represents the network that connects a given set of buildings with the least total length of pipes, thus minimizing the infrastructure cost. In this study, the use of the MST to identify the best (least life cycle cost) thermal network by which to connect a given set of buildings was evaluated as a heuristic for the topology optimization problem, substantially reducing the number of scenarios to be considered. Past work in the area of topology optimization for district thermal energy systems, such as that of [24], [60], and [27], has primarily focused on high-temperature heating-only networks, and has often addressed only radial networks, and treated the connection status of a particular building to a thermal network as a boundary condition. This study is distinct from past work because it addresses both the selection of the set of buildings to connect to a DES as well as the network by which they are connected, and considers 5GDHC systems, which introduce more complexities, and more interesting potential synergistic interactions among building loads, addressing a need

identified by [26]. This work builds on that of [3], who developed a model of a 5GDHC system and evaluated the performance of particle swarm optimization for the network topology optimization problem for a district consisting of three prototypical buildings, with a small search space of 54 scenarios.

4.2.3 Methods

In this study, the MST heuristic was evaluated by performing an exhaustive search of all potential network configurations for a prototypical urban district consisting of five buildings and a central plant and confirming that the MST indeed represented the network with the least life cycle cost to connect a given subset of buildings. The search space consisted of 30,770 possible scenarios, including the "null case" in which all buildings were served by independent systems, with 32 possible subsets of buildings in the district. For each subset, it was confirmed that the MST network had the least life cycle cost relative to other networks connecting the same subset of buildings, or a life cycle cost within a very small margin (0.1%) of the least life cycle cost.

For purposes of this study, the topology optimization problem was formulated based on minimizing the life cycle cost associated with the infrastructure for a district thermal energy system and operating energy costs for heating, ventilating, and air conditioning (HVAC), and associated carbon costs (assuming a carbon fee), for the urban district. The infrastructure cost was defined as the cost associated with pipes for the district thermal energy system. It was assumed that any cost difference between district-level and building-level HVAC generation and distribution equipment would be insignificant. Note that the costs associated with operating energy encompassed all buildings in the considered district, whether or not they were served by the district thermal energy system in a particular scenario. The life cycle cost was calculated for a 30-year time period. The

optimization problem was formulated as follows:

$$\min_{\mathbf{A}} C_{pipes} + C_{elec} UPV_{ele}(E_{de} + \sum_{i=1}^{n} E_{be,i}) + C_{gas} UPV_{gas} \sum_{j=1}^{n} E_{bg,j} + UPV_{CO2} \sum_{t=1}^{30} m_{CO2}(t) C_{CO2}(t) \tag{4.2}$$

where $\mathbf{A}$ is the adjacency matrix representing the connectivity of the thermal network; C_{pipes} is the cost associated with the infrastructure of the DES; C_{elec} and C_{gas} are the costs of electricity and gas per unit of consumption; UPV_{ele}, UPV_{gas}, and UPV_{CO2} are the uniform present value factors used to convert an annual cost to the value over the lifetime of the system for electricity, gas, and carbon, respectively; E_{de} is the energy consumption associated with the centralized DES heat pump and distribution pumps; $E_{be,i}$ is the electricity consumption for HVAC at a given building; $E_{bg,j}$ is the gas consumption for HVAC at a given building; $m_{CO2}(t)$ is the emissions of carbon dioxide associated with the district's energy use for a given year; and $C_{CO2}(t)$ is the unit cost of carbon dioxide emissions in a given year. Note that the gas consumption term exists because buildings with independent HVAC systems are served by gas heating systems. The uniform present value factors associated with electricity and natural gas account for expected escalation in the costs of these utilities projected by the National Institute for Standards and Technology, documented in the work of [88]. The real annual electricity cost escalation rates (between -4% and 2%) and natural gas cost escalation rates (0% to 9%) varied from year to year over the time period considered. Escalation of the carbon price also varies from year to year, ranging from 0% to 33% annually over the time period considered [74].

The economic inputs to the life cycle cost calculation considered in this study, and their sources, are summarized in Table 4.2. In this work, the energy consumption terms in the cost function were evaluated using an energy model developed in Modelica, an object-oriented, equation-based language that is often used for modeling physical systems [36]. Note that for purposes of this study, the calculated energy consumption was taken to be the same for each year in the considered

Table 4.2: Summary of economic parameters in life cycle cost calculation.

Parameter	Value	Source
Discount rate (%)	3%	[3]
Electricity cost, base year ($\frac{\$}{GJ}$)	27.8	[77]
Natural gas cost, base year ($\frac{\$}{GJ}$)	6.48	[77]
Carbon cost, base year ($\frac{\$}{mt}$)	20.0	[88]
Pipe cost ($\frac{\$}{m}$)	548	[26] and [89]

life span of the system (30 years). The model of a 5GDHC system was extended from one developed by [3] as the 5GDHC Topology Analysis Tool. The 5GDHC system considered, similar to the one represented in Figure 4.6, was configured with a two-pipe network, circulating warm water at 26 °C and cool water at 16 °C, with the loop tempered by a ground-source heat pump, and water-source heat pumps tempering the water further at each connected building. The mass flow rate at each building was controlled to maintain a 10°C temperature differential between the "warm pipe" and "cool pipe."

The prototypical district considered consisted of three multi-family buildings, a hospital, and a retail building. The building types were selected based on a thermal load diversity metric developed by [12]. The load diversity metric reflects the extent to which simultaneous heating and cooling loads exist in the district, which improves the exergetic efficiency of a 5GDHC system, by increasing the extent to which buildings can reject heat to or draw heat from the thermal network in a synergistic manner. In the work of [12], a threshold for the diversity metric was established (a value of 0.60), above which 5GDHC systems are likely to exceed distributed building-level HVAC systems in exergetic efficiency. The combination of buildings selected for this study, three multi-family buildings and one hospital, yield a value of the thermal load diversity metric of 0.58, close to this threshold. For purposes of calculating pipe lengths, the locations of the buildings were superimposed on an existing block in Golden, Colorado. The analysis was performed using the Typical Meteorological Year 3 weather file for Golden-NREL (724666).

Building heating and cooling loads were represented using data-driven metamodels, lever-

Table 4.3: Characteristics of prototypical buildings considered in study.

Building	Floor Area(m^2)	Individual HVAC System
Multi-family	3,120	Zone-level direct-expansion cooling and gas heating
Hospital	22,436	Variable-air volume reheat system served by water-cooled chillers and hot water boilers
Retail	2,2956	Roof-top units with DX cooling and gas heating

aging the Metamodeling Framework developed by [31]. The Metamodeling Framework has been demonstrated to represent building loads in an accurate manner and reduces the computational complexity of the district energy model relative to the use of full-order models to represent building loads [3]. The metamodels were trained based on data generated from the DOE prototype building models in EnergyPlus® [64]. Separate metamodels were trained to represent building thermal loads for the case in which the building was connected to the district thermal energy system, and the case in which the building was served by independent systems. For the metamodels representing the case in which the buildings were served by independent systems, the HVAC system types existing in the prototype building models were preserved. For the case in which the buildings were served by a district thermal energy system, the underlying EnergyPlus models were altered to represent a consistent HVAC system type, with water-source heat pumps tied to a heat source and sink at temperatures corresponding to that of the district loop. It was confirmed that the modified HVAC systems continued to meet thermal loads in the modeled buildings. Details of the prototypical buildings are summarized in Table 4.3.

Due to the computational burden of the energy model simulations, hierarchical clustering was performed on the building heating and cooling load profiles to select a smaller set of days to represent an entire year, following an approach similar to that outlined in the work of [90]. It was

found that a set of 30 days could represent the annual heating and cooling load profiles with a coefficient of variation of the root-mean squared error CV(RMSE) of 10.8% and 5.9%, respectively, which was deemed to be acceptable per criteria in ASHRAE Guideline 14 [91].

4.2.4 Results

In this study case, the nature of the set of buildings connected to the network was highly influential on the overall life cycle cost. As shown in Figure 4.8, the inclusion of the prototypical hospital building in the set of connected buildings was necessary in order for the life cycle cost of a particular scenario to be less than that associated with the "null case," in which all buildings are served by independent heating and cooling systems. The hospital building is the only prototypical building for which a connection to the DES results in lower annual building-level energy costs relative to independent systems. For all of the prototypical buildings, a connection to the DES results in lower source- and site-EUI (albeit a very slight reduction in the case of source EUI for the multi-family building), but the low costs of natural gas result in lower annual energy costs when independent systems are employed for the multi-family and retail buildings. Note that the DES considered uses only electricity for both heating and cooling. The prototypical hospital building benefits from a substantial reduction in EUI with a connection to the DES relative to building-level systems due to its year-round base cooling load, which, when the building is connected to the DES, can offset a simultaneous heating load through the shared water loop serving the building's heat pumps and through bi-directional heat and mass flow in the energy transfer station. Note that the zone-level HVAC systems implemented in the "connected" case for the hospital building also eliminate the use of reheat for temperature control. Figure 4.9 shows heating and cooling EUIs, on both a site and source basis, for the prototypical buildings considered, in both their "connected" and "independent" states. This benefit from simultaneous heating and cooling loads at the building level is consistent with results observed in other studies, including that of [92].

District-wide source EUI for HVAC follows a trend similar to the one observed for life cycle cost, as shown in Figure 4.10. Note that this EUI value encompasses energy consumption for

generation and rejection of heat at the building level and at the centralized heat pump serving the DES, and distribution pumping energy for the DES. Site-source multipliers for electricity and natural gas were obtained from [93]. The scenarios in which the hospital building is not served by the DES have a similar source HVAC EUI to the null case, as the prototypical hospital building has the largest thermal load. The scenarios in which the hospital building is served by the DES have an associated source EUI that is approximately 25% lower than that of the null case. This result highlights the potential reductions in source energy and associated carbon emissions from 5GDHC systems, as well as the benefits of optimization in the selection of the subset of buildings to connect to the network.

At a more granular level of comparison, Figures 4.12 and 4.13 show the trajectory of the cooling electricity requirements, and the heating energy delivered, for the multi-family building, over a summer and winter period, respectively. Note that in both the "DES-tied" and "independent" states, each of the prototypical buildings is served by electricity for cooling, but that natural gas provides most of the heating in the "independent" state, while the heating is fully electrified in the "DES-tied" state. Thus, the heating requirements of the two states are compared on the basis of heating energy delivered, and not energy input. The comparison between the two states for the multi-family building is similar to that for the two other prototypical building types considered. Source energy savings generally accrues in heating mode, due to the greater efficiency of heating with efficient heat pumps on a source-energy basis relative to natural gas-fired heating, while the end-use heating requirements of the building in the two states remains similar, as expected. In cooling mode, similar energy end-use requirements or an increase are exhibited through the DES connection. This is partially attributable to the nature of the shared condenser water loop that serves the water-source heat pumps in heating and cooling modes, which helps achieve a reduction in overall HVAC energy use through facilitating the ability of loads to offset each other, but can also appear to "penalize" energy consumption for cooling at the expense of improvement in heating when the energy use attributable to each is disaggregated.

Analysis of the results confirms that the MST network indeed represents the least-cost net-

work to connect any of the thirty-two subsets of buildings associated with the prototypical urban district considered, or results in a life cycle cost within 0.1% of that of the least-cost network. These results are summarized in Figure 4.11 with a plot of the "MST ratio" as a function of network length. The "MST ratio" is defined as the ratio of the life cycle cost of a given scenario to the life cycle cost associated with the MST connecting the same subset of buildings. The fact that the MST ratio is always greater than or equal to unity affirms the validity of the heuristic. Note that the network with the greatest life cycle cost to connect a given subset of buildings never exceeds the cost associated with the MST by more than 20%. In this case study, the selection of the subset of buildings to connect to the DES has more influence on life cycle cost, and source HVAC EUI, than the network by which they are connected. The nature of this result is consistent with expectations based on the type of network configuration considered, in which all loads are connected in parallel, with mass flow rates controlled to a fixed temperature differential. This ensures that all connected loads are served with the same supply temperatures (absent the relatively minute effects of heat loss and gain through the distribution system), and thus, the energy use associated with a connected load is not expected to be altered by the presence or absence of another load, or thermal connection.

For the set of possible networks connecting a given subset of buildings, the life cycle cost generally increases with the length of the network, as the infrastructure cost scales with the network length, and little variation in energy and carbon costs is observed among networks connecting the same subset of buildings. Thus, in Figure 4.11, a linear trend is generally observed in the MST ratio as a function of the total network length.

Figure 4.14 shows a disaggregation of life cycle cost for a random subset of the scenarios considered in this study. Among all scenarios considered, the fraction of life cycle cost attributable to energy costs ranged from 68% to 83%, carbon from 10% to 21%, and infrastructure, 0% to 22% (The null case, representing a scenario in which all buildings are served by independent systems, has no costs for DES infrastructure). The fact that infrastructure-related costs account for less than 25% of the overall life cycle cost in all scenarios in this case study is consistent with the

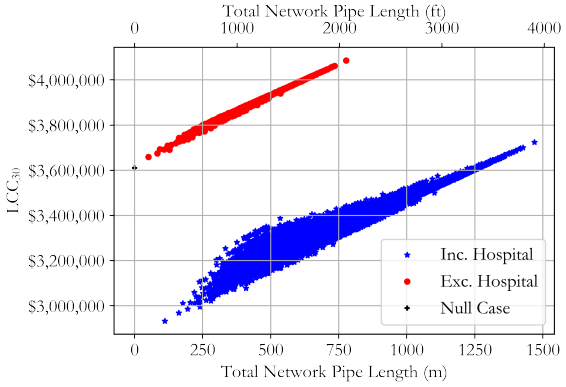

Figure 4.8: Life cycle cost (LCC) as a function of total network pipe length for all scenarios, sub-divided by whether they include or exclude the hospital building.

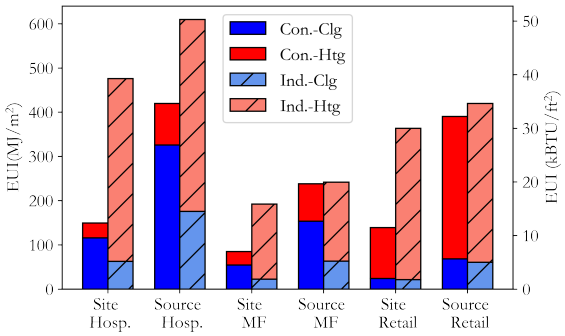

Figure 4.9: Building-level HVAC EUI for prototypical buildings considered.

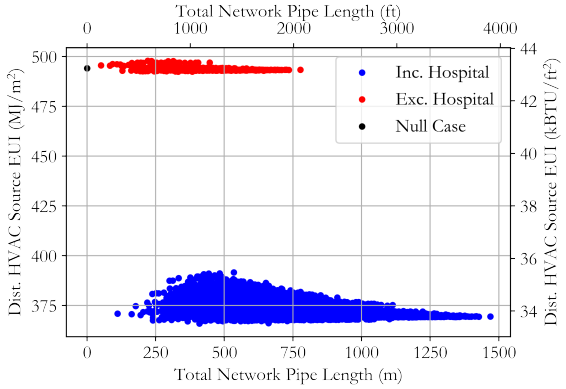

Figure 4.10: District-level HVAC source EUI as a function of total network pipe length for all scenarios.

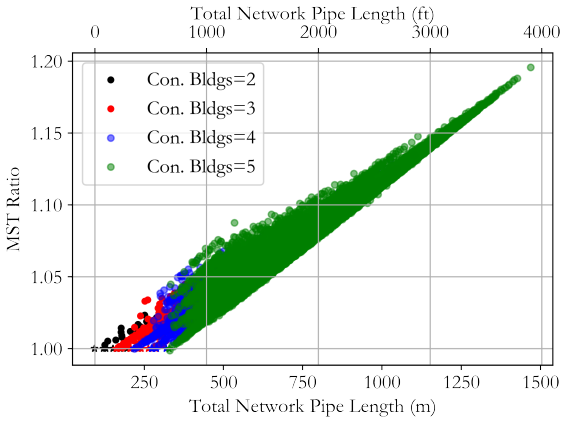

Figure 4.11: MST ratio as a function of total network pipe length for all scenarios considered in this case study.

fact that the selection of the subset of buildings has a greater influence on life cycle cost than the network by which they are connected.

4.2.5 Conclusion

This study has validated the use of the MST as a heuristic for identifying the thermal network with the least life cycle cost for connecting a given set of buildings in an urban district. This study also demonstrated a potential for significant reduction in HVAC-source EUI (on the order

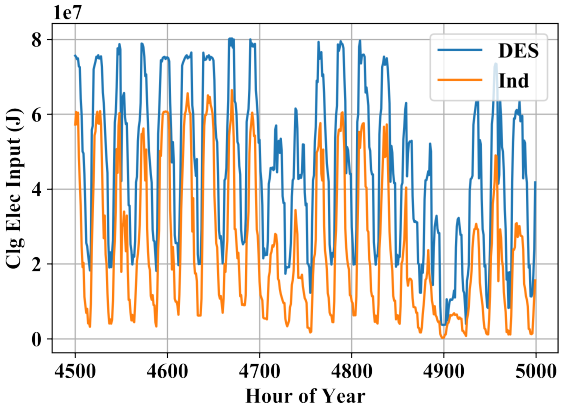

Figure 4.12: Cooling electricity required by the multi-family building, in independent and DES-tied states, during a summer period.

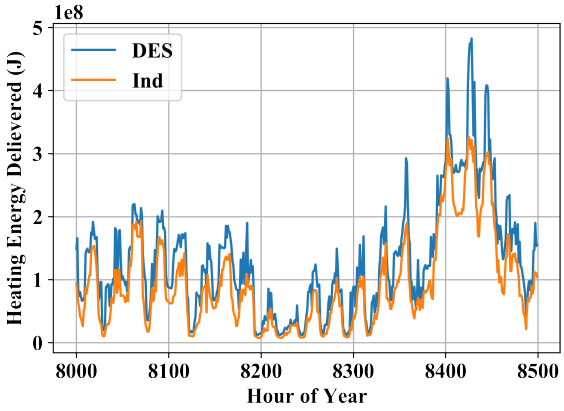

Figure 4.13: Heating energy delivered to the multi-family building, in independent and DES-tied states, during a winter period.

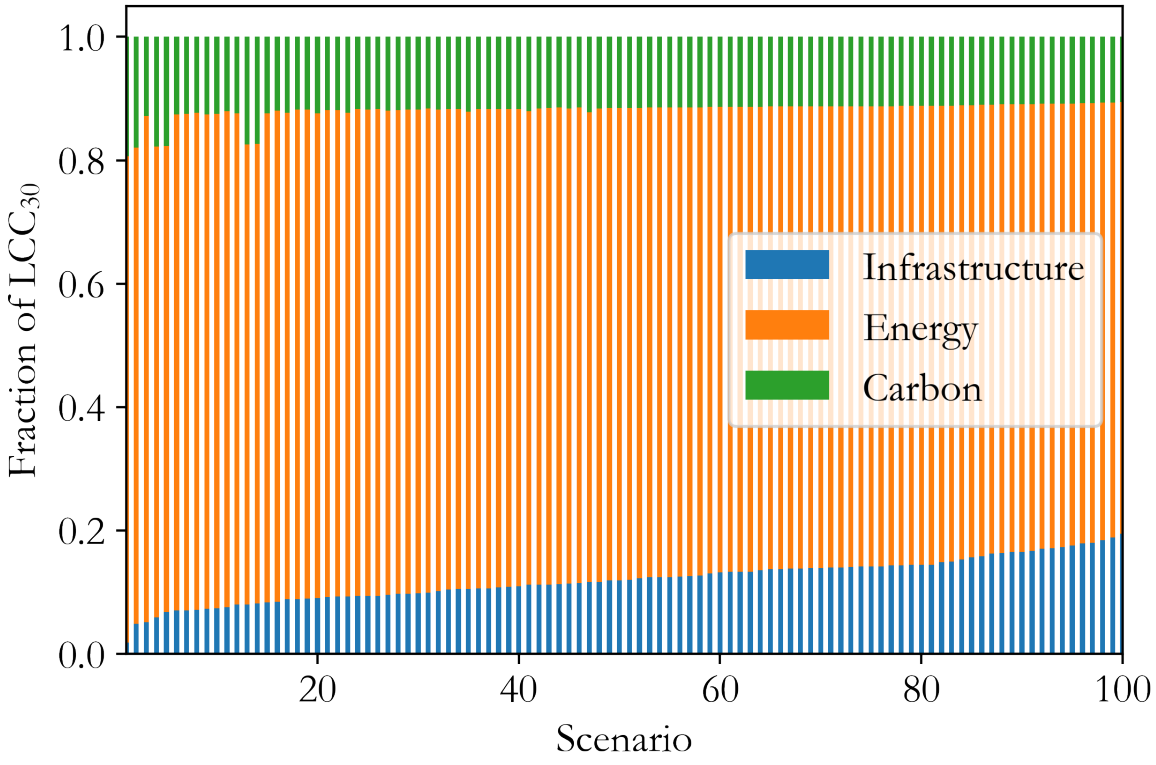

Figure 4.14: Disaggregation of life cycle cost for selected set of representative scenarios.

of 25%) from the use of a 5GDHC system with an optimally selected subset of buildings in an urban district, relative to independent, building-level HVAC systems. Future work will quantify the benefits of integration of available low-temperature waste heat into a similar 5GDHC network, which is expected to improve further the energy and economic performance of the 5GDHC network relative to independent systems. Future work will also investigate the use of an algorithm, such as particle swarm optimization, for selection of the "best" subset of buildings (if any) in an urban district to connect to a 5GDHC network. An approach for selecting the best subset of buildings will be combined with the MST heuristic to create a topology optimization framework for district thermal energy systems. It is anticipated that this framework will help facilitate the adoption of 5GDHC systems in appropriate applications, and contribute to energy and cost savings as well as reduced carbon emissions.

Chapter 5

Validation of particle swarm optimization for the network topology optimization problem

This chapter has been submitted for publication as:

A. Allen, G. Henze, K. Baker, G. Pavlak, and M. Murphy, Development of a framework for topology optimization of district thermal energy systems to achieve energy and cost savings. Energy Conversion and Management, submitted July 2021.

5.1 Abstract

District thermal energy systems operating at near-ambient temperatures have the potential to achieve significant reductions in energy-use intensity and carbon emissions, but face barriers to adoption due to their high infrastructure cost, and design challenges resulting from the large "search space" of potential network configurations. In this work, a topology optimization framework for such district thermal energy systems is presented to address those barriers. The approaches leveraged by the framework are validated, as is the performance of the framework with the implementation of an additional constraint.

5.2 Introduction

A scientific consensus has emerged that widespread electrification of space heating will be necessary to achieve significant reductions of carbon emissions cost-effectively and on the required time scale. A report recently issued by the U.S. National Academies of Science, Engineering, and Medicine called for electrification of heating in new construction in much of the United States by 2030, in order for the country to reach net-zero carbon emissions by 2050, and avert the worst consequences of climate change [94]. Given worldwide trends towards urbanization, it is expected that 68% of people will be living in cities by 2050 [95]. District thermal energy systems operating at near-ambient temperatures facilitate beneficial electrification of heating in urban districts, as well as significant reductions in source-energy use intensity in appropriate applications. However, such systems face barriers to adoption, especially in the United States, due to their high infrastructure costs, and the very large "search space" of potential network configurations, which complicates their design.

In this paper, a novel framework for network topology optimization of district thermal energy systems is presented, and the techniques that it leverages are validated. The Topology Optimization Framework ("Framework") is particularly relevant in the context of 5GDHC systems, but the general approach is extensible to other types of district thermal energy systems as well.

5.2.1 Fifth-generation district heating and cooling systems

Many authors have grouped district thermal energy systems into generations, distinguished by their working fluid (steam or water), and the range of temperatures of the working fluid. Recent studies have generally classified district thermal energy systems into four or five generations. This work will adopt the definition of fifth-generation district heating and cooling (5GDHC) systems proposed by [7]. Such systems are distinguished from earlier generations of district thermal energy systems through their use of water at near-ambient temperatures (15 °C - 25 °C) as a working fluid, and the use of water-source heat pumps at connected buildings, which operate with the network as a heat source and sink [7]. The near-ambient water temperatures used by 5GDHC systems are conducive to the integration of lower-temperature waste heat sources, as well as renewable thermal sources, and facilitate the use of electrically-driven heat pumps, and thus, the decarbonization of source energy for heating [4].

The more moderate operating temperatures of 5GDHC systems also creates the potential for connected loads to act as "prosumers", and exchange heat (or heat rejection) in a synergistic manner [76]. This motivates the consideration of meshed thermal network configurations, beyond the radial or ring networks that are commonly used in earlier generations of district thermal energy systems, and makes the question of network topology optimization especially relevant. Figure 5.1 illustrates common types of thermal network configurations.

5.2.2 Relevant concepts from graph theory

In this work, thermal networks will be described using concepts from graph theory. In mathematics, a "graph" is defined as a set of nodes (vertices) and edges (pairs of vertices) [5]. In the context of a thermal network, nodes represent connected loads and centralized supply equipment, and edges represent thermal connections (pipes carrying the working fluid). A graph can be represented with an "adjacency matrix", a square matrix with dimension equal to the number of nodes. A given element of the adjacency matrix has the value of unity if there exists a connection between

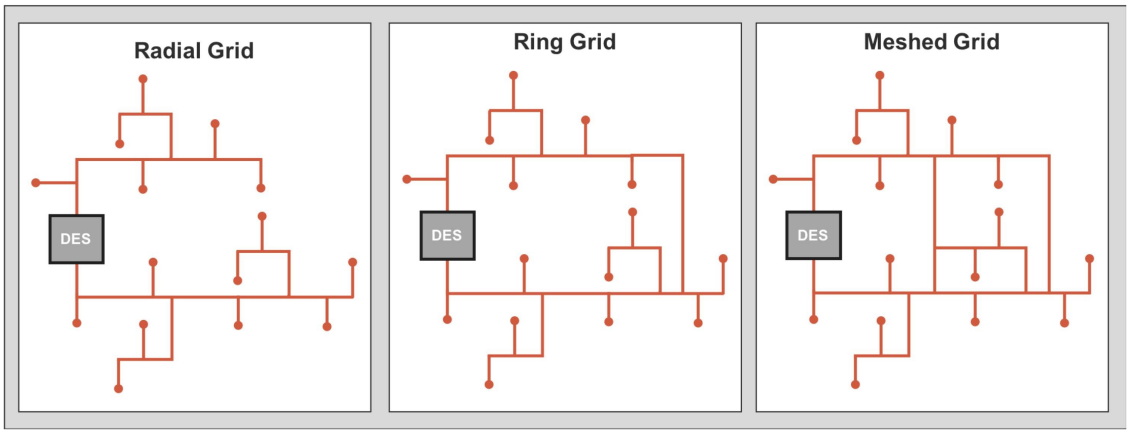

Figure 5.1: Notional representation of thermal network configurations, courtesy of [3].

the corresponding nodes, and a value of zero otherwise. Of particular interest in the context of thermal networks are "connected graphs", in which there exists at least one path between each pair of nodes. A "spanning tree" is a type of connected graph in which there exists *exactly* one path between each pair of nodes. A "minimal spanning tree" (MST) is the spanning tree that connects the given nodes with the least total edge length [5]. In the context of a thermal network, the MST minimizes the total network length, and thus, the infrastructure cost. In general, the infrastructure cost is often a significant fraction of the overall life cycle cost of a district thermal energy system [24].

5.2.3 Particle swarm optimization

Non-convex optimization problems motivate the use of so-called metaheuristic techniques, which, while not offering a guarantee of convergence at the global optimum, are often effective at finding near-optimal solutions, in an efficient manner (relative to an exhaustive search) [96]. Metaheuristics do not require an explicit definition of the objective function or its gradient, making them compatible with the use of a "black box" function evaluator. Most metaheuristic approaches incorporate some degree of stochasticity, which can help prevent the algorithm from getting "stuck" in a local optimum [96]. Particle swarm optimization (PSO) is one such metaheuristic approach. Like other metaheuristics, PSO mimics a search process. In the PSO context, "particles" can be

interpreted as animals acting as part of a swarm in the natural world, seeking a location that maximizes the value of a certain objective [97]. In an optimization problem, this corresponds to the value of the objective function at a given candidate solution, which is visited by a particle as it progresses through the search space. At each iteration of the algorithm, particles are assigned a "velocity," which is used to determine its next position in the search space. Particles retain knowledge of both their own prior best location, and that of the best location visited by any member of the group, and are attracted back to both of these locations, to varying extents. The balance between these two factors is described as a trade-off between *exploration* and *exploitation*. The *cognitive* parameter value scales the degree to which a particle is attracted to its prior best location, and the *social* parameter scales the degree to which a particle is attracted to the global best location [97]. In some implementations of PSO, each particle can "communicate" knowledge of its best position with only a subset of other particles in the swarm. That implementation is known as *local best* (*lbest*) PSO, and the set of particles that can communicate with each other is known as a *neighborhood*. Implementations in which all particles in the swarm can communicate with each other are known as *global best* (*gbest*) PSO [97].

For application to the network topology optimization problem for district thermal energy systems, the implementation of PSO for problems with discrete, binary variables is of interest. The work of [39] developed such an approach, and conceptualized each dimension of the velocity vector as the probability that the corresponding dimension of the position vector would "flip" from one binary value to the other. In the work of [39] the position of a particle $x_{i,j}(t+1)$ (with i being the index in the swarm, and j the dimension) is determined as follows:

$$x_{i,j}(t+1) = \begin{cases} 0, \text{if rand}() \geq S(_{v_{ij}}(t+1)) \\ 1, \text{if rand}() < S(_{v_{ij}}(t+1)) \end{cases} \tag{5.1}$$

where the sigmoid function $S(x)$ is defined as:

$$S(x) = \frac{1}{1 + e^{-x}} \tag{5.2}$$

and the particle's velocity $v_{i,j}(t+1)$ is determined as:

$$v_{i,j}(t+1) = wv_{i,j}(t) + c_1 r_{1j}(t)[y_{ij}(t) - x_{ij}(t)] + c_2 r_{2j}(t)[\hat{y}_j(t) - x_{ij}(t)] \tag{5.3}$$

where w is the inertia weight, c_1 is the cognitive component, c_2 is the social component, $y_{ij}(t)$ is the particle's previous best position, $\hat{y}_j(t)$ is the best position of a particle in the "neighborhood," and $r_{1j}(t)$ and $r_{2j}(t)$ are random numbers.

5.2.4 Optimization of district thermal energy systems

There is an extensive body of work in the area of optimization of different aspects of district thermal energy systems, including network topology and operating parameters, across different system generations. Past studies can be distinguished based on the type of cost function considered, as well as the generation of system, which has implications for the optimization variables. Many past studies addressing network topology optimization have focused on district heating networks only, or uncoupled district heating and cooling systems. The work of [24] addressed a network topology optimization problem to minimize a life cycle cost metric for a district heating system operating at 55 °C. The life cycle cost metric considered encompassed infrastructure (pipes and distribution pumps), energy associated with pumping and heat losses, and a carbon tax. The optimization variables included pipe diameters (with a zero diameter corresponding to the non-existence of a thermal connection) and the location of a central heating plant. The authors formulated the problem as a mixed-integer nonlinear programming problem (MINLP), and employed genetic algorithms to solve it. Only tree network topologies were considered, and the connected building loads were taken as a boundary condition.

The work of [26] addressed a network topology optimization problem for a third-generation district thermal energy system, to minimize a life cycle cost based on costs for piping and trenching, and a limited set of operating costs. The authors compared the optimal network configuration they determined to the network with minimal first cost, and found limited benefits in life cycle cost, though a more significant savings in terms of the internal rate of return. The authors of [26] treated the connected loads as a boundary condition, and also treated the energy consumption of centralized equipment as static. They identified addressing the selection of loads to connect to a district energy system as an area in which further work was needed.

Other past studies have taken a multi-objective approach to optimization of district thermal energy systems. The work of [98] solved an optimization problem for the network topology and selection of primary equipment for a district heating network, to minimize life cycle cost and carbon emissions, using an ϵ-constrained approach. The authors of [98] compared the optimally-designed district heating network to a scenario in which buildings were served by independent heating systems, and found a 23% reduction in carbon emissions, for the same initial investment.

The work of [23] optimized the supply temperature for a 5GDHC system to minimize energy use, using the Nelder-Mead method, with an agent-based control approach implemented to maintain the loop setpoint. They identified energy savings of around 15% from implementing the optimal setpoint, relative to allowing the setpoint to float freely in the range of 12 °C to 20 °C. The authors of [23] also compared the energy consumption associated with uni-directional and bi-directional 5GDHC networks, and found that bi-directional networks saved energy in the two climate zones that they considered.

The work of [99] applied adjoint-based methods to an optimization problem for a district heating system, with the optimization variables including the network topology and pipe diameters, as well as valve positions at connected loads, and the rate of heat supplied by individual pieces of centralized equipment. The authors considered an objective function based on the investment cost of piping and distribution pumps, and the operating cost for pumping. They developed an approach to project a continuous-valued diameter variable onto a set of discrete values of available

pipe diameters, using a modified version of the *projection method* often used in structural topology optimization, and structured the cost function to penalize intermediate values of this variable. The use of adjoint-based methods, in conjunction with constraint aggregation facilitated a large-scale analysis, considering a network with 160 connected loads. Through their topology optimization approach, they identified a network with a 23% reduction in piping cost relative to a base case. The connectivity status of the loads was taken as a boundary condition.

The presented Topology Optimization Framework is novel because it addresses both the selection of loads to connect to a district thermal energy system, as well as the network by which they should be connected (fulfilling a need identified by [26]), and addresses investment and operating costs in a comprehensive way, accounting for all HVAC-related energy consumption by a considered district. The compatibility with an underlying energy model of high fidelity makes it suitable for detailed analysis of potential trade-offs, and distinct from past approaches to network topology optimization for district energy systems, which have focused on model formulations oriented around specific sets of conditions. The framework has been evaluated in case studies involving 5GDHC systems with bi-directional thermal and mass flow in the context of which network topology optimization is particularly interesting and relevant, though it can be applied to district thermal energy systems of any generation. The development of the Topology Optimization Framework builds on the work of [3] and extends previous work by the authors to evaluate the energy-savings potential of 5GDHC systems coupled with low-exergy building level systems [6], and to evaluate the minimal spanning tree heuristic [100].

5.3 Methods

The presented Topology Optimization Framework ("Framework") seeks to address the question, for a given urban district, with known building locations and loads, "What is the best subset (if any) of buildings to connect to a district thermal energy system (DES), and by what network should they be connected, to minimize life cycle cost?" It was hypothesized that a particle swarm optimization (PSO) algorithm could effectively identify the optimal subset of buildings, and that

the minimal spanning tree (MST) heuristic could effectively select the optimal thermal network by which to connect them. The following subsections describe the formulation of the optimization problem, and how these approaches were evaluated in the context of a prototypical district.

5.3.1 Optimization problem

The cost function considered in the network topology optimization problem represents the life cycle cost (LCC) associated with meeting the heating and cooling loads of all buildings in the prototypical district, whether they are served by independent systems or the DES. The LCC considered includes energy costs for HVAC, costs associated with a potential future price on carbon, and infrastructure costs for the thermal network of the DES, evaluated over a thirty-year time period. It was assumed that any differential in costs for building-level HVAC systems observed between buildings tied to the DES and buildings with fully independent HVAC systems would be small relative to the overall LCC. The LCC is calculated as shown in Eqn. 5.4:

$$\begin{aligned}\min_{\vec{L}} & C_{pipes} + C_{elec} UPV_{elec}(E_{de} + \sum_{i=1}^{n} E_{be,i}) + C_{gas} UPV_{gas} \sum_{j=1}^{n} E_{bg,j} \\ & + UPV_{CO2} \sum_{t=1}^{30} m_{CO2}(t) C_{CO2}(t)\end{aligned} \tag{5.4}$$

subject to:

(1) For $i, j \in \{1 \dots n+1\}$, such that $j > i, A_{i,j} = L_{i+j-1}$

(2) If there exists a pipe directly thermally connecting building i and building j, $A_{i,j} = 1$. Otherwise, $A_{i,j} = 0$.

(3) If building i is served by the district thermal energy system, there exists a path from the central plant to node i.

(4) $\forall i, j \in \{1 \dots n+1\}, A_{i,j} = A_{j,i}$.

where $\mathbf{A}$ is the adjacency matrix corresponding to the thermal network, $\vec{L}$ is a vector corresponding to the upper-triangular elements of the adjacency matrix, C_{pipes} is the cost of pipes and trench-

ing, C_{elec} is the electricity cost per unit of consumption, C_{gas} is the natural gas cost per unit of consumption, $E_{be,i}$ is the annual electric consumption for HVAC at building i, E_{de} is the annual electric consumption for the centralized heat pump, $E_{bg,j}$ is the annual natural gas consumption for HVAC at building j, n is the number of buildings considered, UPV_{elec} is the uniform present value factor for electricity, UPV_{gas} is the uniform present value factor for natural gas, $m_{CO2}(t)$ is the annual carbon emissions in a given year, $C_{CO2}(t)$ is the cost associated with carbon emissions in a given year, and UPV_{CO2} is the uniform present value factor associated with carbon pricing. Note that since, in the context of this application, the adjacency matrix $\mathbf{A}$ must be symmetrical, it can be represented with its upper-triangular elements only. The total number of network nodes is equal to $n + 1$, corresponding to all buildings considered and the centralized heat pump.

The uniform present value (UPV) factors are used to convert a cost incurred in one year to a cost over 30 years, accounting for the time value of money at a 3% discount rate. The UPV factors applied for natural gas and electricity account for projected escalation in the costs of those commodities. Note that the time-dependence of carbon emissions and their associated cost is due to the projected future reduction in carbon intensity of electricity in the US, and the consideration of a potential future price on carbon, which escalates over time, in a scenario developed by [88]. The cost function was originally adapted from that used by [3]. Note that the framework's approach is generally extensible to other cost functions based on energy consumption. Table 5.1 shows a summary of values of parameters used in the LCC calculation.

5.3.2 Prototypical district

An exhaustive search, considering all potential thermal network configurations, was performed for a prototypical urban district in order to evaluate the performance of the MST heuristic and the implementation of PSO. The prototypical district consisted of three multifamily buildings, a retail building, and a hospital. An energy model in Modelica was used to calculate the energy use associated with the district thermal energy systems. Modelica is an equation-based, acausal modeling language that is often used for representing physical systems [36]. The energy model was

Table 5.1: Summary of values of economic parameters used in LCC calculation.

Parameter	**Value**	**Units**	**Source**
Discount rate (%)	3%	NA	[3]
Electricity cost, base year	27.8	$\frac{\$}{GJ}$	[77]
Natural gas cost, base year	6.48	$\frac{\$}{GJ}$	[77]
Carbon cost, base year	20.0	$\frac{\$}{mt}$	[88]
Piping and trenching cost	548	$\frac{\$}{m}$	[26]

extended from one developed by [3]. The district thermal energy system modeled operated in a two-pipe configuration, with the "warm pipe" at 26 °C, and the "cool pipe" at 16 °C. A central ground-source heat pump controlled the network temperature.

The U.S. Department of Energy's Prototype Building Models, which are intended to be representative of the characteristics of common commercial building types in the US, and are available in EnergyPlus format, were used to generate the building load profiles [35]. The Prototype Building Models are adapted from the Commercial Reference Building Models, whose development is documented in [101]. The building types were selected in order to create a sufficient level of thermal load diversity, based on the value of a metric proposed by [12]. Higher levels of thermal load diversity in a district increase the potential level of source energy use intensity reductions from a 5GDHC system [12], due to the ability of connected buildings to "offset" each other's loads. For purposes of calculating pipe lengths, these buildings were plotted on an existing block in Golden, Colorado. Figure 5.2 shows a rendering of the district for illustrative purposes. Note that this district was not intended to represent actual buildings at that location.

Since the life cycle cost calculation includes the HVAC energy use of all buildings in the prototypical district, whether or not they are tied to the DES in a particular scenario, a separate energy model is required to represent each building in its "DES-tied" and "independent" cases. In

Table 5.2: Summary of characteristics of prototypical buildings.

Building	**Floor Area** m^2	**Individual HVAC System**
Hospital	22,436	Variable-air volume reheat system served by water-cooled chillers and hot water boilers
Multifamily	3,120	Zone-level direct-expansion cooling and gas heating
Retail	2,295	Roof-top units with DX cooling and gas heating

the "DES-tied" cases, the HVAC systems in the building models were modified to be compatible with hydronic systems. The existing building-level HVAC equipment was replaced with water-source heat pumps. In the "independent" case, the HVAC systems present in the prototype building models were preserved. Table 5.2 summarizes attributes of the prototypical buildings considered. In order to integrate the building energy models with the district model in a computationally efficient manner, data-driven metamodels based on the physics-based models were used to represent the building-level HVAC energy use. The Prototype Building models were used to generate a data set over a sweep of parameter values, and random forest models were trained on the data using the Metamodeling Framework developed by [31].

5.3.3 Evaluation of minimal spanning tree heuristic

An exhaustive search, evaluating the life cycle cost of each potential network configuration corresponding to the five-building prototypical district (a total of 30,770 possible configurations), was performed in order to validate the MST heuristic. For each possible subset of connected buildings, the life cycle cost of the minimal spanning tree network was compared to that of all other possible networks to determine if, in fact, the minimal spanning tree corresponded to the least-cost network. There are thirty-two such subsets, including the "null set", in which all buildings are served by independent systems.

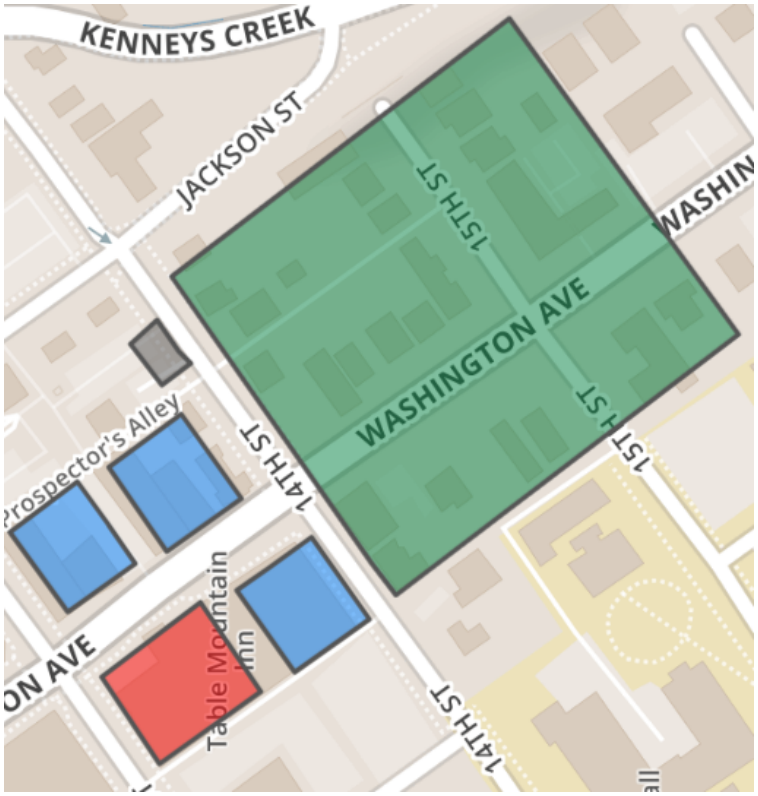

Figure 5.2: Prototypical district for evaluation of MST heuristic and PSO implementation, with the prototypical hospital building shown in green, the prototypical multi-family buildings shown in blue, the prototypical retail building shown in red, and the central plant in brown.

5.3.4 Evaluation of particle swarm optimization

An implementation of the PSO algorithm was evaluated, through comparison of the solution determined by the algorithm to the "ground truth" determined by an exhaustive search of all possible scenarios. This was performed for six cases, distinguished by values of key parameters in the objective function (life cycle cost), in order to affirm the robustness of the conclusion. Parameter values such as costs for energy and carbon in the objective function effectively "weight" different components of the life cycle cost, and thus, varying them potentially alters the solution to the problem, making these changes meaningful extensions of the ground-truth data set.

For programmatic implementation, which was necessary for the evaluation of PSO, the constraints to the optimization problem were formulated in a slightly different manner than previously described. (The objective function was formulated as shown in Eqn. 5.4.) The constraints were implemented in the following manner:

(1) For $i, j \in \{1 \dots n+1\}$, such that $j > i, A_{i,j} = L_{i+j-1}$

(2) $\sum_{i=1,j=1}^{n+1} A_{i,j} = 0$ or $\sum_{j=1}^{n+1} A_{1,j} \geq 1$ and $\sum_{k=0}^{m-1} B^k$ is positive

where node 1 corresponds to the central plant, and $\mathbf{B}$ is an adjacency matrix of dimension m that has been constructed to represent the thermal connectivity of only the loads served by the DES, with $B_{i,i} = 1$ for all $\forall i \in \{1 \dots m\}$. Recall that a "positive" matrix is one in which all elements are greater than zero. This constraint corresponds to confirming that either there are no connected loads, or, if there are, a modified version of the adjacency matrix (representing just the connected loads), is irreducible. Since this modified adjacency matrix has been constructed to have values of unity along the diagonal, this is equivalent to representing a connected graph [5]. Thus, constraint 2 above effectively ensures that any candidate solution conforms to constraint 3 in Eqn. 5.4. The constraint was implemented through returning a high "penalty" value of the cost function

for candidate solutions that violated it. This approach is consistent with that taken by [102], as well as other authors. Constraints 2 and 4 from Eqn. 5.4 are incorporated implicitly, through the approach by which candidate solutions are interpreted in this context.

For each valid candidate solution, the energy model (in FMU format) was modified to represent the thermal network connectivity corresponding to the candidate, using the PyFMI Python package. The PyFMI package was then used to simulate the model [103]. The energy consumption values calculated by the simulation, and the static LCC parameter values were then used to calculate the life cycle cost. Details of the convergence criteria and other aspects of the implementation are discussed in more detail in the following subsection.

Implementation of particle swarm optimization The formulation of the PSO algorithm for a problem with discrete, binary, variables was implemented, using the PySwarms package in Python [41]. For each of the six sets of LCC parameter values considered, the PSO algorithm was executed for a fixed number of iterations, in order to form a consistent basis of comparison. Comparison of the performance of implementations of PSO based on the solution returned after a fixed number of iterations is consistent with the approach taken by [40], among others. Based on the conclusions of past studies that the relative performance of *gbest* and *lbest* is problem-dependent, both forms of the PSO algorithm were initially evaluated for this problem. The lbest algorithm was evaluated using a ring topology, based on the general recommendation of [104]. In the evaluation of *lbest*, three neighborhood sizes (25%, 50%, and 75% of the swarm size) were considered. These swarm sizes are consistent with the range recommended by the work of [105]. In past studies, the performance of the PSO algorithm has been evaluated based on the best value for the objective function returned after a fixed number of iterations [106], and, additionally, on the number of iterations required for the algorithm to reach a certain criteria value of the objective function [107]. In this case, since all implementations of the algorithm succeeded in returning the solution to the optimization problem within the considered number of iterations, a selection was made based on the fraction of the total number of iterations required for convergence to the solution. Due to the

superior performance on this metric of the *lbest* implementation with a neighborhood size equal to 25% of the swarm size, it was selected for implementation in the full analysis. As a proportion of the swarm size, the size of this neighborhood is consistent with the recommendations of [105] based on an empirical analysis. In an initial evaluation of the particle swarm algorithm, it was observed that, in the absence of any control of consideration of duplicate values, a significant proportion (as high as 60%) of values considered were duplicates. Consistent with the work of [102] and [108], a "taboo list" was implemented. In this work, the "taboo list" served to improve the computational efficiency by simply "looking up" the already-determined objective function value for the repeated solution and returning it, instead of re-evaluating the cost function. The repeated value was not penalized with a high value of the cost function.

In this implementation of PSO, the cognitive and social parameters were set such that $c_1 = c_2 = 1.7$, based on guidance from [104] that $c_1 = c_2$ and from [109] that $1.4 \leq c_1, c_2 \leq 2$. The work of [104] reports that the values of the cognitive and social parameters are generally static, and determined empirically. Additionally, an empirical study by [110] demonstrated that fixed values for the cognitive and social parameters resulted in better performance than the use of dynamic values. The inertia weight w was set to a fixed value of 0.85 based on a recommendation by [104] that $1 > w > 0.5(c_1 + c_2) - 1$. The use of $c_1 = c_2$, the selection of a fixed value for w and the magnitudes of c_1, c_2 and w are also consistent with the approach taken by other studies, including that of [105].

In the literature, swarm sizes ranging from 15 to 50 particles have been reported ([102], [97], [40], [105], [111], among others). Swarm sizes of both ten and twenty particles were initially evaluated in this study, and the algorithm's optimization performance was similar in both cases. (See the Appendix for more details of this initial evaluation.) To improve the efficiency of the analysis, a swarm size of 20 particles was used, and evaluation of the particles was executed in parallel.

Based on the work of [112], a threshold for the CV-RMSE of the objective function values for the swarm relative to that of the best objective function thus far was implemented as a convergence

criterion, with CV-RMSE and RMSE defined as shown in Eqn. 5.5:

$$RMSE = \sqrt{\frac{\sum_{i=1}^{n}(y_i - o_{best})^2}{n}} \qquad (5.5)$$
$$CV - RMSE = \frac{RMSE}{var(\vec{y})}$$

where $\vec{y}$ contains the objective function values of the swarm's particles at the current iteration, o_{best} represents the best value of the objective function found thus far, n corresponds to the number of particles in the swarm, and var refers to the variance.

In several trial evaluations of the PSO algorithm, it was observed that the CV-RMSE was often small in magnitude, and did not change significantly, over the execution of the algorithm–that is, that while the particles found improved values of the objective function, they did not "converge" in position over repeated iterations. Thus, an additional criterion for termination of the algorithm was implemented, based on "stall", under which the algorithm will terminate if the global best value of the objective function has not improved for a certain number of iterations. Based on several test evaluations, the number of iterations to trigger termination based on stall was set at 40% of the maximum number of desired iterations. In this implementation of PSO, the maximum number of iterations was set at 500.

Selection of life cycle cost parameter values The six scenarios, distinguished by their parameter values, were selected such that each one resulted in the optimal solution consisting of a different number of buildings served by the thermal network. These parameter values were selected by leveraging the Monte Carlo Simulation Framework (MCS Framework) for 5GDHC Systems, which will be documented in the work of [38]. The MCS Framework performs Monte Carlo analysis varying the values of parameters in the life cycle cost function, to enhance the extensibility of the exhaustive search performed for the five-building prototypical district.

For the prototypical district previously introduced, utility costs were generally found to ac-

count for at least 60% of the LCC across all scenarios. For this reason, parameters related to utility costs–natural gas and electricity rates–were selected to distinguish the scenarios, in addition to the carbon intensity of electricity, and the unit cost of piping and trenching. The carbon intensity of electricity in the US is expected to continue to decline significantly over the next 30 years [88], and from a review of relevant literature, there is a substantial range in the expected unit cost of piping and trenching [26]. The considered range of values for the utility costs was selected based on data from the continental US between 2013 and 2018, and for carbon intensity of electricity, for data from the continental US between 1990 and 2018 [77]. The range of values for the unit cost of piping and trenching was selected based on an extensive literature review, including the work of [26], [60], and [25]. The selected values of parameters for these scenarios are shown in Table 5.3.

Table 5.3: Summary of scenarios for PSO evaluation.

Number of connected buildings	Elec. cost $\frac{\$}{kWh}$	Gas cost $\frac{\$}{therm}$	Elec. carbon intensity $\frac{kg}{kWh}$	Pipe cost $\frac{\$}{m}$
0	0.14	0.57	0.38	922
1	0.15	0.76	0.44	436
2	0.15	1.25	0.75	324
3	0.12	1.20	1.0	311
4	0.11	1.40	0.76	1130
5	0.09	1.20	0.55	815

5.3.5 Constraint evaluation

The performance of the framework was also evaluated in the context of an additional constraint to require a minimum of two direct thermal connections for each connected load, to represent a requirement for redundancy of supply. This constraint was formulated as shown in Eqn. 5.6:

$$\forall i \in \{1 \dots n+1\}, \sum_{j=1}^{n+1} (A_{i,j}) \neq 1 \tag{5.6}$$

where $n+1$ is the dimension of the adjacency matrix, a square. This constraint ensures that each considered load has exactly zero thermal connections, or more than one. The framework was executed for the base case and a subset of the scenarios described in the previous section with this constraint added, to evaluate its performance under those conditions.

5.4 Results

5.4.1 Evaluation of minimal spanning tree heuristic

For the prototypical district considered, the subset of buildings selected for connection to the DES was greatly influential on the life cycle cost, much more so than the choice of network by which a given subset of buildings was connected. Inclusion of the prototypical hospital building among the connected buildings is necessary in order for a given scenario to have a lower life cycle cost than that of the "null case", in which all buildings are served by independent systems. The prototypical hospital building had a significantly higher thermal load density than the multi-family or retail buildings, and also has significant internal load diversity. Other studies, including that of [92], have also concluded that higher internal thermal load diversity, as well as higher district-level thermal load diversity, contributes to greater reductions in source EUI for 5GDHC systems relative to independent systems. The hospital is the only building for which a reduction in energy cost occurs with a connection to the DES, though all buildings exhibit at least a slight reduction in site- and source-energy use intensity through a connection to the DES. For the prototypical retail and multi-family buildings, the lower magnitude of this reduction is eclipsed by the higher unit cost of electricity than natural gas. In the "independent" case, the buildings have natural gas-fired heating systems, while the DES uses only electricity for heating and cooling. Figure 5.3 plots LCC as a function of network length for all scenarios in the search space, with the scenarios disaggregated by whether or not the hospital building was connected to the DES. As shown in Figure 5.3, there is generally a positive correlation between network length and LCC, due to the fact that the infrastructure cost scales with the network length.

Figure 5.4 shows the source energy use intensity (EUI) for HVAC for all scenarios, as a function of the network length. In this space, the results also show a bifurcation among the scenarios based on whether or not the hospital building is connected to the DES, with the scenarios in which the hospital is served by the DES having a significantly lower source EUI for HVAC (approximately 25% lower than in the null case), for the reasons articulated previously. The significantly larger thermal load intensity of the hospital, and the significant difference in its EUI for the DES-tied and independent cases, overrides the differences in EUI for the multi-family and retail buildings in their connected and non-connected states. This result highlights the potential reductions in source EUI through the use of 5GDHC systems. Figure 5.5 shows a comparison of source EUI for HVAC for each prototypical building type, for their connected and non-connected states. The reduction in source HVAC EUI is particularly substantial for the prototypical hospital building in heating mode, due to the fact that the year-round base cooling load can offset some of this heating load through the shared condenser loop serving water-source heat pumps in the building. Note that this HVAC configuration for the prototypical hospital building also eliminates the use of reheat for temperature control, which also contributes to the heating energy savings.

The exhaustive search confirmed the validity of the MST heuristic. For all possible subsets of buildings in the prototypical district, the network corresponding to the MST indeed provided the solution with the least life cycle cost. These results are presented in Figure 5.6, with the "MST ratio" representing the ratio of the life cycle cost of a given scenario to that of the MST connecting the same subset of buildings. For MST scenarios, the value of this ratio is naturally unity. The fact that this ratio never takes on a value less than one demonstrates the validity of the heuristic.

5.4.2 Evaluation of particle swarm optimization

A summary of results for three of the sets of parameter values considered (corresponding to 0, 3, and 5 connected buildings, respectively), are shown in Figures 5.7, 5.8, 5.9. The minimum value in the current swarm and the global minimum thus far, as well as the "ground truth" value, and the maximum value in the search space, are plotted as a function of the number of iterations.

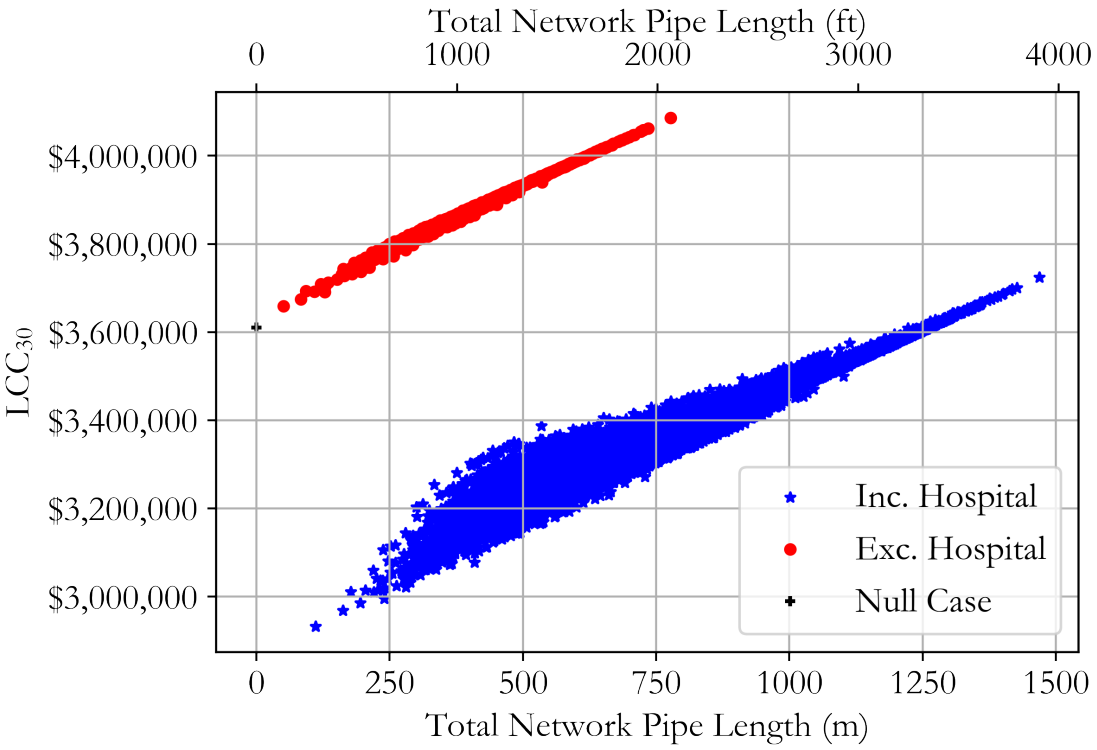

Figure 5.3: Life cycle cost for all scenarios in search space, also presented in [100].

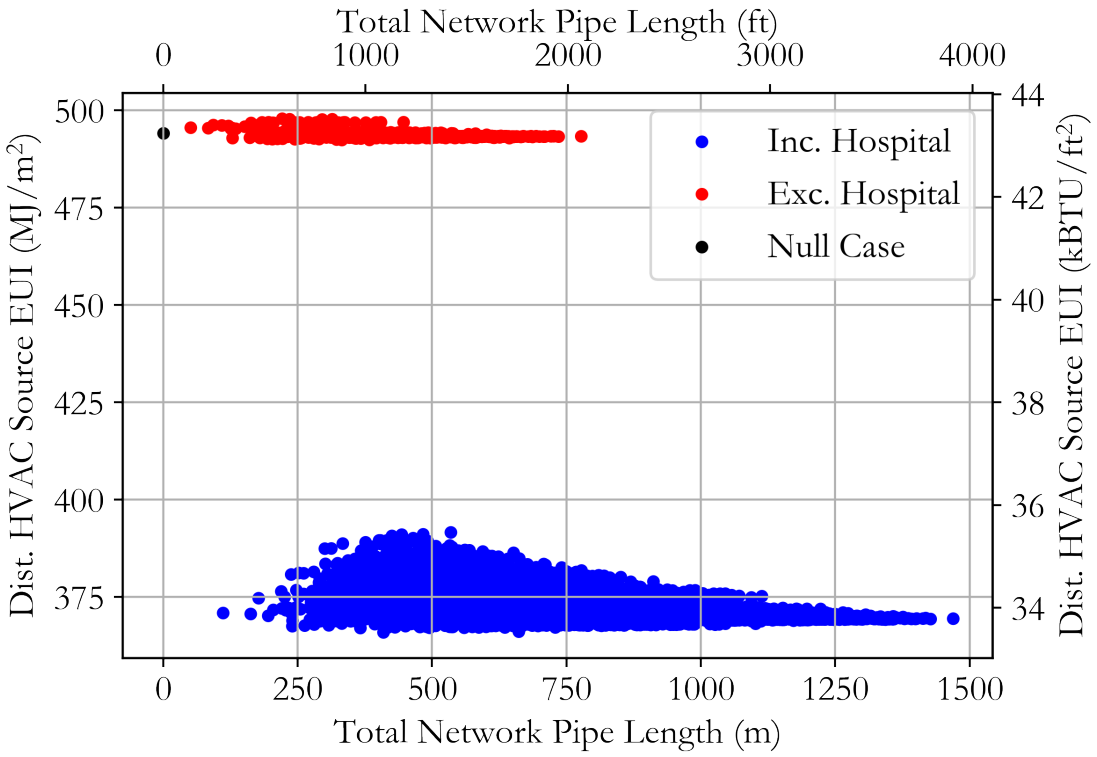

Figure 5.4: Source HVAC EUI for all scenarios in search space, also presented in [100].

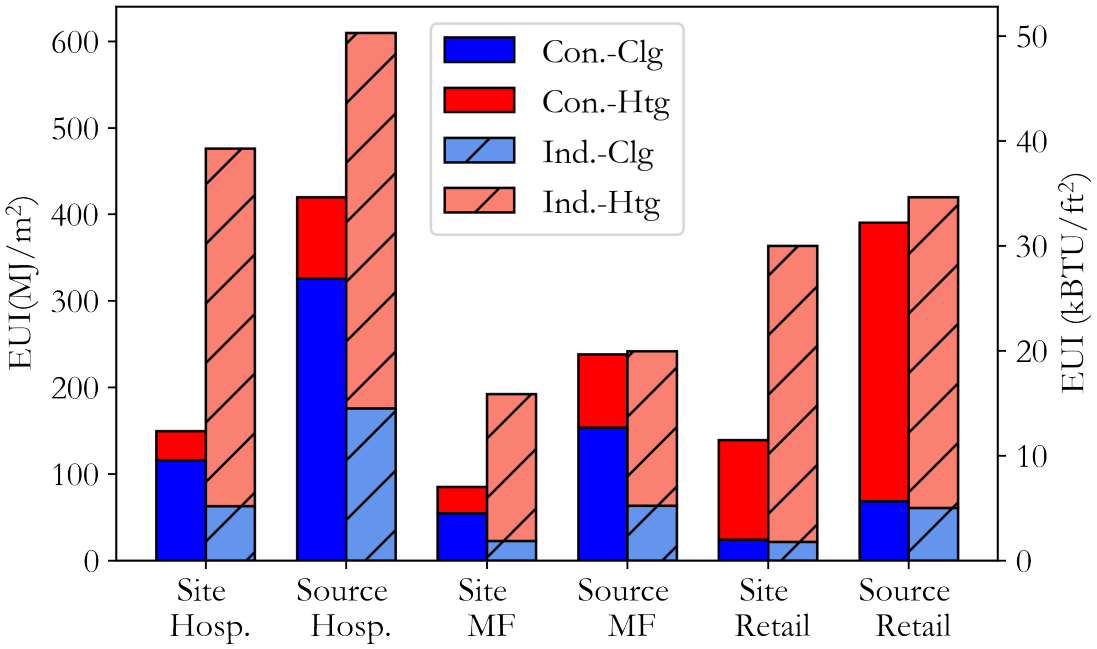

Figure 5.5: Source HVAC EUI for each prototypical building type, also presented in [100].

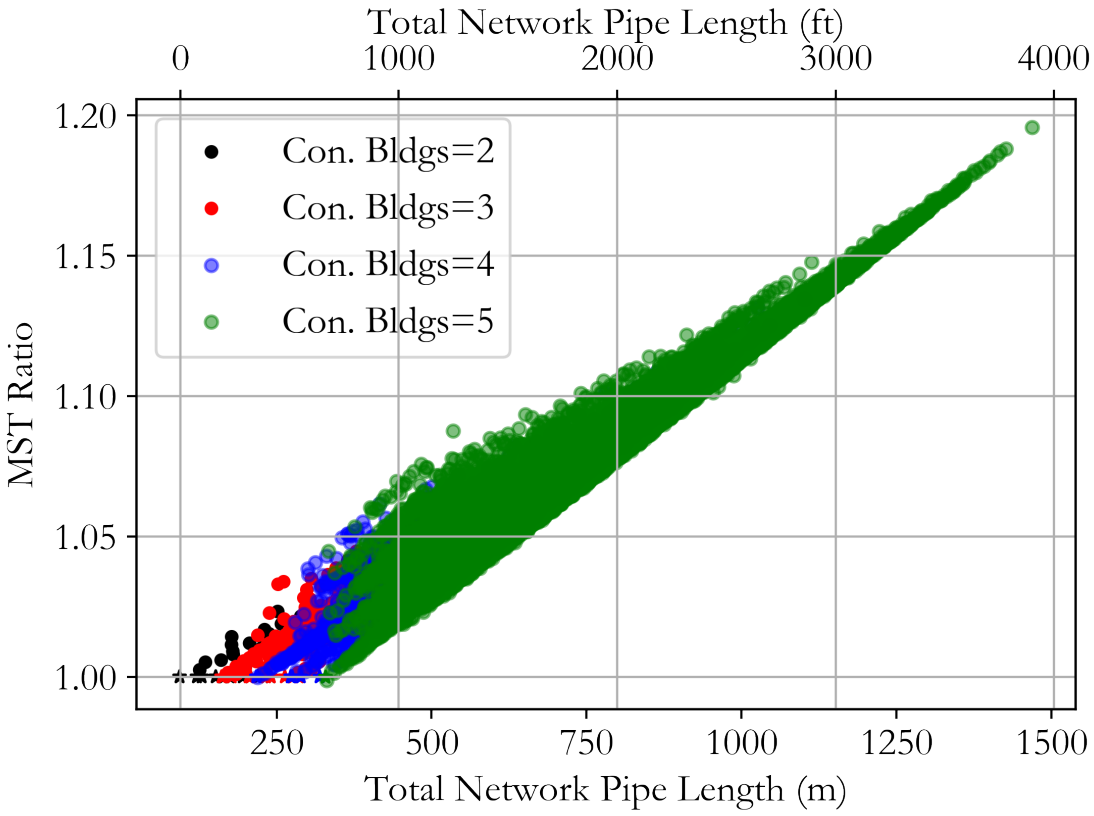

Figure 5.6: Comparison of MST ratio for all scenarios, also presented in [100].

(The scenarios are identified based on the number of connected buildings in the optimal case, with "Scenario 0" corresponding to all buildings having independent systems.) As expected, the global minimum value is monotonically decreasing. In all the scenarios considered, the global best value quickly approached the "ground truth" value, within the first 100 iterations.

In Scenarios 3 and 5, the variation in the swarm minima is small compared with the range between the minimum and maximum values of life cycle cost in the search space. In all scenarios, the swarm minimum did not consistently decrease as the algorithm progressed. This behavior is inherent in the structure of the PSO algorithm to balance exploration of the search space, with exploitation of a "fruitful" area. By definition, once the algorithm has identified what is in fact the "ground truth" solution, it will be impossible to identify a better one, and the algorithm will continue to "explore" other areas of the search space. As observed in the initial evaluations of PSO in this work, and has also been observed by other authors, including [102], the algorithm frequently "returned" to solutions that previously were the minimum value of the swarm, including that corresponding to the ultimate solution. Note that though the optimal network identified in each of the scenarios considered is equivalent to that corresponding to the "ground truth" solution, the calculated values of the objective function were slightly different, due to rounding in the parameter values. In all cases considered, the algorithm terminated due to the stall criteria being met.

5.4.3 Constraint evaluation

A summary of results for three of the sets of parameter values considered for the analysis of an additional constraint (corresponding to the base case, Scenario 3, and Scenario 5, respectively), are shown in Figures 5.10, 5.11, and 5.12. The additional constrained required at least two separate thermal connections for each connected building, which could provide added resiliency to equipment failures. The minimum value in the current swarm and the global minimum thus far, as well as the "ground truth" value, with the inclusion of the constraint, and the maximum value in the search space (compliant with the constraint), are plotted as a function of the number of iterations. The optimal value in absence of the constraint is also shown for reference.

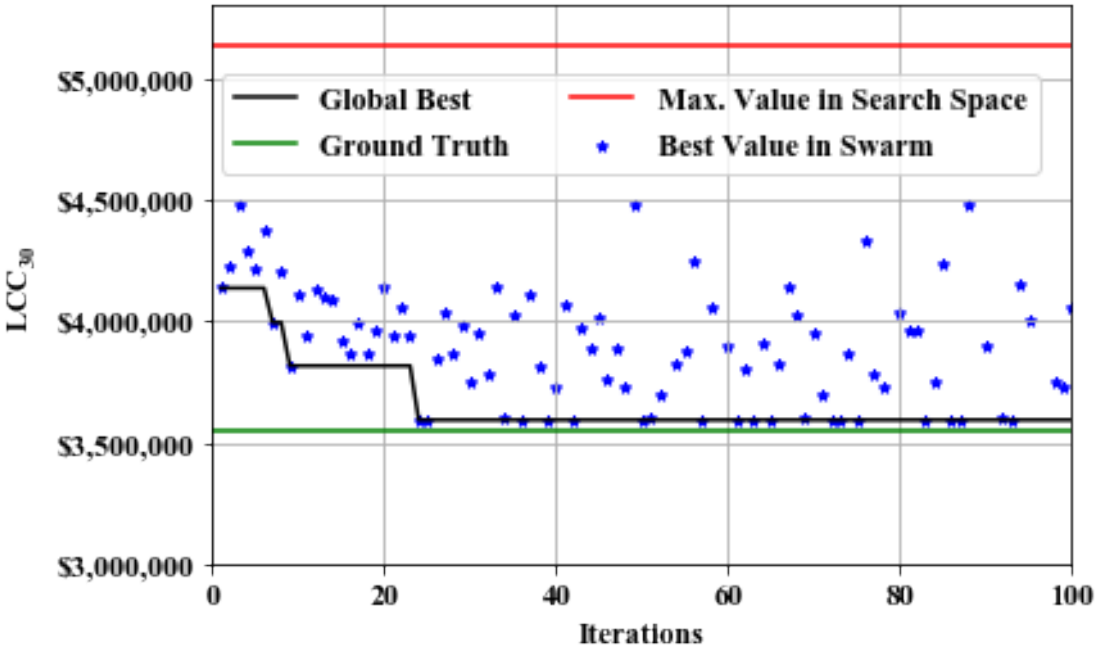

Figure 5.7: Best values over first 100 iterations, implementation for Scenario 0.

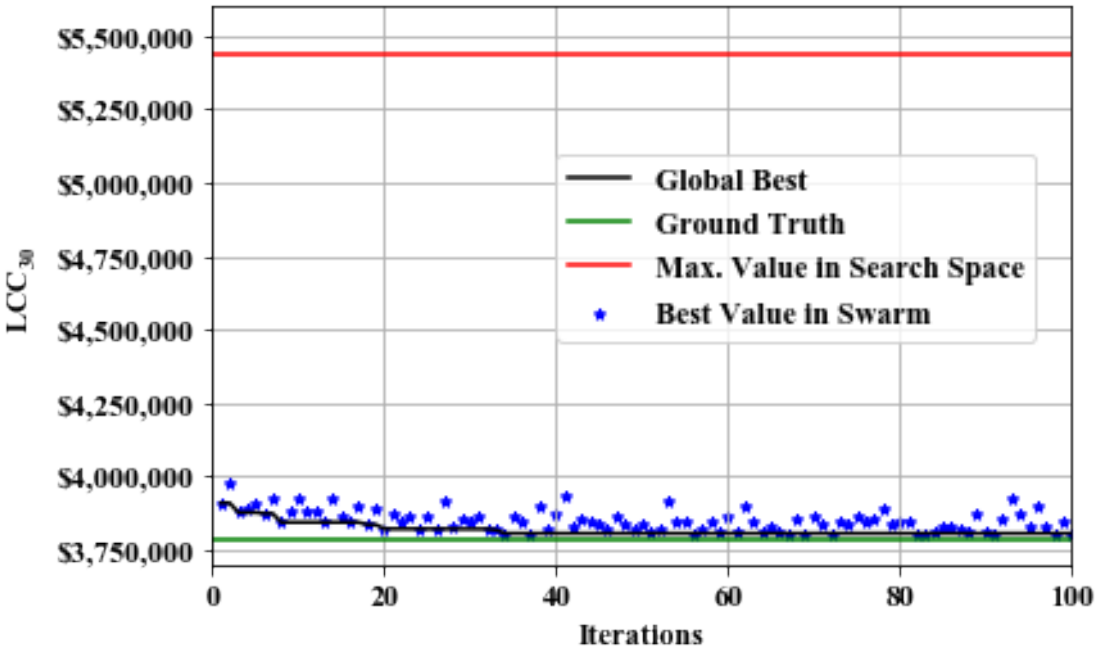

Figure 5.8: Best values over first 100 iterations, implementation for Scenario 3.

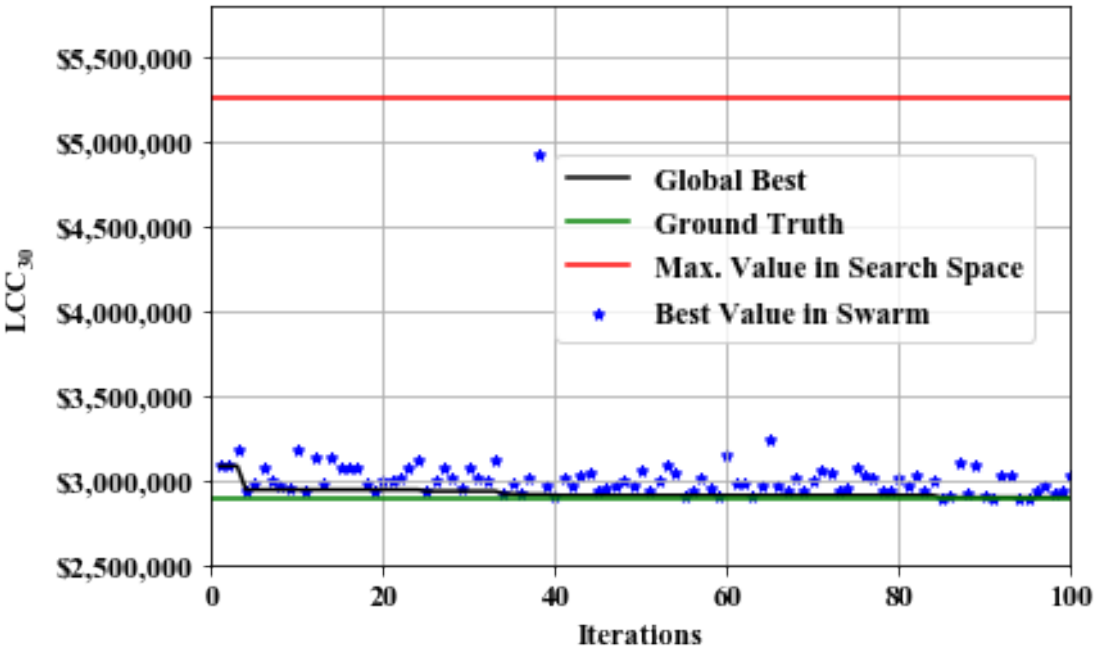

Figure 5.9: Best values over first 100 iterations, implementation for Scenario 5.

For all three sets of parameter values considered, the algorithm terminated due to stall, and reached the solution it ultimately returned within the first 100 iterations. As shown in Figures 5.10, 5.11, and 5.12, the inclusion of the additional constraint did not significantly increase the life cycle cost associated with the optimal solution. The life cycle cost "penalty" associated with enforcing this constraint ranged from 1.1% to 3.4% for the three sets of parameter values considered. For all three cases considered, the optimal solution with the additional constraint ("constrained optimal") was topologically similarly to the optimal solution without the constraint ("unconstrained optimal").

For the base case, the constrained optimal solution involved the connection of an additional load, and two additional thermal connections. (The fact that the constrained optimal solution entailed the connection of an additional load is an artifact of how the search space was defined–such that "duplicate" thermal connections were not permitted–and that the unconstrained optimum in the base case entailed the connection of a single load.) For Scenario 3, the constrained optimal solution involved the connection of one fewer load, and the same number of thermal connections, though the connections were greater in total length. (Note that another candidate solution would have complied with the constraints and connected the same loads, for an incremental "penalty" of less than 0.2% of life cycle cost.) For Scenario 5, the constrained optimal solution involved the same number of connected loads, and an additional thermal connection. The minimal "penalty" associated with compliance with this constraint is expected due to the fact that constraint compliance requires a marginal increase in the infrastructure cost, which is a limited fraction of the overall life cycle cost. For example, in the case of Scenario 5, with the most extensive network, constraint compliance entails an increase of 17% of the network length, and thus also, network cost, while the network cost accounts for only 11% of the overall life cycle cost.

With the addition of the constraint, for the three sets of parameter values evaluated, the framework successfully identified the "ground truth" optimal solution, or a "near-optimal" solution within 1% of the objective function value of the ground truth. For the base case, the solution returned was near-optimal, and for Scenarios 3 and 5, the solution returned was optimal. Thus,

in Figures 5.11 and 5.12, the line corresponding to the global best becomes coincident with the ground truth.

5.4.4 Value of topology optimization

For each of the six sets of parameter values considered in the evaluation of PSO, there is a significant range of associated lifetime carbon emissions and life cycle cost, when statistical outliers are included, as well as significant variation between scenarios. Note that the energy consumption for each case remains the same across scenarios, as the scenarios are distinguished in utility rates, carbon intensity of electricity, and unit cost of infrastructure. Each of the scenarios represents a set of circumstances that is reasonably likely to occur in the United States, and thus, forms a reasonable basis for quantifying benefits of network topology optimization.

Figure 5.13 shows a boxplot depicting the variation in associated lifetime carbon emissions across scenarios and the base case. The variation in lifetime carbon emissions among the scenarios considered is due to the differing rates of carbon intensity of electricity. The variation in carbon intensity of electricity has the effect of scaling the carbon emissions due to electricity use, which are then summed with the carbon emissions attributable to natural gas. The scenarios considering the highest carbon intensity for electricity (Scenario 3 has the highest value for this parameter, at 1.027 kg/kWh), have the least range of carbon emissions within the scenario, since the more carbon-intense electricity serves to reduce the difference in emissions among scenarios due to their differing levels of reliance on natural gas. Scenario 0, which has the least carbon-intense electricity (at 0.379 kg/kWh), has the widest range in carbon emissions within the scenario.

The variation in life cycle cost among the scenarios considered is due to differences in utility rates and infrastructure unit costs, as well as variation in carbon intensity of electricity, which influences the amount of carbon tax accrued. Figure 5.14 shows a boxplot depicting the variation in associated life cycle cost across scenarios and the base case. The wide variation in life cycle cost, carbon emissions, and source EUI among the network configurations in the search space motivates the use of topology optimization. (Note that the energy consumption of a given network

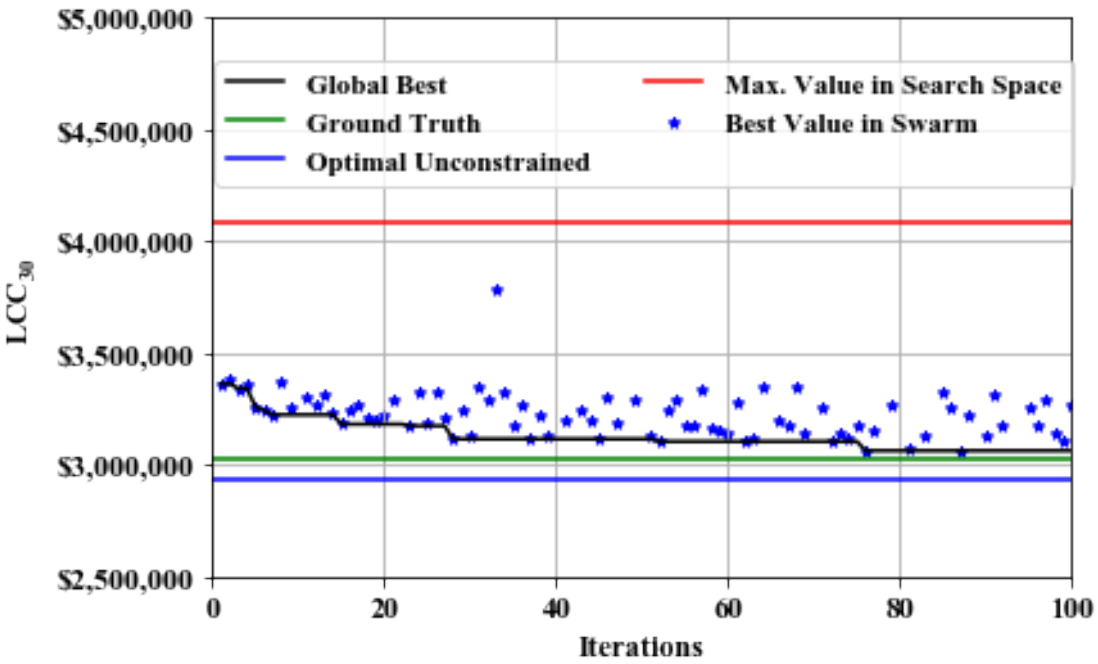

Figure 5.10: Best values over first 100 iterations, implementation for base case, with additional constraint.

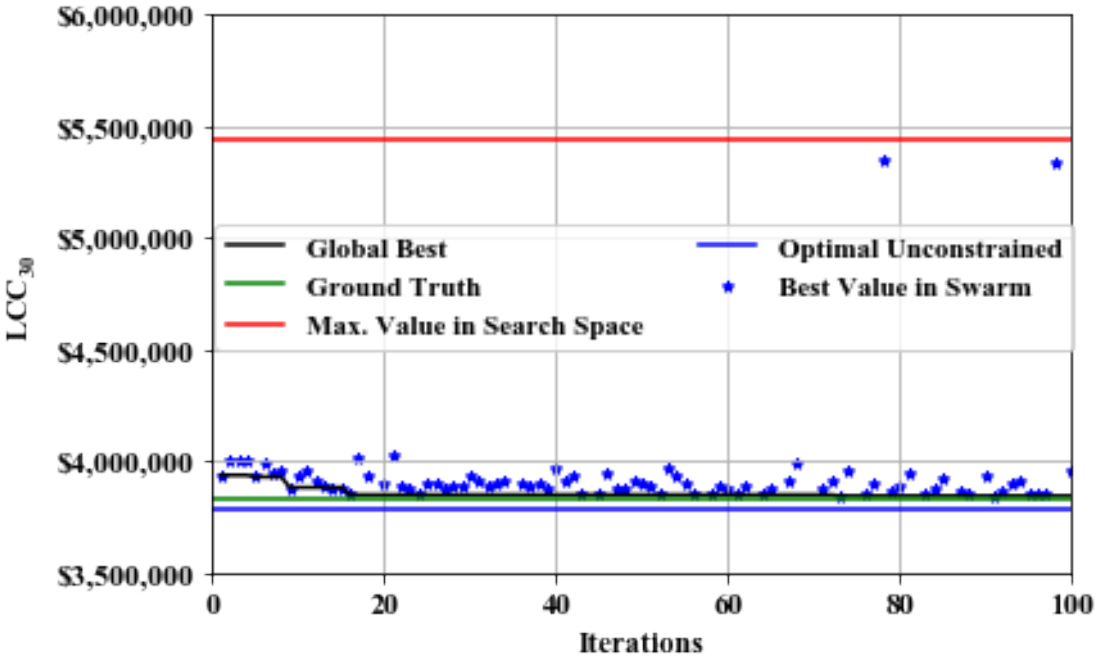

Figure 5.11: Best values over first 100 iterations, implementation for Scenario 3, with additional constraint.

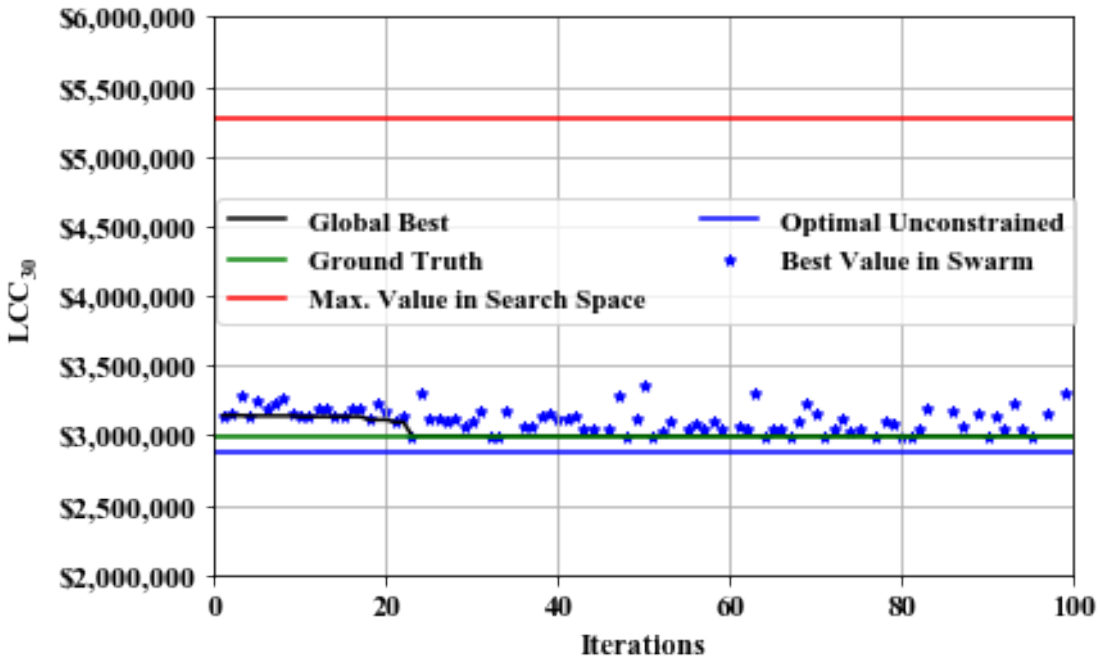

Figure 5.12: Best values over first 100 iterations, implementation for Scenario 5 with additional constraint.

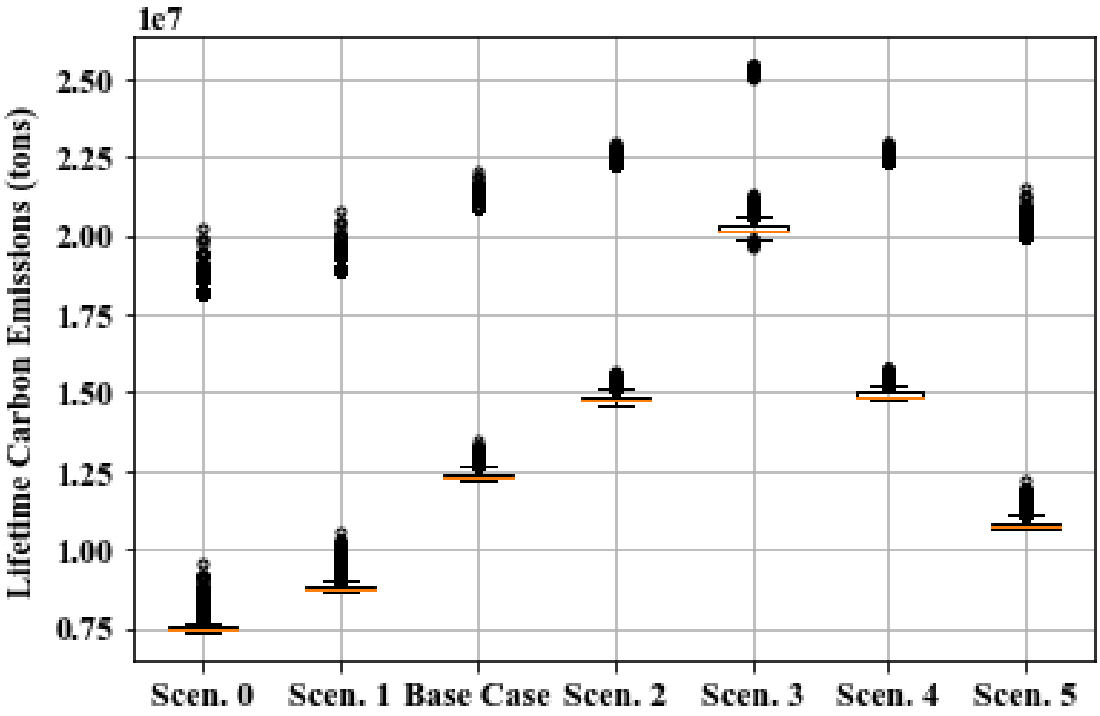

Figure 5.13: Variation in lifetime carbon emissions across scenarios.

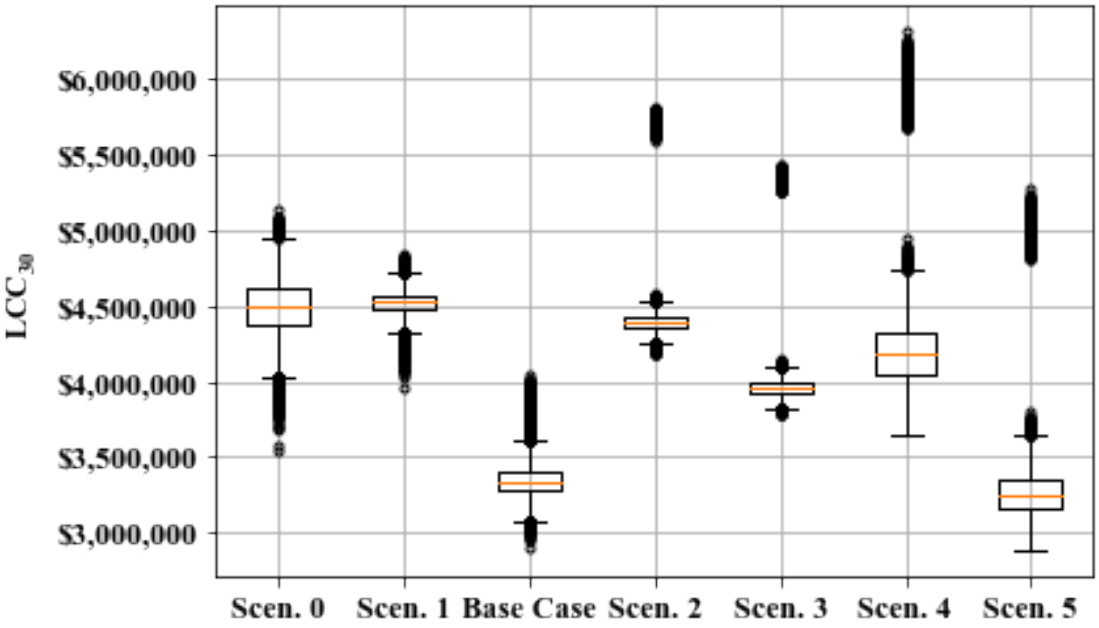

Figure 5.14: Variation in life cycle cost across scenarios.

configuration remain the same across all scenarios considered, and Figure 5.4 shows the range of source EUI for all potential network configurations.) The network configuration with the minimum source EUI has a value that is 28% less than that of the maximum source EUI in the search space. Among the six scenarios considered and the base case, the median range of lifetime carbon emissions is 9.8 megatons, or about 40% of the overall maximum value. Among those same scenarios, the median range of life cycle cost is $1.64 million, or about 26% of the maximum value. Thus, the use of the framework has the potential to provide engineers and planners with opportunities for significant savings in life cycle cost, energy, and carbon emissions.

5.5 Discussion

While the evaluation of the MST heuristic was performed for a particular set of conditions, it is expected that the validation result will be extensible to other climate zones, spatial densities, and building load densities, among those in the range commonly encountered in urban districts, since the results rest on the fact that networks with added thermal connections fail to provide significant enough energy savings benefits to outweigh the additional infrastructure cost. For other 5GDHC system configurations (such as those that incorporate series connections to the DES), the MST validation may not be extensible, as series configurations result in greater variation in supply temperature along the network length.

It is also expected that the validation of the use of the MST heuristic and PSO are extensible to a cost function including electric demand charges. The effect of the consideration of demand charges in the cost function is expected to increase costs for both the “connected” and “independent” states, and more significantly for the “connected” states, due to the use of electrified heating. As discussed previously, the validation of the MST heuristic rests on the lack of compelling energy efficiency benefits from a greater number of network connections, a comparison which is not expected to change if demand charges were considered. The performance of the PSO algorithm is also tied to the nature of the search space, which is characterized by a greater influence on life cycle cost from the selection of a subset of buildings than the network by which they are connected, a

dynamic that is not expected to be altered by the consideration of a demand charge. However, the cost function implemented in the Topology Optimization Framework could be easily modified to account for consideration of a demand charge, or a time-of-use electric rate structure.

Uncertainty exists regarding the trajectory of future costs for electricity and natural gas. An increase in electricity costs relative to those of natural gas would further exacerbate the economic "penalty" observed for heating electrification. Different future escalation rates (positive or negative) in natural gas or electricity rates than those considered in this analysis are not expected to alter the conclusion regarding the validity of the MST heuristic and PSO in the context of this problem. The future trajectory of electric and natural gas rates is not expected to result in energy efficiency benefits associated with the presence of additional thermal connections (which would change the conclusion regarding the MST heuristic) or significantly change the nature of the "search space" of life cycle cost as a function of the adjacency matrix elements. A higher disparity between electric and natural gas rates in the future would likely have the effect of further emphasizing the trend already observed in the search space of the greater influence of the selection of connected loads (through their energy costs) on life cycle cost than the network by which a set of buildings is connected.

The results of this analysis, consistent with that of past work, confirm that buildings with a higher degree of internal load diversity exhibit greater reductions in HVAC source EUI through a connection to a 5GDHC system relative to independent systems. A variety of prototypical buildings represented (in this case, a multifamily building, hospital, and retail building) were shown to exhibit at least some reduction in HVAC source EUI through a connection to a 5GDHC system. This is consistent with the validity of the thermal load diversity metric (proposed by [12]) used to select the collection of prototypical buildings.

Based on the results of the evaluation of the MST heuristic and PSO, the framework leverages both techniques to address the network topology optimization problem. The optimization problem

is formulated as follows:

$$\min_{\vec{L}} C_{pipes} + C_{elec} UPV_{elec}(E_{de} + \sum_{i=1}^{n} E_{be,i}) + C_{gas} UPV_{gas} \sum_{j=1}^{n} E_{bg,j} + UPV_{CO2} \sum_{t=1}^{30} m_{CO2}(t) C_{CO2}(t) \tag{5.7}$$

subject to:

(1) $L_i = 1$ if building i is connected to the DES, and $L_i = 0$ otherwise

(2) If there exists a pipe directly thermally connecting building i and building j, $A_{i,j} = 1$. Otherwise, $A_{i,j} = 0$.

(3) If $\sum_{j=1}^{n+1} \sum_{i=1}^{n+1} A_{i,j} \geq 1, \sum_{j=1}^{n+1} A_{1,j} \geq 1$

(4) $\forall i, j \in \{1 \dots n+1\}, A_{i,j} = A_{j,i}$.

where $\vec{L}$ is now a vector of $n+1$ dimensions, corresponding to the total number of network nodes considered, for each of the buildings and the centralized heat pump. The use of the MST heuristic to determine the network connectivity allows the dimensionality of the problem to be reduced. Constraint 3 ensures that if any load is connected to the network in a candidate solution, the centralized heat pump is also connected. By definition, an MST network is a connected graph, and thus this constraint is now sufficient to ensure network connectivity. Constraints 2 and 4 are incorporated implicitly, through the approach by which candidate solutions are interpreted in this context.

Prim's Algorithm is used to construct the adjacency matrix of the minimal spanning tree graph corresponding to $\vec{L}$ [113]. PSO is implemented with the same parameter values as described previously. In the same manner as described in the evaluation of PSO, PyFMI is used to modify the FMU energy model to match the network connectivity associated with the candidate solution, and simulate the model. The energy consumption values from the model simulation, as well as the fixed parameter values, are then used to calculate the LCC. A diagram illustrating the workflow of

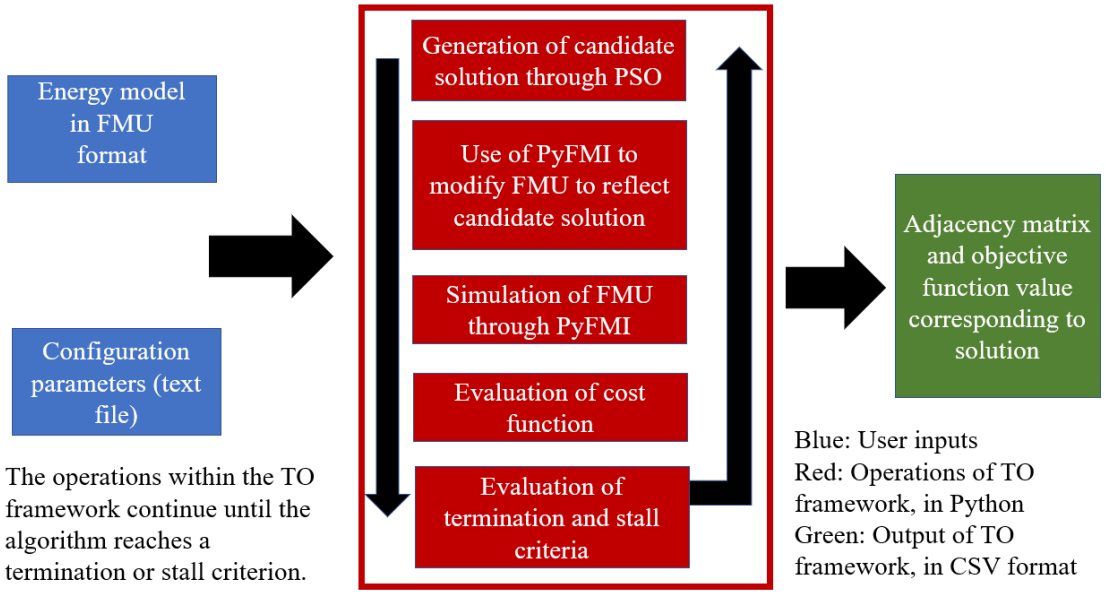

Figure 5.15: Diagram illustrating the workflow of the presented Topology Optimization Framework.

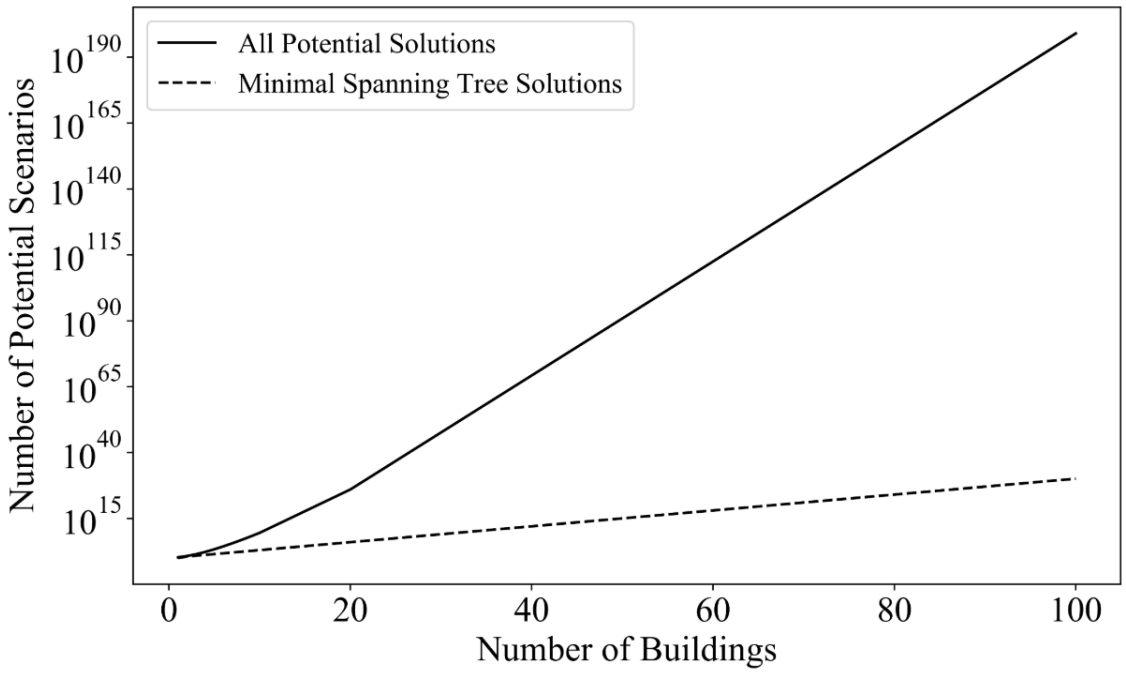

Figure 5.16: Comparison of growth in search space as a function of number of buildings considered, presented also in [6].

the framework is shown in Figure 5.15. The use of the MST heuristic significantly reduces the size of the "search space" and thus improves the computational efficiency of the framework. Figure 5.16 shows the growth in the size of the search space as a function of the number of buildings considered, for all potential solutions, and for MST networks only.

The analysis of an additional constraint, intended to promote redundancy of supply, shows that a requirement for each connected load to be served by at least two thermal connections can be enforced at a life cycle cost penalty of less than 3.5%, for the three sets of parameter values considered. The value of such redundancy to a project could be quantified in terms of the value of potential lost operations, and compared to this margin.

5.6 Conclusion

An exhaustive search evaluating the life cycle cost of all potential thermal network configurations for a five-building prototypical district (more than 30,000 configurations) highlights the motivation for network topology optimization in the context of 5GDHC systems. The scenarios have a range of district-level HVAC source EUI of 28% of the maximum value. An analysis of six different sets of realistic values of high-level LCC parameters revealed a median range of carbon emissions across the scenarios of 40% of the overall maximum value, and a median range of life cycle cost of 26% of the maximum value. Thus, network topology optimization has the potential to facilitate significant reductions in life cycle cost, source EUI, and carbon emissions.

To advance this, a network Topology Optimization Framework has been developed for district thermal energy systems, to address the question "Given a set of buildings with known locations and loads, what is the optimal subset of buildings, if any, to connect to a district thermal energy system, and by what subset should they be connected, to minimize life cycle cost?" The framework is implemented in Python, and takes an energy model of a district thermal energy system in FMU format as an input. The framework uses particle swarm optimization (PSO) to determine the optimal subset of buildings to connect to a DES, and the minimal spanning tree (MST) heuristic to identify the network by which to connect them. In this paper, the use of PSO and the MST

heuristic have been validated through the exhaustive search for the five-building prototypical district, extended with six different sets of realistic parameter values. The framework has also been demonstrated to work effectively with the addition of a constraint to promote redundancy of supply. It is anticipated that the framework can facilitate the adoption of 5GDHC systems in appropriate applications, and thus, opportunities for reductions in energy use and carbon emissions.

Chapter 6

Development of the Topology Optimization Framework

The Topology Optimization Framework is a software module that is intended for use by both researchers and practitioners who are evaluating or designing district thermal energy systems. The Topology Optimization Framework will determine, for a set of buildings with known locations and loads, the optimal subset (if any) of buildings to be served by a district thermal energy system, and the optimal network by which the subset should be connected, to minimize life cycle cost.

6.1 Technical approach

The Topology Optimization Framework uses the minimal spanning tree (MST) heuristic to identify the optimal (with respect to life cycle cost) network by which a given subset of buildings should be connected, and a version of the particle swarm optimization (PSO) algorithm adapted for a discrete problem ([39]) to select the optimal subset of buildings to be connected to the network. The validation of the MST heuristic and PSO for application to this problem, as well as details of the implementation in the framework, are discussed in Chapters 4 and 5. A constraint related to network connectivity is enforced through assignment of a high "penalty" value to the objective function for candidate solutions that violate the constraint. In the context of this research, the topology optimization problem was investigated with life cycle cost as the objective function. The Topology Optimization Framework could be easily adapted to use any objective that is a function of energy consumption, carbon emissions, or life cycle cost.

6.2 Implementation

The Topology Optimization Framework is implemented in a series of Python scripts, which will soon be publicly available through a GitHub repository. The framework takes as inputs a GeoJSON file characterizing the locations of the buildings, and an energy model (in the form of a functional mock-up unit, or FMU) representing a district thermal energy system serving the buildings. The energy model is used to calculate the energy consumption associated with HVAC for all buildings in the district, whether or not they are served by a district thermal energy system in a given scenario. Thus, the energy model must also calculate the energy consumption associated with HVAC for a case in which a considered building is served by independent, building-level HVAC systems. The use of metamodels to represent thermal loads of buildings served by a district thermal energy system to improve the efficiency of simulation, while preserving accuracy, is recommended, and the Metamodeling Framework developed by [31] can accomplish this, as well as modeling HVAC energy use for buildings served by independent systems. See Figure 2.2 for a schematic illustration of the workflow of the Topology Optimization Framework.

Requirements for inputs to the framework An energy model representing the HVAC energy consumption of the considered district must be provided in FMU format. FMUs facilitate the exchange of simulation models in a compact and accessible format. FMUs are generated through the Functional Mock-Up Interface (FMI), and contain an XML file with definitions of the variables used, the equations used by the model, expressed in the form of C functions, as well as additional data that may be required, such as tables of parameter values [114]. Modelica, EnergyPlus, and other modeling tools support exports of models to FMU format, and the focus of the implementation of the framework has been on models created in Modelica.

The energy model must be structured so that each thermal connection in the district thermal energy system can be "enabled" or "disabled" with a binary variable. The energy model must be configured with the "full mesh" (all possible connections) of thermal connections present, so that

any possible network configuration can be explored. The model must also be structured so that the "connectivity status" of each considered building load can be set with a binary variable, so that in "connected mode" the building is thermally and hydronically tied to the district thermal energy system, and in "independent mode", it is served entirely by building-level HVAC systems. The Modelica language provides a convenient format for implementing such a model. The framework manipulates the model in FMU format, and uses the PyFMI Python package to set the values of these binary variables to represent a particular network configuration.

The energy model must output values that are used to evaluate the cost function, including the total amounts of electricity and natural gas that are used for HVAC at the district level, encompassing both buildings served by the district thermal energy system and those with independent systems. The framework reads these output values from the .mat output file resulting from the simulation, using the BuildingsPy Python package [115]. The approach for configuration and manipulation of the energy model is extended from that of [3].

The framework uses a GeoJSON file representing the physical locations of buildings and a centralized heat pump for the district to calculate the lengths of thermal connections. GeoJSON is a commonly used format for encoding geographic data, and can represent points, polygons, linestrings, and other geometry types [116]. By default, the string names assigned to buildings in the GeoJSON file are used to infer names for the thermal connectors in the energy model. Both of these steps can be overriden by a user to manually set the lengths of pipes and their names. A GeoJSON file can be constructed manually, or generated through online tools, including NREL's URBANopt software modules, or the GeoJSON.io interface [117].

Example modeling implementation The energy models used for evaluation and demonstration of the framework were extended from one created by [3] in Modelica. These models are described as an example of how the required energy model could be structured for use by the framework. The Metamodeling Framework developed by [31] was used to generate data-driven metamodels for the HVAC energy use by each considered building, in both its "connected" and

"independent" states. (The training of the metamodels is discussed in more detail in Chapter 3.) For the "connected" state, the supply water temperature from the network is one of the model covariates. In the Modelica model, each considered building load is represented, and associated with it is a binary variable representing its connectivity status. For greater computational efficiency, the metamodels are pre-compiled and heating and cooling energy use (as a function of network water temperature, where applicable) at each time step is cataloged in a table embedded in the district model. At each time step, the district model "looks up" the heating and cooling energy consumption of each building, using the metamodel for the appropriate state. Each possible thermal connection is represented in the district model, and associated with a binary variable that renders it "active" or "inactive," to facilitate the representation of all potential network configurations.

Computational intensity The use of the minimal spanning tree heuristic significantly reduces the size of the "search space" for the topology optimization problem, and thus, the computational intensity. The Topology Optimization Framework parallelized the model simulation task across workers on a given compute node and can be implemented in a high-performance computing (HPC) environment. The computational intensity of the execution of the framework depends primarily on the computational intensity of the underlying DES model, and the number of buildings considered in a prototypical district. For a seven-building prototypical district, and a computationally-intensive DES model (requiring approximately 30 minutes of simulation time), the full execution of the topology optimization framework required around one day of compute time parallelized in an HPC environment.

6.3 Integration with related tools

The topology optimization framework will soon be available as a module in the URBANopt advanced analytics platform developed by NREL [32]. The functionality of the URBANopt platform is discussed in more detail in Chapter 1. As part of URBANopt, the topology optimization framework will leverage the OpenStudio Analysis Framework [118] (OSAF) for cloud-based sim-

ulation. Figure 6.1 shows a schematic illustration of how this workflow could be configured. In Figure 6.1, files are shown in light green, software modules in yellow, and *measures* (scripts that manipulate input files) in red. The processes associated with the topology optimization module are enclosed in a yellow rectangle at the left of the figure. Also shown is a parallel workflow path (terminating at the "eplusout.sql" file), that can modify and simulate the energy model without performing network topology optimization.

The GeoJSON-to-Modelica Translator (GMT) is a software module that programmatically configures Modelica models of district thermal energy systems based on high-level user inputs [119], in the form of a GeoJSON and a system design parameters file. A model generated by the GMT can be exported as an FMU, and used as an input to the topology optimization module. The OSAF will use an optimization algorithm selected by the user to generate candidate solutions to the topology optimization problem, and modify and simulate the FMU energy model to evaluate them. The OSAF's operations, such as the choice of algorithm and related hyper-parameters, can be configured through the "OSAF analysis JSON" file. This process will continue until a convergence or termination criterion is met. The energy model and the set of inputs used to generate it can be modified programmatically at several stages: through a measure acting on the JSON file ("JSON measure"), a measure acting on the Modelica model ("Modelica measure") or a measure acting on the model in FMU form ("FMU measure"). The outputs can be processed through the use of a reporting measure.

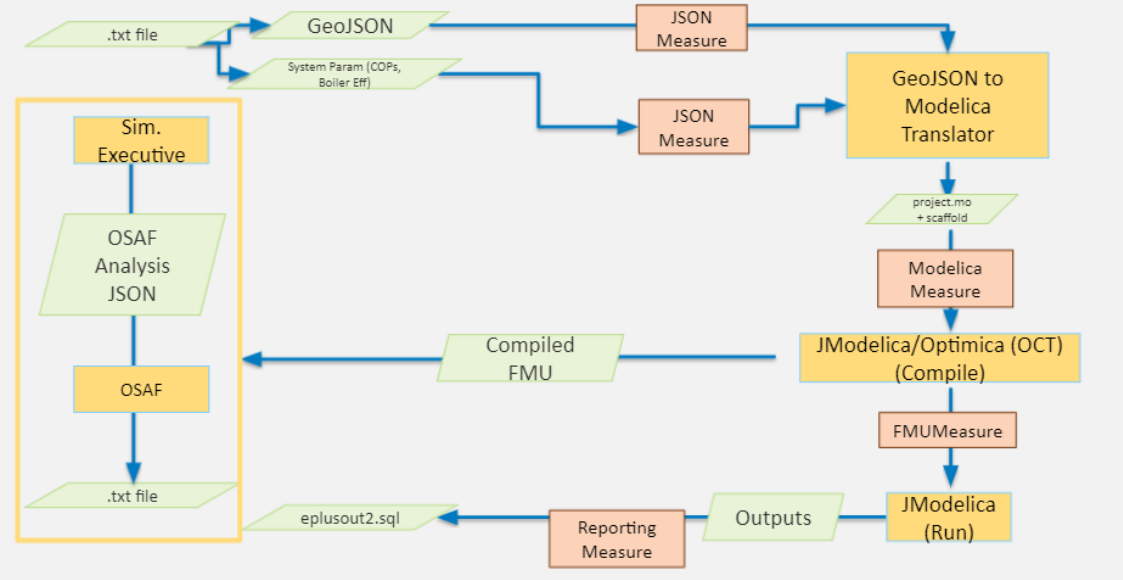

Figure 6.1: Schematic illustration of workflow of the topology optimization module in the context of URBANOpt.

Chapter 7

Demonstration of the topology optimization framework

This chapter is based on a paper that will be presented as:

A. Allen, G. Henze, K. Baker, G. Pavlak. "Quantification of the Benefits of Topology Optimization for Advanced District Thermal Energy Systems," to be presented at 2021 SDEWES Conference, October 2021.

7.1 Abstract

In this paper, a network topology optimization framework was developed and applied to a prototypical district to determine the best design solutions for a district thermal energy system with respect to life cycle cost. The analysis focused on an advanced, fifth-generation district system operating at near-ambient temperatures. The framework leverages a particle swarm optimization algorithm and a minimal spanning tree heuristic to select an optimal subset of buildings and optimal network configuration. The topology optimization approach identified solutions resulting in life cycle cost savings of 14% to 72% (depending on the reference case) relative to designs based on heuristics. Analysis of the results indicates that advanced district thermal energy systems have the potential to achieve significant reductions in energy use and emissions relative to building-level systems, but face obstacles to cost-competitiveness due to the prevalence of natural gas heating and low natural gas costs in the U.S.

7.2 Introduction

This work seeks to evaluate and quantify the potential benefits of network topology optimization in the design of a district thermal energy system operating at near-ambient temperatures, commonly referred to also as a fifth-generation system. In this context, topology optimization is used to address the questions, "Given an urban district with known building locations and loads, what is the best subset of buildings to connect to a district thermal energy system to minimize life cycle cost, and by what thermal network should that subset be connected?" A novel topology optimization framework is then applied to a prototypical new construction district in the setting of a university campus.

7.2.1 Fifth-generation district heating and cooling systems

The evolution of district thermal energy systems is often characterized by "generations", with systems progressing from the use of steam to water as a working fluid for heating, and then to the

use of water at more moderate temperatures, over time [4]. Fifth-generation district heating and cooling (5GDHC) systems are characterized by their use of water at near-ambient temperatures (often in the range of 15-25°C) and the use of water-source heat pumps to meet thermal loads at connected buildings, using the district network as both a heat source and a sink [7]. Through their use of more moderate water temperatures, 5GDHC systems facilitate the beneficial electrification of heating. 5GDHC systems also offer potential reductions in energy consumption and carbon emissions through their ability to facilitate the integration of renewable thermal and waste heat sources, as well as the reduction of unwanted heat losses and gains through the distribution system [4].

The use of network topology optimization is especially valuable in the context of 5GDHC systems. The moderate water temperatures characteristic of 5GDHC systems facilitate the exchange of heat (and heat rejection) among connected buildings and motivate consideration of network configurations outside of the typical ring or radial networks used by older generations of district systems [3]. This dramatically increases the "search space" of potential network configurations under consideration, motivating the need for a topology optimization approach in order to select the best solution, as the number of potential configurations grows factorially with the number of buildings in the district. Figure 7.1 illustrates this conceptually for a prototypical district of only three buildings, which creates fifty-four potential network configurations. The size of the search space grows quickly to more than 30,000 potential configurations for a district of five buildings.

Previous work by the authors has also demonstrated the motivation for network topology optimization for 5GDHC systems, identifying a reduction in life cycle cost on the order of 2/3 by the optimal, relative to non-optimal, network configurations [6], in the context of a small prototypical district. Previous work by the authors has also validated the use of a heuristic for the topology optimization problem [120]. This study extends this previous work by creating a network topology optimization framework, which implements the heuristic, in conjunction with an optimization algorithm, to address the problem in a computationally efficient manner.

The work of [4] says that the increased adoption of 5GDHC systems in the context of in-

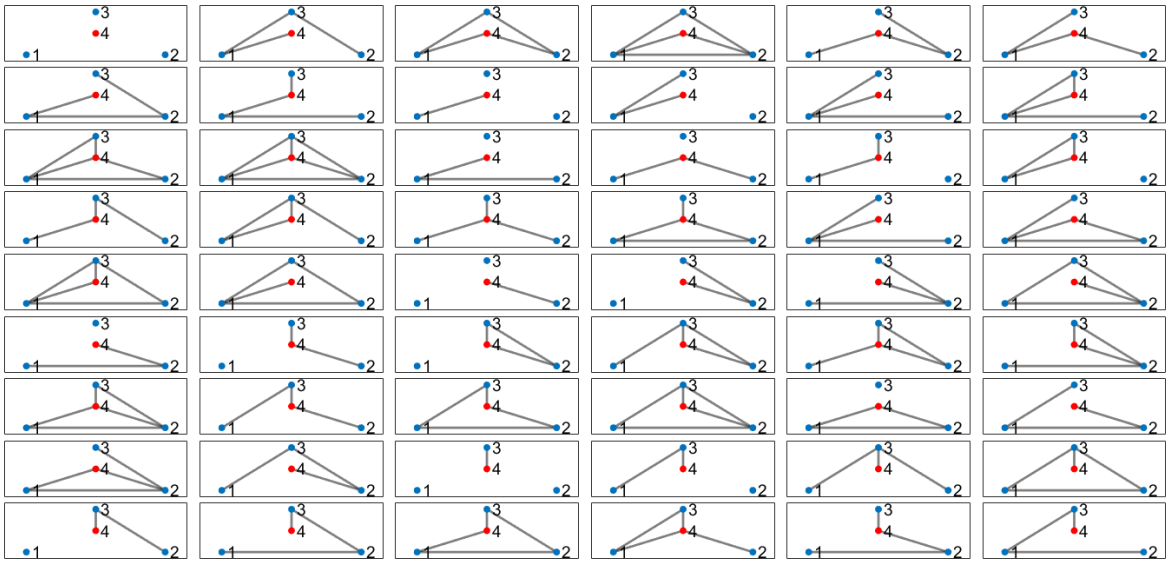

Figure 7.1: Illustration of all potential thermal network configurations associated with three buildings (represented with blue nodes) and a central plant (represented with a red node), originally presented in [6].

creasing penetration of renewable electric generation will require "advanced energy system analysis tools of coherent systems." Past work in the realm of topology optimization for district thermal energy systems has primarily focused on heating-only systems, with the work of [24] addressing a low-temperature district heating network, and the work of [25] addressing a "cascade" district heating system operating at two different temperatures. The work of [26] performed network topology optimization for a third-generation district heating and cooling system, with an objective function based on costs for piping and trenching and certain operating costs, finding a limited reduction in life cycle cost, though a more significant benefit in internal rate of return, for the life cycle cost-optimal network, relative to the best network with respect to initial cost. The work of [26] considered only the network configuration, and not the selection of connected loads. Additionally, [26] treated the energy use associated with centralized equipment as a static condition.

Past studies have also addressed topology optimization with a multi-objective approach. The work of [121] sought to optimize the network configuration and pipe diameter of an existing district heating network in Turin, for the objectives of investment cost and robustness, with robustness defined in terms of minimal fluctuation of minimum supply pressure, using an ϵ-constrained approach. The work of [122] performed optimization for the network topology and selection of primary equipment for a district heating network, for the objectives of carbon emissions and life cycle cost, also using an ϵ-constrained approach, and identified reductions in carbon emissions of 23% through the use of a district heating network, for the same investment cost as building-level heating systems. The present work is novel because it addresses both aspects of topology optimization (selection of a subset of buildings and of a network configuration, a need highlighted by [26]) and is presented in the context of a 5GDHC system with bi-directional thermal and mass flow, which presents the greatest potential benefits for this approach.

7.2.2 Optimization approaches and relevant concepts from graph theory

In the context of optimization problems, it is convenient to represent thermal networks as "undirected graphs." An "undirected graph" is a set of nodes (vertices) and edges, which can be

defined by the two vertices that they connect [5]. A relevant concept is a graph known as a "minimal spanning tree (MST)," in which a given set of vertices is connected with the least total edge length, and there exists exactly one path between each pair of nodes [5] . In the graph theoretical context, a thermal network can be represented with an "adjacency matrix," which is a square matrix with its dimension corresponding to the number of nodes in the graph. The matrix has binary values, with a value of one in a given position if there exists a connection between the corresponding nodes, and a value of zero otherwise [5].

Particle swarm optimization (PSO) is a method for optimization of continuous, non-convex functions developed by [37]. The algorithm does not rely on an explicit definition of the objective function or its derivative. While PSO does not provide a guarantee of convergence to a global optimum, the characteristics of PSO have been shown to mitigate the risk of becoming "stuck" at a local minimum [112] relative to other approaches for non-convex problems. Conceptually, PSO emulates the behavior of animals in the natural world acting as part of a swarm and being attracted towards a location that satisfies an objective through both each individual's knowledge and the group's collective knowledge of the location and terrain. In the context of optimization, the individuals represent vectors that are potential solutions, and the goal is to minimize an objective function. Each iteration of the algorithm involves evaluation of a "swarm" of these candidate solutions, termed particles. At each iteration of the algorithm, the value of each candidate solution, represented with the location of a particle in the solution space, is updated, using a "velocity" that seeks to drive each particle towards both its prior best solution, and the prior best solution of the swarm as a whole. The velocity also incorporates a stochastic component [37]. In the velocity update step, the current velocity is multiplied by a scalar, known as the "inertia weight," which controls the influence of the existing velocity in directing the motion of the particle through the search space [37].

In the PSO algorithm, the value of the cognitive parameter (c_1) scales the degree to which a particle is attracted back to its prior best position, and the value of the social parameter (c_2) scales the degree to which a particle is attracted back to the prior best position of the group. The

set of other particles with which a given particle can "communicate" knowledge of best positions is described as a "neighborhood" [37]. When this "neighborhood" consists of a number of particles that is less than the swarm size at a given iteration, the approach is called "local best" (*lbest*) PSO. When each particle can communicate with all others, the approach is known as "global best" (*gbest*) PSO.

7.2.3 Case study definition

The prototypical district considered in this case study consists of seven buildings: three office buildings, three multi-family housing buildings, and a restaurant. To provide realism, the general building types and locations are based on those of real buildings on the campus of the University of Colorado Boulder (CU Boulder), with some adjustments. CU Boulder is located in a dry, high-altitude climate with hot summers and cold winters. The intention is not to represent the load profiles of those buildings exactly, but to reflect the nature of loads that tend to exist in urban developments. In this case study, the life cycle cost and energy performance of a district thermal energy system configuration determined through network topology optimization, and a district thermal energy system serving the prototypical district designed based on high-level metrics that are often used to assess district energy potential, are compared.

Given the emerging nature of district thermal energy systems operating at near-ambient temperatures, metrics to assess their techno-economic potential have not yet been widely adopted, though some authors, including [12], have proposed metrics to assess their energy performance. Existing metrics for assessing techno-economic potential of district thermal energy systems largely focus on third-generation (or earlier) versions of district heating systems. Due to their ability to leverage less costly distribution infrastructure (such as plastic pipes), systems operating at near-ambient temperatures can potentially be favorable on a life-cycle cost basis at lower load densities than higher-temperature district heating systems [7]. An annual load-per-area density metric was used by [87] to evaluate the techno-economic potential for district heating systems in the U.S. Based on modelled building loads, this prototypical district has an annual heating load density (8.45 $\frac{GWh}{km^2}$)

that exceeds the lower value used by [87] as a threshold (5 $\frac{GWh}{km^2}$). Another metric used to assess potential for district heating systems is the linear heating power demand density (LHPDD), with a lower threshold of 1.25 $\frac{kW}{m}$ often considered [2], with the heating power corresponding to the system's installed thermal capacity. The authors of [7] note that operating examples of fifth-generation systems have values of LHPDD less than this threshold. For this district, the value of the LHPDD is 0.77 $\frac{kW}{m}$, which is within the range of values for operating fifth-generation systems surveyed in [7].

Based on these criteria, interpreted in the context of the expected lower infrastructure costs for fifth-generation systems, it is concluded that this prototypical district would be a plausible application for a fifth-generation district thermal energy system, and thus, the inclusion of all buildings in the prototypical district will serve as the basis for comparison in this case study, in four different network configurations: radial, ring, the minimal spanning tree, and a full mesh network with all possible thermal connections present. Ring and radial network configurations are commonly used in district thermal energy systems, and the minimal spanning tree and full mesh networks represent the two extremes of network connectivity.

7.3 Methods

In this study, a novel topology optimization framework was applied to a prototypical urban district, to determine the best potential network configuration for a district thermal energy system operating at near-ambient temperatures, to minimize life cycle cost. The results of the topology optimization process were compared with several "base cases" representing network designs determined through common heuristics. To perform this analysis, an energy model of the district energy system and the prototypical building loads was applied. The energy models and the topology optimization framework are discussed in the following sub-sections.

7.3.1 Building load models

In this study, the U.S. DOE Prototype Building models, with modifications, are used to represent the building thermal load profiles, for three prototypical building types: a medium office building (three instances), a multi-family housing building (three instances), and a full-service restaurant (one instance). The Prototype Building models are designed to represent characteristics of common commercial building types in the U.S. and are available in formats corresponding to several recent energy code standards, and all U.S. climate zones [35]. The Prototype Building models are adapted from the Commercial Reference Building models, whose development is documented in [101]. This analysis was performed for the location of Boulder, Colorado, using the 724699 TMY3 weather file (Boulder/Broomfield/Jefferson County AP), and the versions of the prototype building models that are compliant with 2013 ASHRAE 90.1. for Climate Zone 5B (in which Boulder is located) were applied.

The prototypical office building has lighting and plug loads reflective of typical office space and light computer equipment. The prototypical multi-family building consists of dwelling units, as well as a small office space on the ground floor. The prototypical restaurant building consists of a kitchen and a dining area, with the kitchen having electric and natural gas-fired equipment for cooking and food preparation, and reach-in refrigeration cases. For illustration, a schematic representation of this district is shown in Figure 7.2, and a satellite image of the location shown in Figure 7.3. Notionally, these prototypical buildings correspond to university administration buildings, dormitories, and a large cafeteria that exist in this location on the CU Boulder campus. (Note that a student health center also exists at this location, and a suitable match for this building type does not currently exist among the DOE Prototype Building models.) It is not expected that the Prototype Building models would represent the nuances of the operating schedules and load densities of these particular buildings, but that they would capture some expected elements of the load diversity (balance between heating and cooling loads) of a plausible new construction district. New construction also more readily facilitates the drilling of wells tied to the ground-source heat

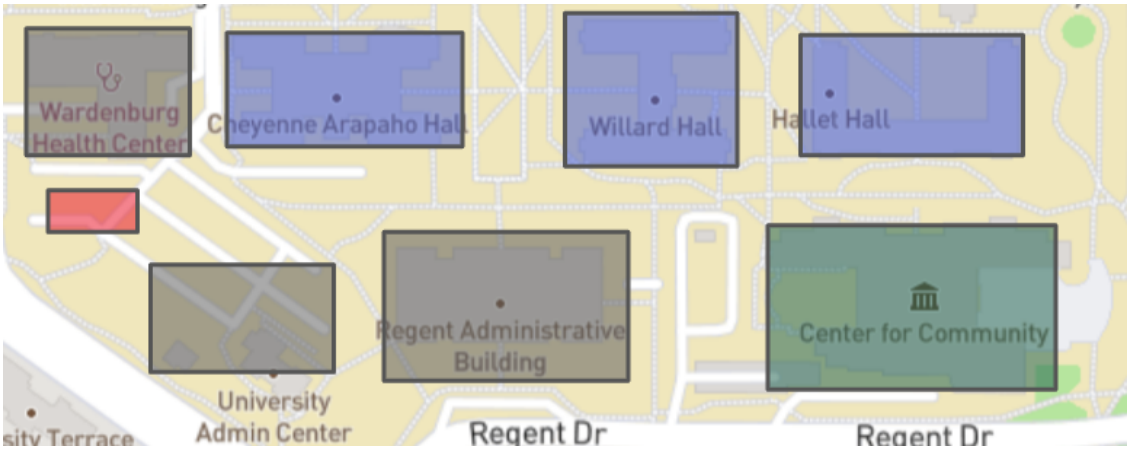

Figure 7.2: Prototypical district analysed in this case study, with multi-family buildings shown in blue, offices in grey, a restaurant in green, and the central plant in red. Note that the rectangles representing the buildings are not shown to scale for building area.

pump that serves the district thermal energy system considered in this study.

To represent the full scope of potential network configurations, the load of each prototypical building must be represented for two cases: one in which the building is tied to the district thermal energy system, and one in which the building is served by independent, building-level HVAC systems. To represent the case in which the building is served by a district thermal energy system, the HVAC systems in the prototype building models were modified to incorporate water-source heat pumps tied to the district network. (The modifications were based on OpenStudio measures developed by [31].) To represent the case in which the building was served by independent HVAC systems, the HVAC systems present in the prototype building model were preserved. Characteristics of the prototype building models applied in this study are summarized in Table 7.1 and Table 7.2. Note that heating and cooling are entirely supplied by electricity for buildings tied to the DES, whereas the buildings with independent systems have heating supplied primarily by natural gas. For each of the building energy models considered, it was confirmed that there were fewer than 300 hours annually in which zone-level temperature setpoints were not met, as recommended by [66] .

Figure 7.3: Satellite image of location considered in this case study, courtesy of Google Earth.

Table 7.1: Envelope characteristics of building load models.

Building Type	Floors	Floor Area(m^2)	Envelope
Office	3	4,980	Reinforced concrete construction with built-up roof, 33% window-to-wall ratio (WWR)
Multi-family	4	3,130	Steel frame construction with built-up roof, 20% WWR
Full-service restaurant	1	510	Steel frame construction with attic above wood joists, 18% average WWR (varying by façade)

Table 7.2: HVAC system types for independent ("indep") and district energy system-tied ("DES") cases for building models.

Building Type	HVAC-Indep.	HVAC-DES.
Office	Packaged variable air volume (VAV) unit with direct-expansion (DX) cooling, gas heating, and electric reheat	Zone-level water-to-air heat pumps with electric reheat
Multi-family	Split-system with DX cooling and gas heating	Zone-level water-to-air heat pumps
Full-service restaurant	Packaged unit with DX cooling and gas heating	Zone-level water-to-air heat pumps

7.3.2 District energy system model

A model created in Modelica, an object-oriented, equation-based language for representing physical systems, was used to calculate the energy consumption associated with the district thermal energy system [36]. The model was extended from the one in [3]. In this case study, the district thermal energy system considered operated in a two-pipe configuration, facilitating bi-directional thermal and mass flow. A centralized ground-source heat pump controlled the loop temperature, with the "warm pipe" operating at 26 °C, and the "cool pipe" at 16 °C. Based on ground temperatures for the location, and guidance from [123] regarding design of ground-source heat pump systems, the model assumed an evaporator temperature for the heat pump of 4.4 °C in heating mode, and a condenser temperature of 21 °C in cooling mode. Each building was equipped with an "energy transfer station" with water-source heat pumps, whose energy consumption was calculated through the use of the building load model.

7.3.3 Topology optimization framework

The novel topology optimization framework developed by the authors and applied in this study uses an energy model to determine the "best" configuration of a district thermal energy system with respect to life cycle cost. The life cycle cost considered encompasses the energy costs associated with HVAC systems for buildings in the district of interest, the cost of installing the thermal network itself, and costs associated with a potential future price on carbon. The framework leverages the PSO algorithm to determine the best subset of buildings (if any) to connect to the network and applies the MST heuristic to specify the best network by which to connect a given subset of buildings. The MST minimizes the length of the thermal network, and thus, the infrastructure cost. The use of the MST heuristic was validated in [120]. Development of the framework has been documented in [6] and [120].

The PSO algorithm, in its alternate formulation for a problem with discrete, binary variables, is implemented in the framework using the pyswarms package available in Python [41]. For a

candidate solution with valid connectivity, the corresponding minimal spanning tree network is constructed using Prim's Algorithm [113]. The energy model, in functional mock-up unit (FMU) format, representing the district thermal energy system, is then modified through the Python PyFMI package to represent the building and network connectivity corresponding to the candidate solution [103]. The energy model is simulated (also by leveraging the PyFMI package) and the outputs, as well as parameter values related to infrastructure and utility costs, are used to evaluate the cost function. The framework incorporates several termination criteria, including one based on "stall," which will terminate the algorithm if the best value of the objective function does not improve after a fixed number of iterations (in this case, 50% of the maximum number of iterations, 1,000). In this analysis, the algorithm terminated based on stall.

Based on an evaluation of the performance of the PSO algorithm on a similar problem, to be documented in [124], the lbest version of PSO, with a swarm size (n) of 20 particles, and a neighbourhood size (k) of 5 particles, was implemented for this study. As a proportion of the swarm size, the size of this neighbourhood is consistent with the recommendations of [105] based on an empirical analysis. The values of hyperparameters for the PSO algorithm that were used in this study, and references used to determine them, are shown in Table 7.3.

Table 7.3: Values of hyperparameters used in configuration of PSO algorithm in this study.

Parameter	**Value**	**Selected References**
c_1, c_2	1.7	[104], [105], [109]
w	0.85	[104], [105]
n	20	[102], [97], [40]
k	5	[105]

In this case study, the topology optimization framework was configured to perform optimization

based on the cost function shown in Equation 7.1:

$$\min_{\mathbf{A}} C_{pipes} + C_{elec} UPV_{ele}(E_{de} + \sum_{i=1}^{n} E_{be,i}) + C_{gas} UPV_{gas} \sum_{j=1}^{n} E_{bg,j} + UPV_{CO2} \sum_{t=1}^{30} m_{CO2}(t) C_{CO2}(t) \tag{7.1}$$

where $\mathbf{A}$ is the adjacency matrix corresponding to the connectivity of the thermal network, C_{pipes} is the cost of the DES infrastructure, C_{elec} and C_{gas} are the costs of electricity and natural gas per unit of consumption, UPV_{ele}, UPV_{gas}, and UPV_{CO2} are the uniform present value factors used to convert an annual cost to the value over the lifetime of the system for electricity, gas, and carbon, respectively, E_{de} is the electricity consumption associated with the centralized DES heat pump and system distribution pumps, E_{be} is the electricity consumption for HVAC at a given building, E_{bg} is the natural gas consumption for HVAC at a given building, $m_{CO2}(t)$ is the emissions of carbon dioxide associated with the district's HVAC energy use for a given year, and $C_{CO2}(t)$ is the unit cost of carbon dioxide (CO_2) emissions in a given year, under a potential future carbon pricing scenario outlined by [88]. A constraint was imposed to ensure that if any loads were connected to the network in a given scenario, the centralized heat pump was also connected. The uniform present value factors, developed by [88], account for projections of future escalation in utility costs, as well as the time value of money. Note that declining values of carbon intensity for electricity are used over the project's lifespan, per a scenario outlined by [88].

The life cycle cost was evaluated over 30 years. The infrastructure cost component consists of the cost associated with piping and trenching for the thermal network, calculated as a linear function of the network length. It was assumed that differences in the cost associated with building-level HVAC equipment for DES-tied or independent scenarios would be negligible relative to the life cycle cost of the system. This is consistent with the approach taken in [6] and [3]. Note that the objective function encompasses the energy costs associated with HVAC systems for all buildings in the prototypical district, whether or not a given building is tied to the district thermal network.

The building-level HVAC energy use considered encompasses the energy use associated with heating and cooling coils, heat pumps, and hydronic distribution pumps (if present), and does not include fan energy use. Table 7.4 shows a summary of values of parameters used in the life cycle cost calculation. The cost function itself and these values are consistent with those used in [124].

Table 7.4: Values of economic parameters in life cycle cost calculation.

Parameter	**Value**	**Units**	**Source**
Discount rate	3%	NA	[3]
Electricity cost, base year	27.8	$\frac{\$}{GJ}$	[88]
Natural gas cost, base year	6.48	$\frac{\$}{GJ}$	[88]
Carbon cost, base year	20.0	$\frac{\$}{mt}$	[88]
Pipe cost	548	$\frac{\$}{m}$	[26], [89]

7.4 Results and discussion

The application of the topology optimization framework identified design solutions with life cycle costs significantly lower than that of the designs based on heuristics. Specifically, the topology optimization framework identified four design solutions with very similar values of life cycle cost, a value which is 14% lower than that of the best-performing base case (the minimal spanning tree network), and 72% lower than that of the worst-performing base case (the full mesh network). Attributes of the solutions determined through the framework, as well as the base case scenarios, are summarized in Table 7.5. Optimal solutions are numbered in increasing order of associated life cycle cost. A plot of all the candidate solutions evaluated by the topology optimization framework, as well as the base cases, in terms of the total network length and life cycle cost, is shown in Figure 3. (Note that two among these best solutions have very similar values of network length, due to the fact that two buildings in the prototypical district are roughly equidistant from the hypothetical central plant location.)

As shown in Table 7.5 and Figures 7.4 and 7.5, all four solutions identified through the topology optimization process entail a limited district thermal energy network (serving at most two buildings), or no network at all. Of these four solutions with very similar values of LCC, the

Table 7.5: Summary of optimal solutions and base case scenarios.

Scenario	**LCC**	**Network Length (m)**	**Con. Bldgs.**	**Source EUI ($\frac{MJ}{m^2}$)**
Opt-1	$979,867	0	0	176.9
Opt-2	$980,377	64	1	170.2
Opt-3	$981,602	65	1	170.3
Opt-4	$982,381	130	2	163.6
Base-Ring	$1,254,779	803	7	141.6
Base-Radial	$1,430,558	1,136	7	140.4
Base-Full Mesh	$3,500,538	4,924	7	139.4
Base-MST	$1,137,870	589	7	141.6

one with the least LCC ("Opt-1") corresponds to the case in which all buildings in the prototypical district are served by independent HVAC systems. The networks corresponding to the "Opt-2", "Opt-3", and "Opt-4" solutions are visualized in Figures 7.6, 7.7, and 7.8. Note that the Opt-2 and Opt-3 solutions correspond to the shortest possible networks that can be created to serve at least one building, and that Opt-4 entails only a marginally longer network. (There are two possible networks with lengths intermediate to those of Opt-3 and Opt-4, with a marginally higher LCC.) The nature of these results is consistent with the theme that, though the DES connection provides a reduction in source energy use intensity for each building type, the energy savings is offset by the higher unit costs of heating by electricity instead of natural gas, and the infrastructure costs further compound these higher costs. Thus, in this scenario, the most cost-effective networks are generally the shortest ones.

The four base case scenarios all result in very similar values of district-level source energy use intensity and vary chiefly in terms of the associated network length. As discussed in a following sub-section, this trend is also borne out by the candidate solutions evaluated by the optimization algorithm, when they are sub-divided based on the number of connected buildings. Due to its high life cycle cost (driven by the associated infrastructure cost), and lack of benefit in reduction of source energy use intensity in this case, it appears unlikely that the full mesh network would be implemented in practice, but it is included among the base case scenarios for completeness, as

representing one of the extremes of network length (the longest possible network). Ring, radial, and full mesh networks can also provide benefits in terms of redundancy of supply. Resilience or robustness were not objectives considered in this analysis, though they may be identified as important objectives in some applications.

The candidate solutions explored by the optimization algorithm offer insights into the factors influencing the energy and economic performance of 5GDHC systems in this case. Note that these candidate solutions represent a subset of the total possible "search space" of network configurations, and that the stochastic element of the PSO algorithm introduces some randomness into the identification of candidate solutions. It is useful to characterize the candidate solutions as a function of the corresponding number of DES-connected buildings, as this significantly influences the life cycle cost. In this study, the PSO algorithm converged before exploring any potential solutions involving a connection of all seven buildings in the prototypical district to the DES. For purposes of comparison, the four "base case" scenarios (representing thermal networks connecting all seven buildings to the DES) are also plotted alongside candidate solutions explored by the optimization algorithm. Note that while all the candidate solutions explored by the optimization approach correspond to MST networks, only one of the base case scenarios corresponds to an MST.

Figures 7.9 and 7.10 show, in boxplot form, the variation in overall life cycle cost, and the energy and infrastructure components specifically, for the candidate solutions evaluated by the topology optimization framework, and the base cases, sub-divided based on the number of connected buildings. The case in which all buildings are served by independent systems is represented as a single point. (For purposes of concision, the "full mesh" base case, which has a significantly higher infrastructure cost, is not represented on this plot.) Generally, a higher number of connected buildings results in higher life cycle costs. Though the district thermal energy network results in reduced source energy use intensity (as will be discussed further in a following sub-section), this effect is dominated by the higher infrastructure costs associated with network connectivity. As shown in Figure 7.10, variation in infrastructure cost, corresponding to different network lengths, explains most of the variation in life cycle cost among scenarios with the same number of buildings

connected to the network. All the scenarios explored by the optimization algorithm represent minimal spanning tree networks, whereas only one of the "base case" scenarios is a minimal spanning tree network, resulting in greater variability in the thermal network length among the scenarios with all seven buildings tied to the DES. For a given number of connected buildings, the variation in energy cost among different scenarios explored (corresponding to the selection of different subsets of buildings), is very limited in this case. This trend is further elucidated by the boxplot showing variation in district-level source EUI in Figure 7.12. Shown in Figure 7.11 is a boxplot showing the variation in the component of life cycle cost associated with carbon, as a function of the number of buildings connected. For a given number of connected buildings, there is limited variation in the source EUI, and correspondingly, in the associated carbon emissions and carbon cost.

Among the scenarios evaluated by the optimization algorithm, energy cost dominated as a fraction of the overall life cycle cost, ranging from 63% to 84% of the overall life cycle cost. The fraction of life cycle cost attributable to infrastructure ranged from 0% (for the null case) to 27%, and the fraction attributable to a price on carbon ranged from 10% to 16%. The high cost of electricity relative to natural gas in the US as a whole and in this region contributes to the fact that energy costs constitute a significant fraction of the life cycle costs of the systems considered.

Figure 7.12 shows the range of source EUI for HVAC as a function of the number of buildings tied to the network. This value is based on the total district-level HVAC energy use, as used by the cost function, and the total floor area of buildings in the prototypical district. Though the restaurant building has a significantly higher source EUI than the multi-family or office buildings (discussed in more detail in a following section), the overall building-level thermal loads, especially in heating mode, are relatively similar among the three building types, resulting in limited variation for district-level HVAC source EUI for a given number of connected buildings.

The median district-level source EUI for HVAC among the four "base case" scenarios representing the connection of all buildings to the DES is 20% lower than that of the "null case" in which all buildings have independent systems. For intermediate numbers of connected buildings, the median source HVAC EUI is monotonically decreasing between these two values. However,

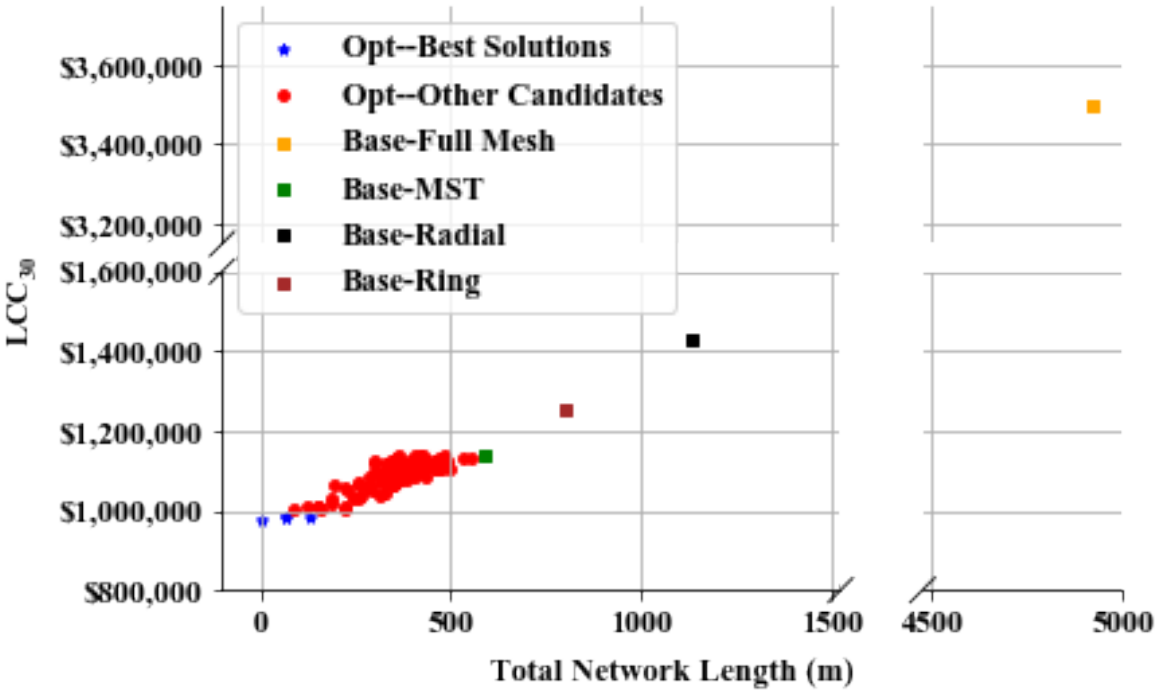

Figure 7.4: Life cycle cost as a function of total network length, for all scenarios. Note the broken axes in the plot.

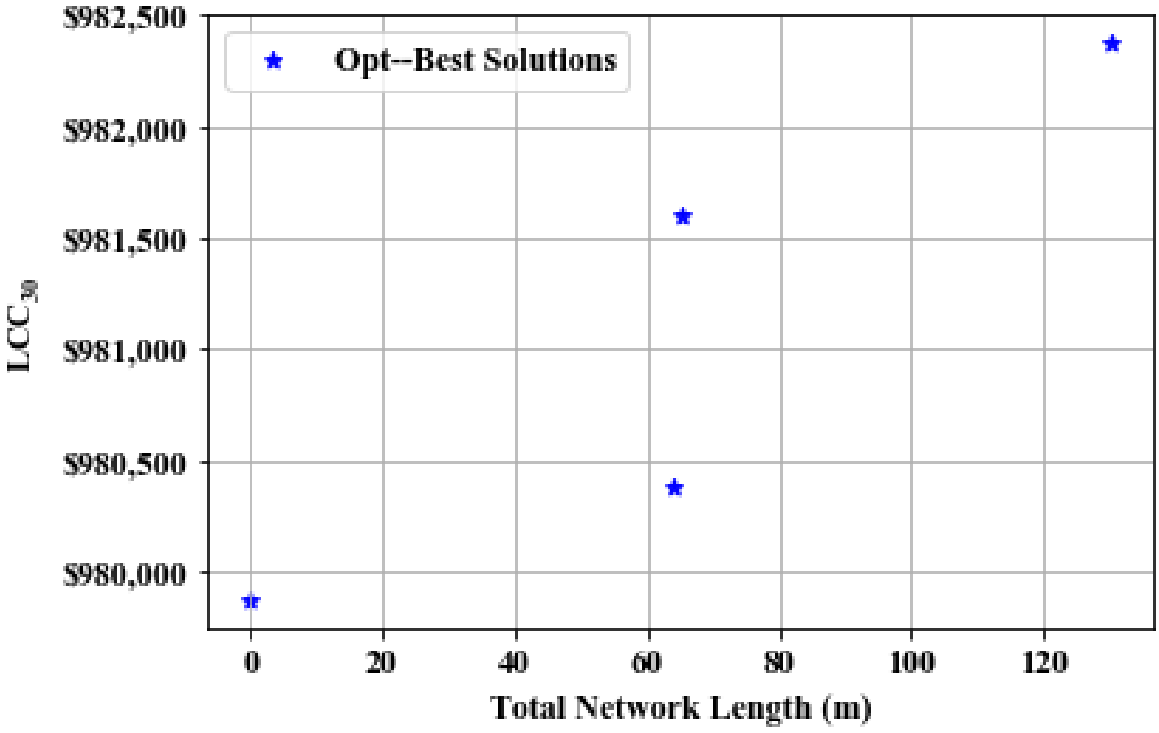

Figure 7.5: Best solutions identified by the topology optimization framework.

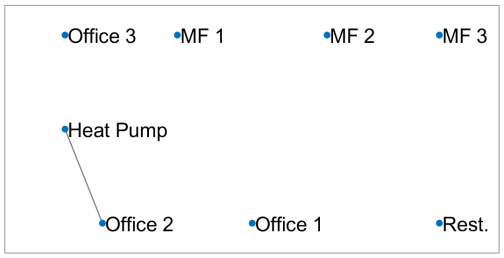

Figure 7.6: Graph corresponding to "Opt-2" solution.

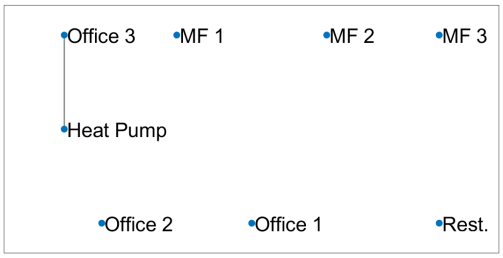

Figure 7.7: Graph corresponding to "Opt-3" solution.

the median energy cost component of the LCC is reduced by only 14% (a reduction of roughly $114,500) between the same two comparison points. This is largely driven by the lower cost associated with meeting a given heating load with natural gas relative to electricity under the utility pricing scenario considered in this study, with the unit cost of electricity 4.3 times that of natural gas. The reduction in energy costs is eclipsed by the increase in infrastructure costs of $531,300 between the same two points. The median infrastructure cost as a function of the number of connected buildings also increases monotonically between these two points and is a linear function of the network length.

7.4.1 Source energy use intensity comparison

Each of the prototypical building types considered in this study exhibits a reduction in source energy use intensity (EUI) for HVAC when tied to the district thermal energy system. For this comparison, in the DES-tied scenario, energy use by the centralized heat pump was allocated to each individual building based on the annual average coefficient of performance (COP) values in heating and cooling modes, to approximate an annual source HVAC EUI for each prototypical building, encompassing heating, cooling, and distribution pump energy use. (Note that this approximation introduces a slight imprecision due to variations in loop operating temperatures as a function of the nature of the connected buildings.) Site-to-source conversion factors for natural gas and electricity were obtained from [93]. Figures 7.13 and 7.14 show the HVAC source EUI, disaggregated by

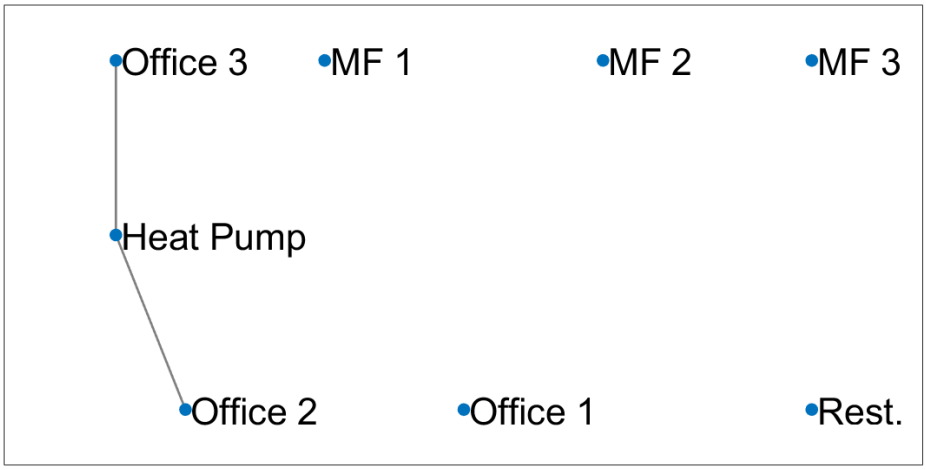

Figure 7.8: Graph corresponding to "Opt-4" solution.

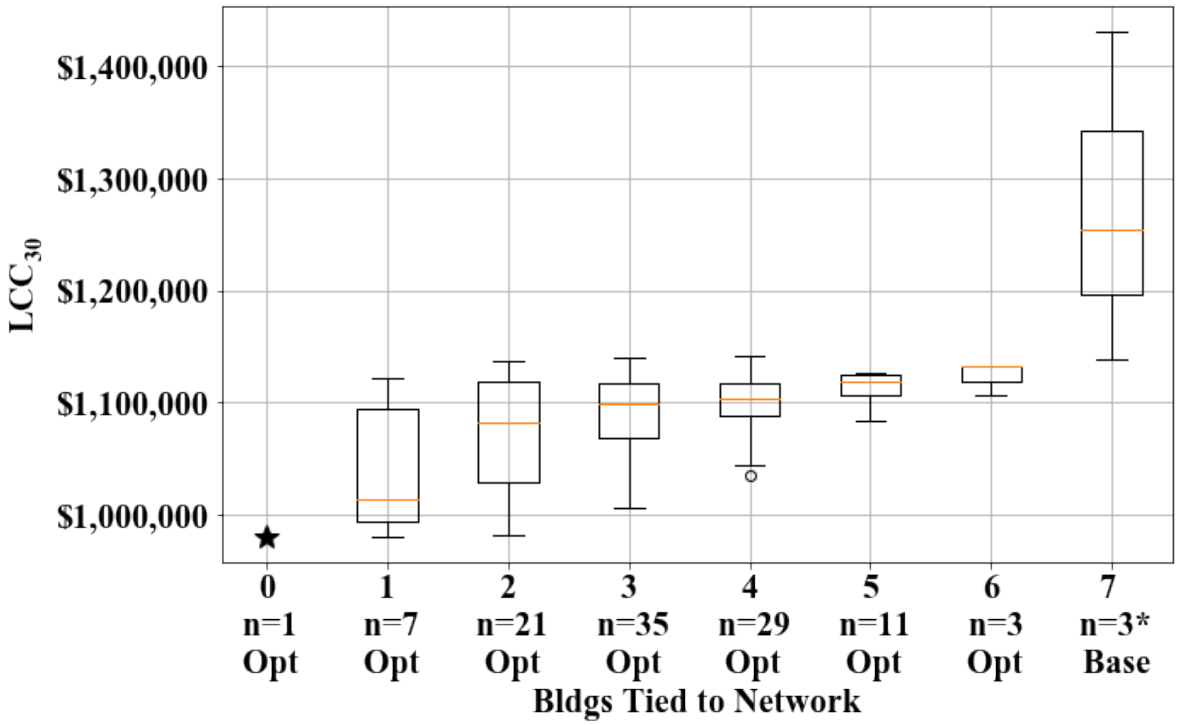

Figure 7.9: Boxplot showing range of variation of LCC, as a function of the number of buildings tied to the network.Note that for concision, one of the base case scenarios, corresponding to the "full mesh" network with seven connected buildings, is excluded from this plot due to its significantly higher LCC.

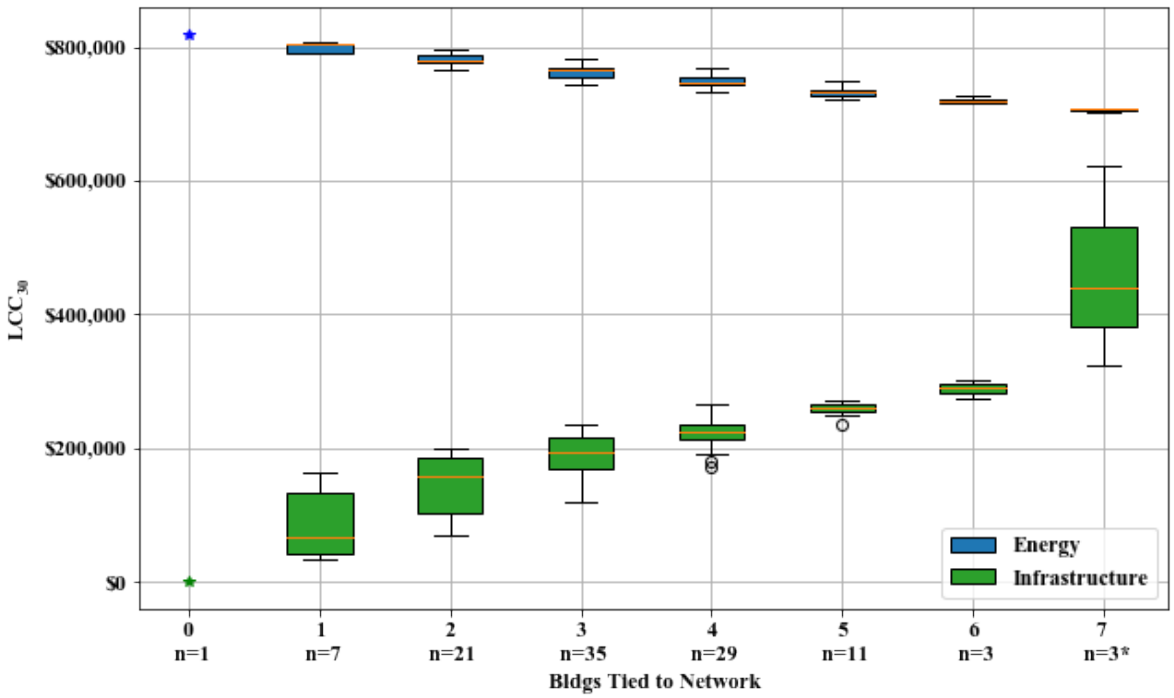

Figure 7.10: Boxplot showing range of variation of LCC for energy and infrastructure cost components of the LCC. Note that for concision, one of the base case scenarios, corresponding to the "full mesh" network with seven connected buildings, is excluded from this plot due to its significantly higher LCC.

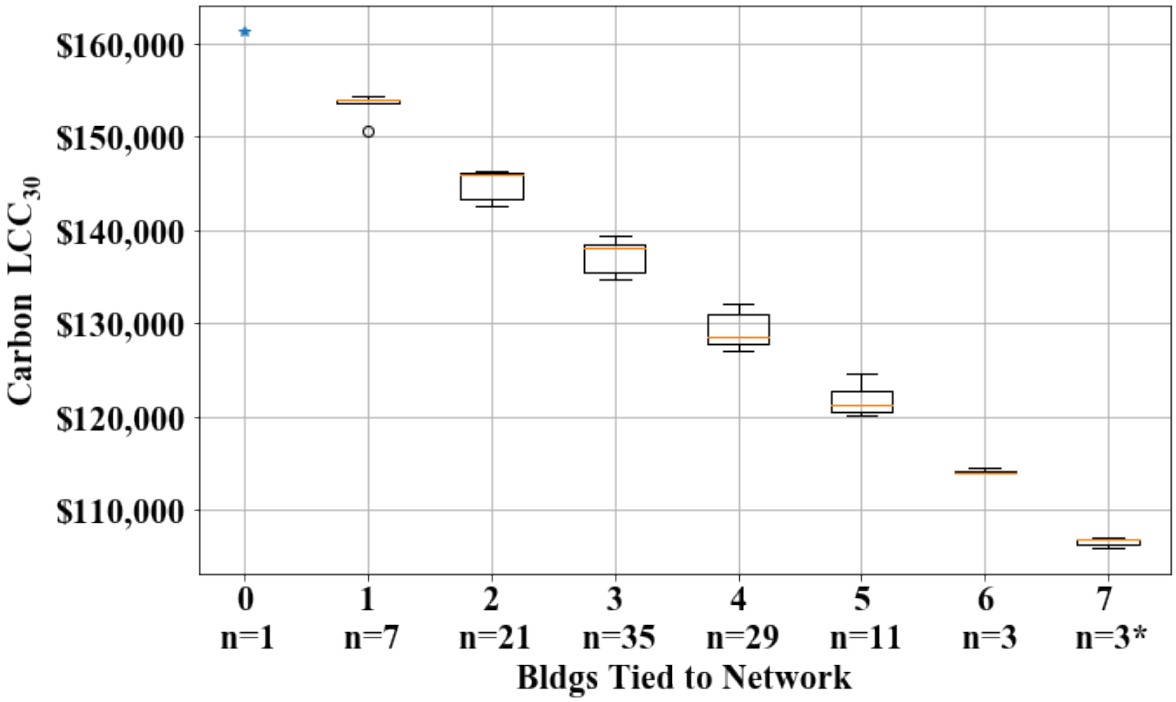

Figure 7.11: Boxplot showing range of LCC for carbon emissions as a function of the number of buildings tied to the network.

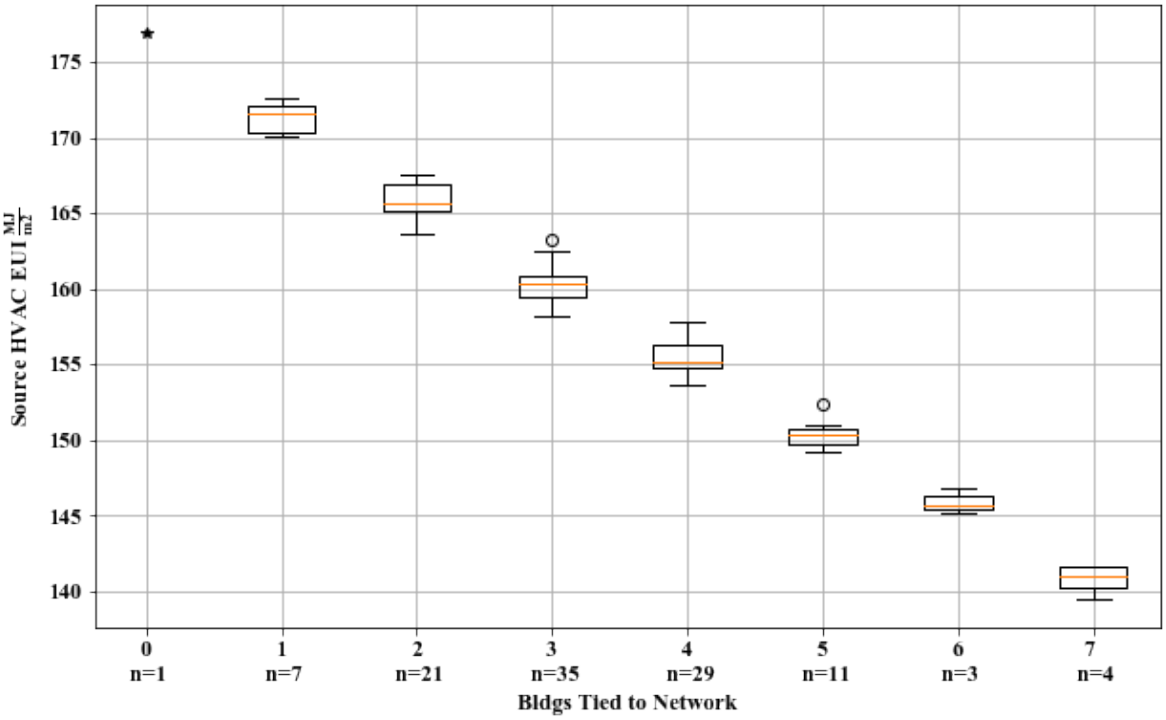

Figure 7.12: Boxplot showing range of district source HVAC EUI as a function of the number of buildings tied to the network.

heating and cooling, for each prototypical building type, when served by independent, building-level systems ("indep") and by the DES ("DES"). Note that the prototypical restaurant building has a significantly higher source EUI for HVAC than the office or multi-family buildings, due to its high ventilation loads, magnified by its smaller physical footprint. The restaurant building accounts for around 13% of the overall source energy use of the prototypical district.

A connection to the DES results in an annual reduction in source EUI of 15% for the multi-family and restaurant buildings, and 21% for the office building. The reduction in source EUI is exhibited primarily in heating energy use. The centralized ground-source heat pump considered in this analysis operates between an evaporator temperature of 4.4 °C and a condenser temperature of 26 °C in heating mode, allowing it to achieve an annual average COP on the order of 6.0. The building-level heat pumps operate with the district loop as a heat source or sink and have nominal COPs in the range of 5.0 to 6.0 for the loop temperatures of 16 °C in cooling and 26 °C in heating. In heating in particular, this represents a significant improvement in exergetic efficiency relative to the 80% efficient natural gas heating coils that serve the buildings with independent systems.

One of the factors contributing to the greater proportionate reduction for the office building is the greater amount of time during which, in the DES-tied configuration, simultaneous heating and cooling occurs at the building level. During 42% of the time in which heating or cooling is required in the office building, at least one zone in the building requires heating while another requires cooling. This thermal diversity within the office building is contributed to by the configuration of the building into core and perimeter thermal zones. The building-level water-source heat pump loop facilitates the ability of simultaneous heating and cooling loads to partially (or fully) offset each other, mitigating demand on the district-level loop. Simultaneous heating and cooling at the building level occurs in just 10% of the time in which heating or cooling is required for the prototypical multi-family building, and virtually never for the restaurant building. The restaurant building model is configured with two thermal zones (corresponding to the kitchen and dining area, respectively), and both have high ventilation loads, resulting in little thermal diversity within the building itself. In addition to the benefits of building-level thermal diversity, the zone-level HVAC

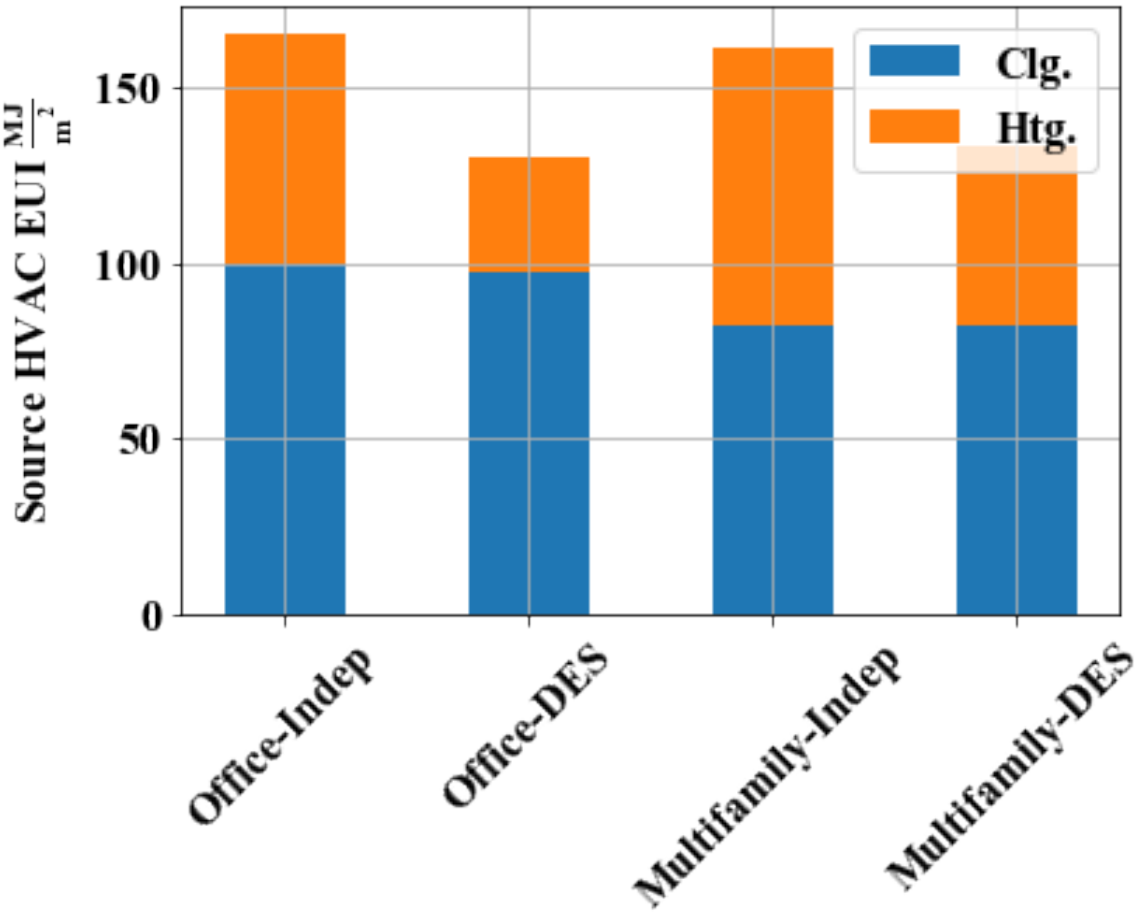

Figure 7.13: Source energy use intensity (EUI) for the prototypical office and multi-family buildings considered in this study, for the cases in which the buildings are served by building-level systems ("Indep") and the district thermal energy system ("DES").

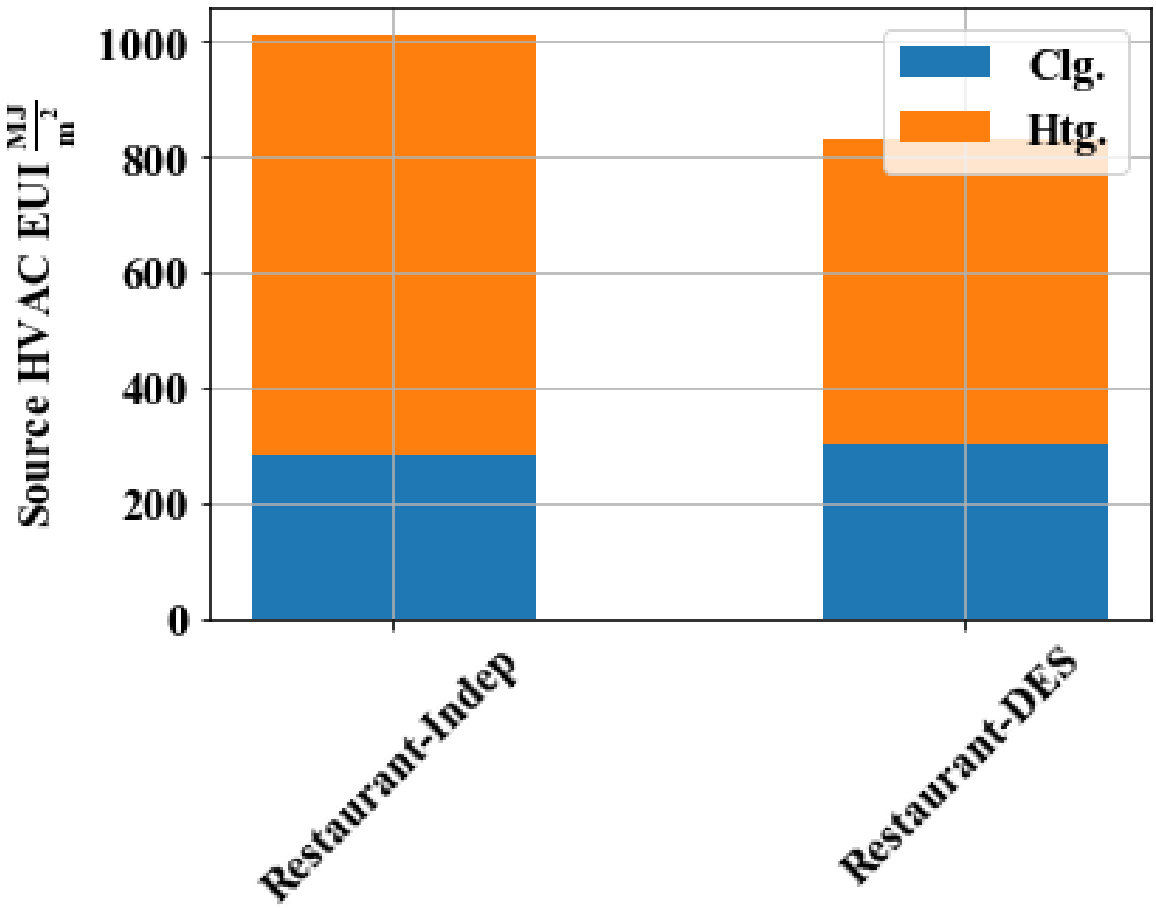

Figure 7.14: Source energy use intensity (EUI) for the prototypical restaurant building considered in this study, for the cases in which the building is served by building-level systems ("Indep") and the district thermal energy system ("DES").

systems used in the DES-tied case for the office building eliminate the use of reheat purely for temperature control, though not for humidity control.

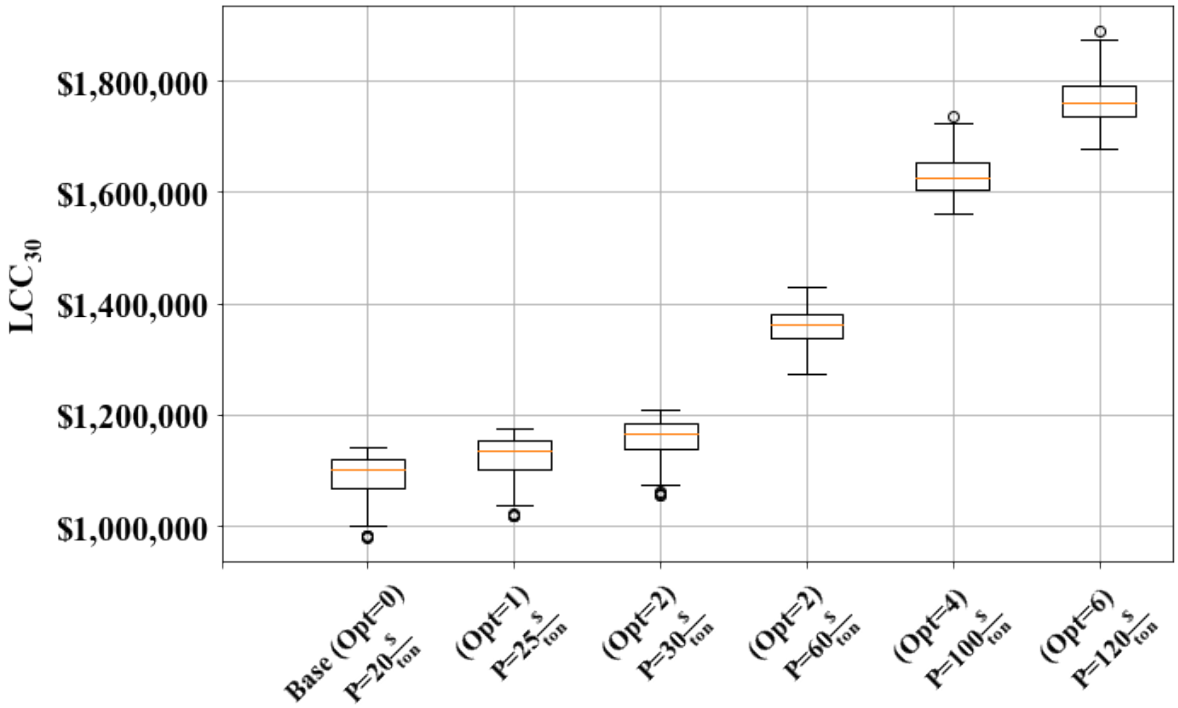

Figure 7.15: Summary of results of sensitivity analysis for carbon price, presented with the carbon price in the first year.

A sensitivity analysis for the price on carbon was performed using post-processing, based on the data set generated from the points evaluated by the framework. The results from this analysis are presented in a boxplot in Figure 7.15. For purposes of the sensitivity analysis, the carbon pricing trajectory was scaled by a constant factor, and the price on carbon in the initial year is used to represent the scenario. Several scenarios are presented, based on the resulting optimal level of network connectivity, in terms of the number of buildings. There were no candidate solutions evaluated that entailed the connection of all seven buildings to the network, so that level of connectivity was not encompassed by the sensitivity analysis.

In general, in this study, a larger number of connected loads resulted in a higher life cycle cost, due to higher energy costs (resulting from a greater degree of electrification of heating), and higher

costs associated with network infrastructure. Thus, a higher price on carbon was required to offset these costs and result in an optimum solution with a greater degree of network connectivity. The significant increase in the carbon price required to result in an optimal connection of four buildings compared with two is due to the significantly (28%) longer mean network length associated with the candidate solutions consisting of three connected buildings, relative to two. (The limited number of candidate solutions explored through the optimization—108—results in some discontinuities in the results of this sensitivity analysis.) It is worth underscoring that in this study, a carbon pricing scheme with rates scaled by a factor of 6 (for an initial rate of $\frac{\$120}{ton}$) from those projected as a potential future scenario by NIST are required for the optimum solution to entail a high degree of network connectivity (six connected loads), all other things being equal.

7.5 Conclusion

In this study, a topology optimization framework developed by the authors was applied to the design of a 5GDHC system for a prototypical urban district to identify a network configuration that would minimize life cycle cost. The results from the topology optimization process were compared to four "base cases," in which the district thermal energy system served all buildings in the prototypical district, with a network design based on heuristics. The topology optimization approach identified four solutions (with very similar values of life cycle cost), which would provide reductions of life cycle cost ranging from 14% to 72% relative to the base cases, depending on the base case scenario considered, highlighting the benefits of topology optimization in this context. Though the study is tied to a particular set of conditions, the selection of prototypical buildings based on a thermal load diversity metric ensures that it provides an evaluation of 5GDHC systems in a "competitive" context.

All four solutions identified through topology optimization involved a limited district thermal energy network, or the absence of a network at all. It is evident that while a 5GDHC system serving all buildings in the prototypical district would provide reductions in source energy use intensity (on the order of 20%), as well as energy cost savings, the scale of the energy cost savings are insufficient

to offset the additional investment in infrastructure required. The low cost of natural gas relative to electricity contributes to this disparity. A carbon tax of at least $\frac{\$30}{ton}$ under the initial conditions, and increasing with time, is found to be necessary for even a moderate degree of network connectivity to be cost-effective relative to distributed, building-level systems. Extending this analysis to a case with electrified building-level heating systems, such as air-source heat pumps, is an area for future work. This study has demonstrated the value of a network topology optimization approach for the design of 5GDHC systems, as well as the potential benefits of 5GDHC systems themselves in reducing the energy- and carbon-intensity of HVAC systems. Changes in utility costs or policy interventions are likely to be necessary for these reductions in emissions to be cost-effective relative to building-level HVAC systems.

Chapter 8

Conclusions and future work

As part of the work underlying this dissertation, the energy performance benefits associated with low-exergy HVAC systems have been quantified, motivating a focus on network topology optimization in the context of advanced district thermal energy systems. From a case study focusing on multi-family housing buildings, it was concluded that low-exergy HVAC systems could achieve reductions on the order of 25% in source energy use for HVAC relative to third-generation hydronic HVAC systems, in appropriate applications. Low-exergy systems in the form analyzed in this work — radiant hydronic thermo-active building systems — are best suited to buildings with high-performance envelopes, limited sensible loads, and minimal dehumidification loads, due to the limits on surface temperatures to avoid condensation. Low-exergy systems facilitate the use of district thermal energy systems operating at near-ambient temperatures. The potential for connected loads served by such 5GDHC systems to act as "prosumers", and exchange heat, and heat rejection, in a synergistic manner, motivates the consideration of the network topology optimization problem. In this context, network topology optimization seeks to answer the question, "Given a prototypical urban district with known building locations and loads, what is the best subset of buildings, if any, to connect to a district thermal energy system, and by what thermal network should they be connected, to minimize life cycle cost?"

An approach for optimization of network topology for district thermal energy systems — namely, the use of the minimal spanning tree heuristic and particle swarm optimization — has been validated, in the context of systems operating at near-ambient temperatures, with an exhaustive

search evaluating the full "solution space" of more than 30,000 potential network configurations for a five-building prototypical district. The MST heuristic and a PSO algorithm have been combined to create a topology optimization framework, which will soon be integrated with NREL's URBANopt advanced analytics platform, and publicly available for use as a software module by researchers and practitioners. A PSO algorithm is used to determine the optimal subset of buildings (if any) to connect to a district thermal energy system, and the MST heuristic is used to select the thermal network by which to connect them. In this way, the MST heuristic serves to significantly reduce the size of the "search space." The Topology Optimization Framework takes as inputs an energy model of a district thermal energy system in FMU format, and a GeoJSON file with data on the physical locations of the buildings considered. A PSO algorithm is used to generate candidate solutions, and the FMU energy model is programmatically modified to represent the solution, using the MST network. The energy model is simulated and its outputs, as well as other parameter values, are used to evaluate the objective function. The process repeats until a convergence or termination criterion is met. Topology optimization has been applied to two prototypical districts (one of five buildings and one of seven buildings), with promising results regarding reduction in source energy use intensity and life cycle cost, relative to a network designed based on rules-of-thumb.

The application of the Topology Optimization Framework to a prototypical new-construction district in Colorado revealed that the relative costs of electricity and natural gas present a significant barrier to the cost-effectiveness of 5GDHC systems in the US, since they entail the electrification of space heating. The reductions in source energy use associated with beneficial electrification, while notable, are not sufficient to offset the higher costs associated with electricity. In Colorado, electricity costs per unit are 4.3 times that of natural gas, and similar disparities exist across the US [77]. In the prototypical district considered, a carbon tax of at least $ 30/ton, increasing with time, was found to be necessary in order for even a moderate degree of thermal network connectivity to be optimal. Consistent with other case studies performed in the course of this work, it was found that the use of a district thermal energy system to serve all buildings in the prototypical district resulted in a reduction on the order of 20% of source energy use for HVAC, relative to a case in which all

buildings were served by independent systems. This motivates the consideration of policy efforts that would improve the relative cost-effectiveness of beneficial electrification of space heating. In this and other case studies performed as part of this work, it was found that the selection of the subset of buildings to connect to a district thermal energy system was much more influential on the source energy use for HVAC of the district than the particular network configuration, though the selection of network configuration could lead to significant variation in life cycle cost through the varying infrastructure cost, especially with a greater number of buildings served.

The Topology Optimization Framework as developed can address cost functions related to energy consumption, carbon emissions, and life cycle cost. Related work that is currently ongoing applies the Topology Optimization Framework to objectives of carbon emissions and life cycle cost in a multi-objective approach, and applies Monte Carlo analysis to the values of key parameters in the cost function. It is anticipated that multi-objective optimization can identify trade-offs between reductions in life cycle cost and carbon emissions that could guide decisionmaking. The application of Monte Carlo analysis is expected to illustrate the ranges of values of particular parameters in the life cycle cost function that either "promote" or "discourage" the connection of more loads to the thermal network.

Additional ongoing work concerns the analysis of the integration of low- to moderate-temperature waste heat sources into 5GDHC systems. It is anticipated that such sources, including commercial refrigeration and data centers, will improve the relative cost-effectiveness of 5GDHC systems, as well as further reducing the energy use and carbon emissions associated with meeting space heating loads. The network topology optimization problem could also be extended to consider the locations at which waste heat should be integrated, and additional work could consider the optimal temperature level and control of waste heat integration.

Further refinements could be made to the Topology Optimization Framework. In its current form, the framework has been demonstrated to support the implementation of additional constraints related to network connectivity, through the approach of assigning high "penalty" values to the cost function when candidate solutions violate such constraints. In the future, the framework could

be adapted to incorporate constraints into the optimization problem directly. Another relevant area for further research, to mitigate the computational complexity associated with the network topology optimization problem, is the development of metamodels to represent district-level energy consumption for a thermal network. When integrated as part of the URBANopt platform, the Topology Optimization Framework will be available to a wider array of potential users, including researchers and practitioners. Research by others has concluded that, depending on the demand density threshold considered, the techno-economic potential for district heating systems in the US is on the order of 12% to 43% of the current energy consumption for space heating [87]. District energy systems operating at near-ambient temperatures can facilitate the integration of moderate-temperature waste heat sources, which can further serve to improve the cost-effectiveness of such systems. It is anticipated that the Topology Optimization Framework can help facilitate the adoption of advanced district thermal energy systems in appropriate applications, and thus, help achieve reductions in source energy use and associated carbon emissions, as well as addressing additional research questions.

Bibliography

[1] UNEP. The Sustainable Development Goals Report. Technical report, 2018.

[2] Joan Fitzgerald and Jennifer Lenhart. Eco-districts: can they accelerate urban climate planning? Environment and Planning C: Government and Policy, 34(2):364–380, 2016.

[3] Justus von Rhein, Gregor P. Henze, Nicholas Long, and Yangyang Fu. Development of a topology analysis tool for fifth-generation district heating and cooling networks. Energy Conversion and Management, 196(March):705–716, 2019.

[4] Henrik Lund, Sven Werner, Robin Wiltshire, Svend Svendsen, Jan Eric Thorsen, Frede Hvelplund, and Brian Vad Mathiesen. 4th Generation District Heating (4GDH). Integrating smart thermal grids into future sustainable energy systems. Energy, 68:1–11, 2014.

[5] Francesco Bullo, Cortes Jorge, Dorfler Florian, and Martinez Sonia. Lectures on network systems. Kindle Direct Publishing, 2019.

[6] Amy Allen, Gregor Henze, Kyri Baker, and Gregory Pavlak. Evaluation of low-exergy heating and cooling systems and topology optimization for deep energy savings at the urban district level. Energy Conversion and Management, 222:113106, 2020.

[7] S. Buffa, M. Cozzini, M. D'Antoni, M. Baratieri, and R. Fedrizzi. 5th generation district heating and cooling systems: A review of existing cases in Europe. Renewable and Sustainable Energy Reviews, 104, 2019.

[8] Matthias Sulzer, Artem Sotnikov, and Tobias Sommer. Reservoir-Niedertemperatur Netztopologie für die Vermaschung von thermischen Netzen. brenet Conference Proceedings, (September 2018):590, 2018.

[9] Michael Wetter and Jianjun Hu. Quayside Energy Systems Analysis. 2019.

[10] Tobias Sommer, Stefan Mennel, and Matthias Sulzer. Lowering the pressure in district heating and cooling networks by alternating the connection of the expansion vessel. Energy, 172:991–996, 2019.

[11] Natasa Nord, Mohammad Shakerin, Tymofii Tereshchenko, Vittorio Verda, and Romano Borchiellini. Data informed physical models for district heating grids with distributed heat sources to understand thermal and hydraulic aspects. Energy, 222:119965, 2021.

[12] R. Zarin Pass, M. Wetter, and M. A. Piette. A thermodynamic analysis of a novel bidirectional district heating and cooling network. Energy, 144:20–30, 2018.

[13] Víctor F. Sanchez, Amaia Uriarte, Eneritz Barreiro, and Matteo Porta. Smart dual thermal network. International Journal of Energy Production and Management, 2(4):315–326, feb 2018.

[14] Ole Sigmund and Kurt Maute. Topology optimization approaches. Structural and Multidisciplinary Optimization, 48(6):1031–1055, 2013.

[15] Sigmund Bendsoe, Olhoff. Topological Design Optimization of Structures, Machines, and Materials. 2006.

[16] Aycan Erentok and Ole Sigmund. Three-dimensional Topology Optimized Electrically-Small Conformal Antenna (1) Department of Mechanical Engineering , Section for Solid Mechanics , Technical University of Denmark , DK-2800 Lyngby , Denmark. IEEE Antennas and Propagation Society International Symposium, (1):1–4, 2008.

[17] M. Beckers. Topology optimization using a dual method with discrete variables. Structural Optimization, 17(1):14–24, 1999.

[18] Satafa Sanogo and Frédéric Messine. Design of space thrusters: a topology optimization problem solved via a Branch and Bound method. Journal of Global Optimization, 64(2):273–288, 2016.

[19] Tingting Fang and Risto Lahdelma. State estimation of district heating network based on customer measurements. Applied Thermal Engineering, 73(1):1211–1221, dec 2014.

[20] Hariharan Gopalakrishnan and Dragoljub Kosanovic. Economic optimization of combined cycle district heating systems. Sustainable Energy Technologies and Assessments, 7:91–100, 2014.

[21] Keith O'Donovan, Reinhard Pertschy, Gerald Schweiger, Ingo Leusbrock, Wolfgang Streicher, Georg Engel, Richard Heimrath, Basak Falay, and Peter Nageler. District energy systems: Modelling paradigms and general-purpose tools. Energy, 164:1326–1340, 2018.

[22] Gerald Schweiger, Per-Ola Larsson, Fredrik Magnusson, Patrick Lauenburg, and Stéphane Velut. District heating and cooling systems – framework for modelica-based simulation and dynamic optimization. Energy, 137:566–578, 2017.

[23] Felix Bunning, Michael Wetter, Marcus Fuchs, and Dirk Müller. Bidirectional low temperature district energy systems with agent-based control: Performance comparison and operation optimization. Applied Energy, 209(July 2017):502–515, 2017.

[24] Hongwei Li and Svend Svendsen. District Heating Network Design and Configuration Optimization with Genetic Algorithm. Journal of Sustainable Development of Energy, Water and Environment Systems, 1(4):291–303, 2013.

[25] T. Mertz, S. Serra, A. Henon, and J. M. Reneaume. A MINLP optimization of the configuration and the design of a district heating network: Academic study cases. Energy, 116:236–248, 2016.

[26] Robert E. Best, P. Rezazadeh Kalehbasti, and Michael D. Lepech. A novel approach to district heating and cooling network design based on life cycle cost optimization. Energy, 194:116837, 2020.

[27] Tobias Falke, Stefan Krengel, Ann Kathrin Meinerzhagen, and Armin Schnettler. Multi-objective optimization and simulation model for the design of distributed energy systems. Applied Energy, 184:1508–1516, 2016.

[28] Hrvoje Dorotić, Tomislav Pukšec, and Neven Duić. Multi-objective optimization of district heating and cooling systems for a one-year time horizon. Energy, 169:319–328, 2019.

[29] Ahmed S. Zamzam, Emiliano Dall'Anese, Changhong Zhao, Josh A. Taylor, and Nicholas D. Sidiropoulos. Optimal water-power flow-problem: Formulation and distributed optimal solution. IEEE Transactions on Control of Network Systems, 6(1):37–47, 2019.

[30] Lena C. Altherr, Philipp Leise, Marc E. Pfetsch, and Andreas Schmitt. Resilient layout, design and operation of energy-efficient water distribution networks for high-rise buildings using MINLP. Optimization and Engineering, 20(2):605–645, 2019.

[31] Nicholas Long. Reduced Order Models for Rapid Analysis of Ambient Loops for Commercial Buildings. Master's thesis, University of Colorado Boulder, Boulder, CO, 2018.

[32] Benjamin Polly, Chuck Kutscher, Daniel Macumber, and Marjorie Schott. From Zero Energy Buildings to Zero Energy Districts. In 2016 ACEEE Summer Study on Energy Efficiency in Buildings, pages 1–16, Asilomar, CA, 2016.

[33] URBANopt SDK Documentation. `https://docs.urbanopt.net/`, 2021.

[34] Brian L. Ball, Nicholas Long, Katherine Fleming, Chris Balbach, and Phylroy Lopez. An open source analysis framework for large-scale building energy modeling. Journal of Building Performance Simulation, 13(5):487–500, 2020.

[35] U.S. Department of Energy. Commercial prototype building models.

[36] Modelica Association. Modelica language. `https://www.modelica.org/modelicalanguage`, 2020. [Accessed 20/02/2020].

[37] J. Kennedy and R. Eberhart. Particle swarm optimization. In Proceedings of ICNN'95 - International Conference on Neural Networks, volume 4, pages 1942–1948 vol.4, 1995.

[38] Z. Fallahi, A. Allen, M. Murphy, and G.P. Henze. Conditions conducive for the adoption of feasible fifth-generation district heating and cooling networks. In 2021 Conference on Sustainable Development of Energy, Water, and Environment Systems, In preparation.

[39] J. Kennedy and R. Eberhart. A discrete binary version of the particle swarm algorithm. In 1997 IEEE International Conference on Systems, Man, and Cybernetics. Computational Cybernetics and Simulation, volume 5, pages 4104–4108 vol.5, 1997.

[40] J. Kennedy. Small worlds and mega-minds: effects of neighborhood topology on particle swarm performance. In Proceedings of the 1999 Congress on Evolutionary Computation-CEC99 (Cat. No. 99TH8406), volume 3, pages 1931–1938 Vol. 3, 1999.

[41] Lester James Miranda. Pyswarms: a research toolkit for particle swarm optimization in python. Journal of Open Source Software, 3(21):433, 2018.

[42] Trieu T Mai, Paige Jadun, Jeffrey S Logan, Colin A McMillan, Matteo Muratori, Daniel C Steinberg, Laura J Vimmerstedt, Benjamin Haley, Ryan Jones, and Brent Nelson. Electrification Futures Study: Scenarios of Electric Technology Adoption and Power Consumption for the United States. Nrel/Tp-6a20-71500, 2018.

[43] European Commission. An EU strategy on heating and cooling 2016. Journal of Chemical Information and Modeling, 53(9):1689–1699, 2016.

[44] Henrik Lund, Poul Alberg Ostergaard, Miguel Chang, Sven Werner, Svend Svendsen, Peter Sorknæs, Jan Eric Thorsen, Frede Hvelplund, Bent Ole Gram Mortensen, Brian Vad Mathiesen, Carsten Bojesen, Neven Duic, Xiliang Zhang, and Bernd Möller. The status of 4th generation district heating: Research and results. Energy, 164:147–159, dec 2018.

[45] Cara Carmichael and Victor Olgyay. Managing Deep Energy Retrofits. May 2012.

[46] D. Connolly, H. Lund, B. V. Mathiesen, S. Werner, B. Möller, U. Persson, T. Boermans, D. Trier, P. A. Østergaard, and S. Nielsen. Heat roadmap Europe: Combining district heating with heat savings to decarbonise the EU energy system. Energy Policy, 65:475–489, 2014.

[47] Henrik Lund, Neven Duic, Poul Alberg Østergaard, and Brian Vad Mathiesen. Future district heating systems and technologies: On the role of smart energy systems and 4th generation district heating. Energy, 165:614–619, 2018.

[48] Lin-Shu Wang. Application of exergy: A low-exergy solution to building heating and cooling. In Tolga Taner, editor, Application of Exergy, chapter 2. IntechOpen, Rijeka, 2018.

[49] Gregor P. Henze, Clemens Felsmann, Doreen E. Kalz, and Sebastian Herkel. Primary energy and comfort performance of ventilation assisted thermo-active building systems in continental climates. Energy and Buildings, 40(2):99 – 111, 2008.

[50] Ioan Sarbu and Calin Sebarchievici. A study of the performances of low-temperature heating systems. Energy Efficiency, 8(3):609–627, Jun 2015.

[51] B Olesen. Radiant heating and cooling by embedded water-based systems. 2011.

[52] Jingjuan (Dove) Feng, Stefano Schiavon, and Fred Bauman. Cooling load differences between radiant and air systems. Energy and Buildings, 65:310 – 321, 2013.

[53] Kyu-Nam Rhee, Bjarne W. Olesen, and Kwang Woo Kim. Ten questions about radiant heating and cooling systems. Building and Environment, 112:367 – 381, 2017.

[54] Christoph F. Reinhart and Carlos Cerezo Davila. Urban building energy modeling – a review of a nascent field. Building and Environment, 97:196 – 202, 2016.

[55] Julia Sokol, Carlos Cerezo Davila, and Christoph F. Reinhart. Validation of a bayesian-based method for defining residential archetypes in urban building energy models. Energy and Buildings, 134:11 – 24, 2017.

[56] Y. Heo, R. Choudhary, and G.A. Augenbroe. Calibration of building energy models for retrofit analysis under uncertainty. Energy and Buildings, 47:550 – 560, 2012.

[57] Christina J. Hopfe and Jan L.M. Hensen. Uncertainty analysis in building performance simulation for design support. Energy and Buildings, 43(10):2798 – 2805, 2011.

[58] Linn Laurberg; Jensen, Daniel Trier, Marcus; Brennenstuhl, Marco; Cozzini, and Belen Gómez-Uribarri Serrano. D3 . 1 – Analysis of Network Layouts in Selected Urban Contexts. Technical report, PlanEnergi, 2017.

[59] T Schluck, P Kräuchi, and M Sulzer. Non-linear thermal networks - How can a meshed network improve energy efficiency? CISBAT 2015 Lausanne, pages 779–785, 2015.

[60] Fabien Marty, Sylvain Serra, Sabine Sochard, and Jean-Michel Reneaume. Simultaneous optimization of the district heating network topology and the organic rankine cycle sizing of a geothermal plant. Energy, 159:1060 – 1074, 2018.

[61] Adriano Sciacovelli and Vittorio Verda. Topology optimization of robust district heating networks. Journal of Energy Resources Technology, 140(February):1–9, 2018.

[62] Bram van der Heijde, Annelies Vandermeulen, Robbe Salenbien, and Lieve Helsen. Integrated optimal design and control of fourth generation district heating networks with thermal energy storage. Energies, 12(14), 2019.

[63] Gregor P. Henze and Alexander G. Floss. Evaluation of temperature degradation in hydraulic flow networks. Energy and Buildings, 43(8):1820–1828, 2011.

[64] U.S. DOE. EnergyPlus, 2018. [Accessed 01/12/2018].

[65] U.S. EPA. The difference between source and site energy. 2018. [Accessed 01/12/2019].

[66] American Society of Heating, Refrigeration, and Air Conditioning Engineers. Standard 90.1 2013: Energy Standard for Buildings Except Low-Rise Residential Buildings. 2013.

[67] Richard Karl Strand and Curtis O. Pedersen. Implementation of a radiant heating and cooling model into an integrated building energy analysis program. ASHRAE Transactions, 103(1):949–958, 1997.

[68] Chanvit Chantrasrisalai, Vinay Ghatti, D E Fisher, and D G Scheatzle. Experimental validation of the EnergyPlus low-temperaturer radiant simulation. ASHRAE Transactions, 109:614–623, 2003.

[69] COMNET, 2016. [Accessed 26/02/2020].

[70] State of California. Title 24 2013: Building Energy Efficiency Standards for Residential and Non-Residential Buildings. 2012.

[71] R Hendron and C Engebrecht. Building America Research Benchmark Definition. 2009.

[72] P.O. Fanger. Thermal Comfort: Analysis and Applications in Environmental Engineering. Danish Technical Press, 1972.

[73] American Society of Heating, Refrigeration, and Air Conditioning Engineers. HVAC Systems and Equipment. ASHRAE, 2016.

[74] Priya D. Lavappa and Joshua D. Kneifel. Energy Price Indices and Discount Factors for Life-Cycle Cost Analysis – 2015 Annual Supplement to NIST Handbook 135. National Institute of Standards and Technology . U.S Depatrtement of Commerce, (April 2005):67, 2015.

[75] EURAC Research. Flexynets, . [Accessed 23/02/2020].

[76] Justus von Rhein. Modeling, Simulation, and Life-Cost Analysis of Fifth-Generation District Heating and Cooling Networks, 2018.

[77] U.S. Energy Information Administration. U.S. Energy Information Administration - EIA - Independent Statistics and Analysis, 2018. [Accessed 14/02/2020].

[78] A. Allen, G. Henze, K. Baker, and G. Pavlak. Analysis of HVAC systems for deep energy savings at the urban district level. In Conference on Sustainable Development of Energy, Water and Environment Systems, Dubrovnik, Croatia, 2019.

[79] American Society of Heating, Refrigeration, and Air Conditioning Engineers. Handbook of Fundamentals. 2017.

[80] J. Kennedy and R. Eberhart. Particle swarm optimization. In Proceedings of ICNN'95 - International Conference on Neural Networks, volume 4, pages 1942–1948 vol.4, Nov 1995.

[81] United Nations Environment Programme. The Sustainable Development Goals Report. New York City: United Nations, 2018.

[82] Arup U.S. EPA, CH2MHill. *District-Scale Energy Planning:Smart Growth Implementation Assistance to the City of San Francisco*. Technical report, 2015.

[83] Kate Doubleday, Faeza Hafiz, Andrew Parker, Tarek Elgindy, Anthony Florita, Gregor Henze, Graziano Salvalai, Shanti Pless, and Bri-Mathias Hodge. Integrated distribution system and urban district planning with high renewable penetrations. WIREs Energy and Environment, 8(5):e339.

[84] Priya D Lavappa and Joshua D Kneifel. Energy Price Indices and Discount Factors for Life-Cycle Cost Analysis – 2015 Annual Supplement to NIST Handbook 135. Washington, DC: National Institute of Standards and Technology, U.S Department of Commerce, 2015.

[85] Amy Allen, Gregor P. Henze, Kyri Baker, and Greg Pavlak. Evaluation of low-exergy hvac systems and topology optimization for deep energy savings at the urban district level. Energ. Convers. Manage., under review, 2019.

[86] US Department of Energy. Quadrennial Technology Review: Chapter 5: Increasing Efficiency of Building Systems and Technologies. 2015.

[87] Hans Christian Gils, Janusz Cofala, Fabian Wagner, and Wolfgang Schöpp. Gis-based assessment of the district heating potential in the usa. Energy, 58:318–329, 2013.

[88] Priya D. Lavappa and Joshua D. Kneifel. Energy Price Indices and Discount Factors for Life-Cycle Cost Analysis – 2019 Annual Supplement to NIST Handbook 135. National Institute of Standards and Technology . U.S Depatrtement of Commerce, page 67, 2019.

[89] K Rafferty. Selected Cost Considerations for Geothermal District Heating in Existing Single-Family Residential Areas. 1996.

[90] Paul Nahmmacher, Eva Schmid, Lion Hirth, and Brigitte Knopf. Carpe diem: A novel approach to select representative days for long-term power system modeling. Energy, 112:430–442, 2016.

[91] American Society of Heating, Refrigeration, and Air Conditioning Engineers. ASHRAE GUIDELINE 14.

[92] Marco Wirtz, Lukas Kivilip, Peter Remmen, and Dirk Müller. Quantifying demand balancing in bidirectional low temperature networks. Energy and Buildings, 224:110245, 2020.

[93] U.S. EPA. Energy Star Portfolio Manager Technical Reference. 2018.

[94] National Academies of Sciences, Engineering, and Medicine. Accelerating Decarbonization of the U.S. Energy System. 2021.

[95] Population Division, Department of Economic and Social Affairs. World Urbanization Prospects: The 2018 Revision. United Nations, 2018.

[96] Raghu Nandan Sengupta, Aparna Gupta, Joydeep Dutta, Sunith Bandaru, and Kalyanmoy Deb. CRC Press, 2020.

[97] A. P. Engelbrecht. Particle swarm optimization: Global best or local best? In 2013 BRICS Congress on Computational Intelligence and 11th Brazilian Congress on Computational Intelligence, pages 124–135, 2013.

[98] Boran Morvaj, Ralph Evins, and Jan Carmeliet. Optimising urban energy systems: Simultaneous system sizing, operation and district heating network layout. Energy, 116:619–636, 2016.

[99] Maarten Blommaert, Y. Wack, and M. Baelmans. An adjoint optimization approach for the topological design of large-scale district heating networks based on nonlinear models. Applied Energy, 280:116025, 2020.

[100] Amy Allen, Gregor Henze, Kyri Baker, Gregory Pavlak, and Michael Murphy. ASHRAE Winter Conference. 2021.

[101] M Deru, K Field, and D Studer. U.S. Department of Energy Commercial Reference Building Models of the National Building Stock. 2011.

[102] Charles D. Corbin, Gregor P. Henze, and Peter May-Ostendorp. A model predictive control optimization environment for real-time commercial building application. Journal of Building Performance Simulation, 6(3):159–174, 2013.

[103] Modelon AB. PyFMI. `https://pypi.org/project/PyFMI/`, 2018.

[104] Andries P. Engelbrecht. Computational intelligence: an introduction. John Wiley & Sons, 2008.

[105] Juan Rada-Vilela, Mengjie Zhang, and Winston Seah. A performance study on synchronicity and neighborhood size in particle swarm optimization. Soft Computing, 17:1019–1030, 2013.

[106] S. B. Akat and V. Gazi. Particle swarm optimization with dynamic neighborhood topology: Three neighborhood strategies and preliminary results. In 2008 IEEE Swarm Intelligence Symposium, pages 1–8, 2008.

[107] J. Kennedy and R. Mendes. Population structure and particle swarm performance. In Proceedings of the 2002 Congress on Evolutionary Computation. CEC'02 (Cat. No.02TH8600), volume 2, pages 1671–1676 vol.2, 2002.

[108] Peter T. May-Ostendorp. Offline Model Predictive Control of Mixed Mode Buildings for Near-Optimal Supervisory Control Strategy Development. PhD thesis, University of Colorado Boulder, Boulder, CO, 2012.

[109] M.R. AlRashidi and M.F. AlHajri. Optimal planning of multiple distributed generation sources in distribution networks: A new approach. Energy Conversion and Management, 52(11):3301 – 3308, 2011.

[110] P. N. Suganthan. Particle swarm optimiser with neighbourhood operator. In Proceedings of the 1999 Congress on Evolutionary Computation-CEC99 (Cat. No. 99TH8406), volume 3, pages 1958–1962 Vol. 3, 1999.

[111] M. F. AlHajri, M. R. AlRashidi, and M. E. El-Hawary. Hybrid particle swarm optimization approach for optimal distribution generation sizing and allocation in distribution systems. In 2007 Canadian Conference on Electrical and Computer Engineering, pages 1290–1293, 2007.

[112] Peter May-Ostendorp, Gregor P. Henze, Charles D. Corbin, Balaji Rajagopalan, and Clemens Felsmann. Model-predictive control of mixed-mode buildings with rule extraction. Building and Environment, 46(2):428 – 437, 2011.

[113] John Morris. Data structures and algorithms: Graph algorithms. `https://www.cs.auckland.ac.nz/software/AlgAnim/prim.html`, 1998.

[114] Functional mock-up interface. `https://fmi-standard.org/`.

[115] Lawrence Berkeley National Lab. Buildingspy. `https://pypi.org/project/buildingspy/`, 2020.

[116] Geojson. `https://geojson.org/`, 2016.

[117] MapBox, Open Street Map. Geojson.io. `geojson.io`.

[118] Brian L. Ball, Nicholas Long, Katherine Fleming, Chris Balbach, and Phylroy Lopez. An open source analysis framework for large-scale building energy modeling. Journal of Building Performance Simulation, 13(5):487–500, 2020.

[119] Long, Nicholas, Summer, Ted. Geojson-to-modelica translator. `https://pypi.org/project/geojson-modelica-translator/`, 2021.

[120] Amy Allen, Gregor Henze, Kyri Baker, and Gregory Pavlak. Evaluation of Topology Optimization to Achieve Energy Savings at the Urban District Level, 2021.

[121] Alberto Pizzolato, Adriano Sciacovelli, and Vittorio Verda. Topology optimization of robust district heating networks. Journal of Energy Resources Technology, 140(2), 2017.

[122] Boran Morvaj, Ralph Evins, and Jan Carmeliet. Optimising urban energy systems: Simultaneous system sizing, operation and district heating network layout. Energy, 116:619–636, 2016.

[123] American Society of Heating, Refrigeration, and Air Conditioning Engineers. HVAC Applications. 2019.

[124] Amy Allen, Gregor Henze, Kyri Baker, Gregory Pavlak, and Michael Murphy. Development of a topology optimization framework for district thermal energy systems. To be submitted to Energy Conversion and Management, 2021.